Palaeoecology of the middle to late Cambrian Rogersville Shale, Conasauga Group, eastern Tennessee

Author: Leslie Ann Campbell

Persistent link: http://hdl.handle.net/2345/351

This work is posted on eScholarship@BC,
Boston College University Libraries.

Boston College

The Graduate School of Arts and Sciences

Department of Geology and Geophysics

PALAEOECOLOGY OF THE MIDDLE TO LATE CAMBRIAN ROGERSVILLE SHALE, CONASAUGA GROUP, EASTERN TENNESSEE

a thesis

by

LESLIE ANN CAMPBELL

submitted in partial fulfillment of the requirements for the degree of

Masters of Science

August, 2008

ABSTRACT

Palaeoecology of the Middle to Late Cambrian Rogersville Shale,

Conasauga Group, eastern Tennessee

Leslie Ann Campbell

Advisor: Dr. Paul Strother

The Rogersville Shale of the Middle to Late Cambrian Conasauga Group was deposited on the margins of Laurentia, in what is now eastern Tennessee. Based on 21 thin section samples from the ORNL-Joy2, core five distinct microlithofacies are described, trace fossils characterized, and palynological data interpreted. This investigation concluded that the Rogersville Shale was deposited in a shallow, restricted marine or possibly estuarine environment that would have been exposed to terrestrial runoff. Previous work on the Conasauga Group placed deposition of the Rogersville Shale within an intercratonic basin in approximately 250m of water, perhaps significantly deeper. This investigation found that the Rogersville Shale was likely deposited in a lagoonal setting or restricted estuarine environment that had freshwater input.

Table of Contents

ACKNOWLEDGEMENTS

To begin I would like to thank Boston College, the Graduate School of Arts and Science and the Geology and Geophysics Department for being given the opportunity to continue my education. I would like to thank Professor Paul Strother for his guidance and patients throughout this long process. I would also like to thank Professor Chris Hepburn and Professor Judy Hepburn for their efforts. To John Beck and Ken Galli I would like to extend special thanks for always having helpful suggestions and advice.

To my family Mom, Dad, Ian, and Rodney and my friends thank you for you love and constant support. To Tim, thank you for all your help along the way, this would not have been possible without you.

Chapter 1

Introduction

Purpose and Scope

The focus of this research has been to reconstruct the palaeoecologic conditions of the Middle to Late Cambrian, Rogersville Shale using a multidisciplinary approach to identify palaeoenvironmental conditions.   Part of the Conasauga Group, the Rogersville Shale, represents one palaeoenvironment in a series of three progradational and retrogradational events. The six formations of the Conasauga Group were formed as Cambrian sea-levels fluctuated across the continental margins.

Previous Works

While the Conasauga Group has been studied in great detail (Glumac and Walker, 1998; Glumac and Walker 2000; Glumac and Walker 2002; Markello and Read 1981; Srinivasan and Walker 1993; Byerly et al. 1986; Haase, Walls, and Farmer 1985; Hasson and Haase 1988; Walker, Foreman, and Srinivasan 1990), the Rogersville Shale has been less completely investigated. Walcott's (1898) Fossil Medusæ, which illustrates and describes fossils found within the Rogersville Shale, was one of the first references to the unit. Markello and Read (1981) briefly describe the Rogersville Shale in their paper on the

Nolichucky Shale. Byerly et al. (1986) describe a classic outcrop of the Conasauga Group at Thorn Hill in which the Rogersville Shale is mentioned. Haase et al. (1985) is a thorough description of the formations within the Conasauga Group. Their paper is a review of the ORNL-Joy2 core which this investigation is based on. Hasson and Haase (1988) describe the lithofacies and palaeogeography of the formations of the Conasauga Group. The most recent investigation of the Rogersville Shale was done by Walker et al. (1990).

The conclusion of this study is in contrast to Walker et al. (1990), who estimated water depths of 100-250m, perhaps substantially more, for deposition of the Rogersville Shale. Their estimate of water depth was based on five particular observations:

1. The presence of paper-laminated shales

2. The presence of allochthonous carbonate beds (resulting from both debris flows and turbidites)

3. The absence of bioturbation

4. The abundance of glauconite

5. The pyritic nature of the shale

Some of these five characteristics were not found to exist within the Rogersville Shale when observed on the scale of thin sections, while others were interpreted differently. When combined, the five observations made by Walker et al. (1990) lead to an interpretation of the paleoenvironment that is different than the findings of this research.

General Geologic Setting

After the Late Precambrian to Early Cambrian breakup of the supercontinent Rodinia, the passive margin of Laurentia was established (Bond et al. 1984) (Figure 1). According to Glumac and Walker (1997, 1998, 2000, and 2002) the margin of what is now eastern North America developed a broad carbonate platform throughout the early Paleozoic. To the west an intercratonic basin was formed.

N
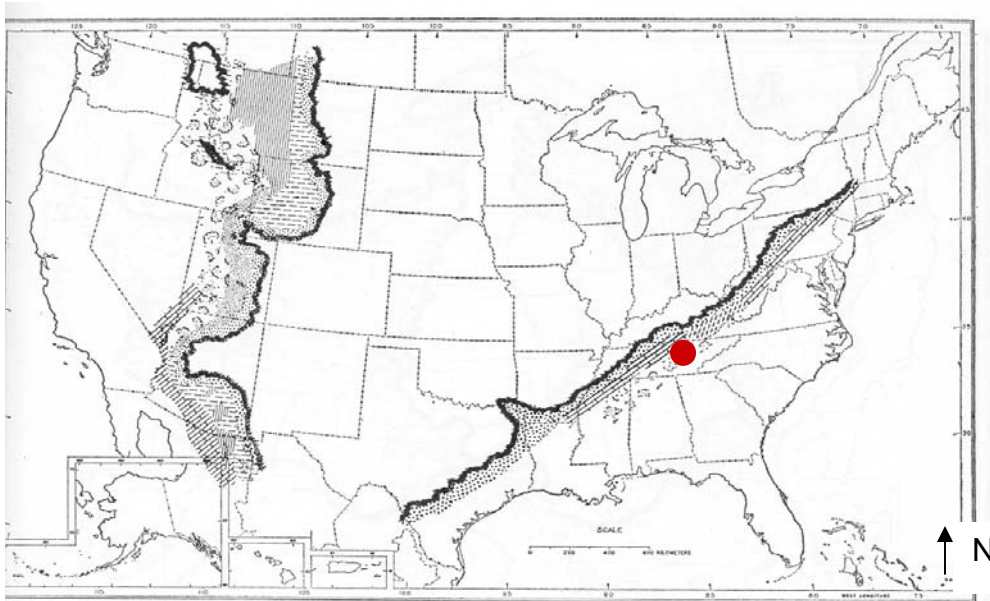
Figure 1. Diagram showing the margins of Laurentia and the Iapetus Ocean during the Middle Cambrian (Lochman-Balk, 1971). The red dot represents the location of the Conasauga Group in the study area

GENERALIZED GEOLOGIC MAP OF TENNESSEE
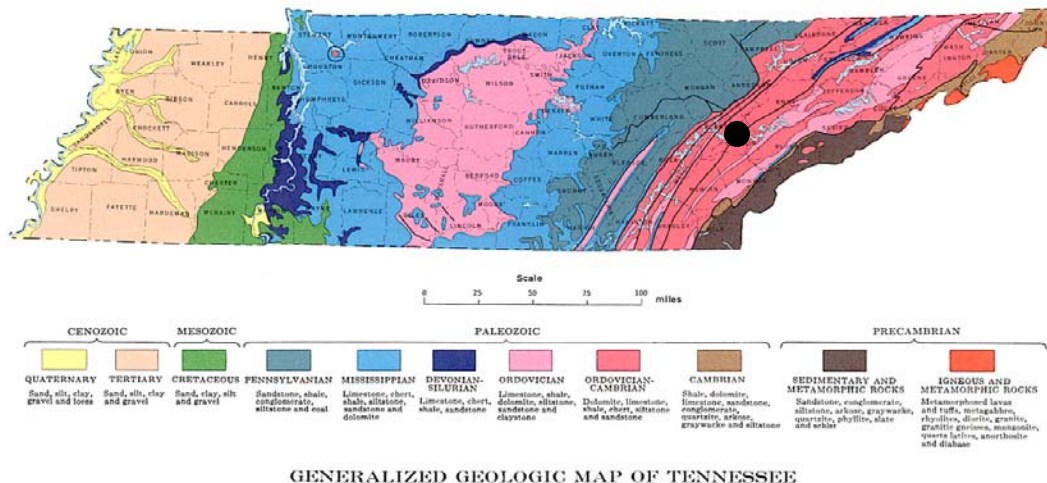
Figure 2. Geologic map of Tennessee with sample location marked with a black dot. [http://www.tn.gov]

Figure 2, a geologic map of Tennessee show the location of the sample location within the study region. The Conasauga Group in eastern Tennessee represents the interfingering and overlapping of carbonates from the east and clastic material in west (Figure 3).
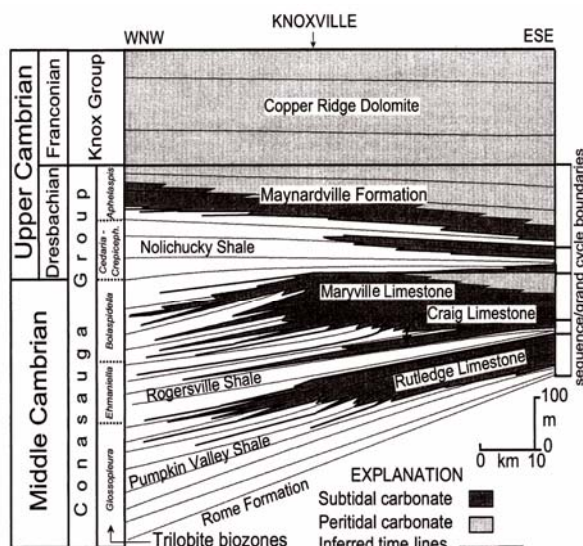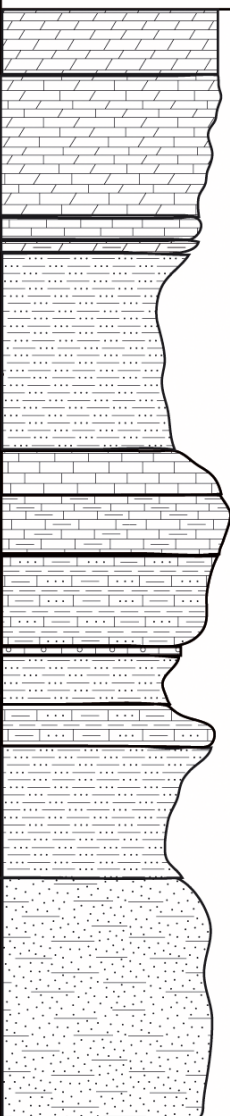
Figure 3. Middle to Upper Cambrian stratigraphy of the eastern Tennessee Appalachians. The Conasauga Group represents a complex overlapping and interfingering of carbonate and siliclastic units. [Glumac and Walker, 2000, p. 953]

Glumac and Walker (2000) believed the Conasauga Group can be divided into three grand cycles characterized by three different clastic to carbonate transitions resulting in six different stratigraphic formations (each formation represents a half-cycle). Glumac and Walker (2000) cite several different authors (Aitken 1978; Bond et al. 1988; Rankey et al. 1994; Walker et al. 1990; Srinivasan and Walker 1993) in establishing the complex interdependency of the factors that ultimately led to the deposition of the Conasauga Group. These conditions include eustatic sea-level changes, tectonism, rate of sedimentation and sediment supply.

The intermixed carbonate and clastic rocks of the Conasauga Group are broadly transitional between the underlying Rome Formation, which is essentially carbonate-free, and the overlying Knox Group, which is essentially clastic-free (Haase et al. 1985). The summary presented here starts with the lowest (oldest) stratigraphic unit the Rome Formation and finishes with the youngest formation, the Copper Ridge Dolomite of the Knox Group (Figure 4).

Figure 4. Stratigraphic column representing the lithology present in the ORNL-Joy2 core. The stratigraphic column ranges from the Rome Formation, through the six stratigraphic units of the Conasauga Group and into the Copper Ridge Dolomite of the Knox Group. Biostratigraphic data is compiled from Glumac & Walker (1998), Sundberg (1989), and Hasse et al. (1985). Formation thickness data is also from Hasse et al. (1985).

Trilobite Zone	Lithology	Formation
Taenicephalus		Copper Ridge Dolomite 43 m
Elvinia		
Dunderbergia Prehousia Dicanthopyge Aphelaspis		Maynardville Limestone 98 m
Crepicephalus Cedaria		Nolichucky Shale 167 m
Bolaspidella		Maryville Limestone 141 m
Ehmaniella		Craig Member Rogersville Shale 39 m
		Rutledge Limestone 30 m
Glossopleura		Pumpkin Valley Shale 94 m
		Rome 188 m

Left margin labels: Conasauga Group; Rome; Knox; Upper Cambrian; Middle Cambrian

Legend for lithologies in Figure 4
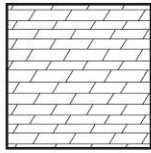
A. Dolomite found within the Copper Ridge Dolomite of the Knox Group

B. Limestone interbedded with dolomite, found within the Maynardville Limestone of the Conasauga Group
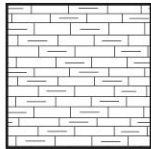
C. Argillaceous Limestone, a limestone that contains variable amounts of shale, found within the Nolichucky Shale and the Maryville Limestone of the Conasauga Group
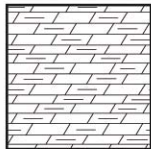
D. Argillaceous Dolomite, a dolomite that contains variable amounts of shale, found within the Nolichucky Shale of the Conasauga Group
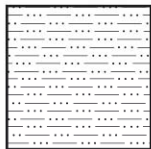
E. Silty Shale, this material is common throughout the Conasauga Group, and is found within the Nolichucky Shale, the Rogersville Shale and the Pumpkin Valley Shale
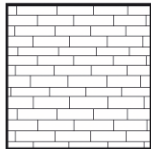
F. Limestone, found within the Maryville Limestone of the Conasauga Group
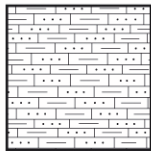
G. Limestone that contains silt and shale, found within the Maryville Limestone of the Conasauga Group
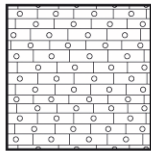
H. Oolitic Limestone, found within the Craig Limestone member of the Rogersville Shale of the Conasauga Group
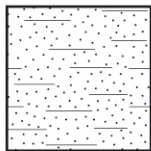
I. Sandstone that contains some shale, found within the Rome Formation

ORNL-Joy2 Core

The core was drilled by the U. S. Department of Energy (DOE) to determine the stratigraphy of the Conasauga Group on the Copper Creek fault block on the U.S. DOE's Oak Ridge National Laboratory on the Oak Ridge Reservation. Drilled near Melton Lake, the ORNL-Joy2 core bore hole is located in Anderson County, Tennessee on the United States Department of Energy Oak Ridge Reservation (Figure 5).
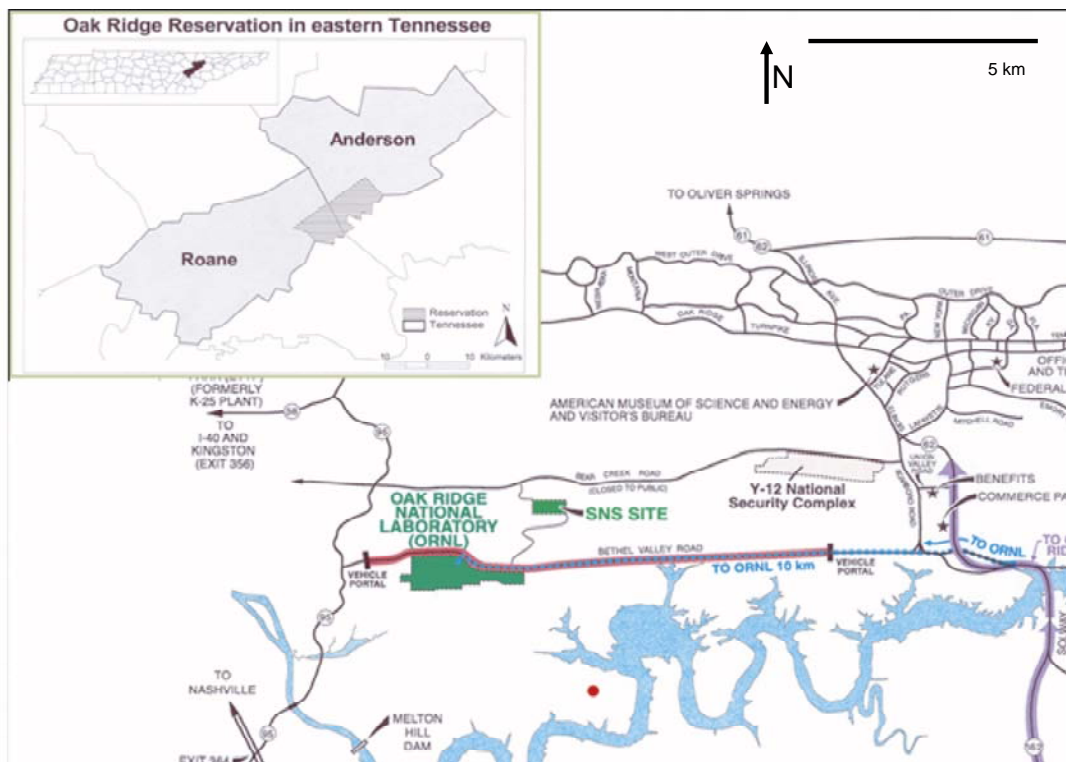
Figure 5. Map of the Oak Ridge Reservation in eastern Tennessee and the ORNL-Joy2 drill core, marked with a red dot. [From http://www.em.doe.gov]

The bore-hole, located on the Copper Creek fault block, is approximately 5km southwest of the Oak Ridge National Laboratory plant (Haase et al.1985).

Drilling operations were conducted by the Contract Drilling Division of Joy

Manufacturing Company, Inc. from August 26, 1982 through December 15, 1982

(Haase et al.1985). The core was drilled to a depth of nearly 830 meters,

penetrating the Copper Ridge Dolomite of the Knox Group, the six stratigraphic

formations of the Conasauga Group, and the Rome Formation (Haase et

al.1985).

Descriptions of the ORNL-Joy2 Core

Descriptions of the eight formation of the ORNL-Joy2 core are presented

in the following section. The descriptions are based on investigation of thin

section samples of the core in addition to those of Haase et al. (1985), who

provided a detailed summary of the ORNL-Joy2 core.   Descriptions of all eight

formations are included to summarize the depositional history of the area.

Rome formation

Due to the location of several thrust faults in the Valley and Ridge

Province in Tennessee, the Rome formation has experienced substantial

deformation, causing intervals of lithology to be repeated or completely removed

at the core site. The ORNL-Joy2 core went through nearly 190m of the Rome

Formation; although the true thickness of the formation is known to be

significantly less in the area surrounding the bore hole. The complex structural

history of the area is particularly apparent in the lower Rome Formation; it is

generally characterized by "severe deformation and extremely chaotic stratification patterns" (Haase et al. 1985 pg. 52). Preliminary investigations of the lithology of the lower Rome Formation, performed by Haase et al. (1985), reveal that nearly all the intervals contained within the lower member are lithologically the same as the upper Rome Formation, but have been repeated due to extensive tectonism. Unlike the lower Rome Formation, the upper Rome Formation has not been affected by tectonic activity to the degree seen in the lower Rome Formation. Deformation that does occur in the upper Rome Formation is generally localized and small in scale. Lithologically, the upper Rome Formation is a complex mixture of several lithologically distinct sandstones interbedded with shales and mudstones. Subarkosic to quartz arenitic sandstones within the upper Rome Formation account for 60 – 80% of the member. The rest of the formation is composed of sandstones and siltstones interbedded with silty mudstone and shales (Haase et al. 1985).

The Conasauga Group

Pumpkin Valley Shale

Moving up section into the Middle Cambrian, the lowermost clastic formation in the Conasauga Group is the Pumpkin Valley Shale, it is the first half cycle of the three grand cycles. The Pumpkin Valley Shale has not been formally divided into different members, although it can be informally separated into an upper and lower member. The lower member is characterized by interbedded

bioturbated siltstones and mudstones with abundant glauconite pellets in the bioturbated siltstone intervals (up to 40% in some instances). The upper member is similar lithologically to the lower member- mudstones and is interbedded with subarkosic siltstones. The upper member is not as strongly bioturbated as the lower member. Glauconite in the upper member is ubiquitous throughout both the siltstone intervals (like the lower member) and the mudstones.

Rutledge Limestone

Overlying the Pumpkin Valley Shale is the Rutledge Limestone, a 30m thick ribbon-bedded carbonate that is clastic-rich in some intervals. In the vicinity of the core, the Rutledge Limestone can be divided into an upper and lower limestone member separated by a third unusually clastic rich interval. DeLaguna et al. (1968) referred to the lower member of the Rutledge Limestone as a 6m thick interval, with three limestone beds interstratified with two mudstone-rich intervals. The middle clastic-rich interval of the Rutledge Limestone is composed of mudstones and shales and contains lenses of siltstones. The upper member of the Rutledge Limestone is characterized by lenticular ribbon-bedded micrites, fossiliferous pelloidal wackestones and packstones, and lenticular bedded silty calcarenites. The transition from the Rutledge Limestone to the overlying mudstones of the Rogersville Shale is abrupt.

Rogersville Shale

The Rogersville Shale is characterized by massive to laminated noncalcareous mudstones and evenly bedded to wavy current-rippled calcarenites and subarkosic siltstones which exhibit substantial bioturbation (Haase et al. 1985). At the core site, the Rogersville Shale is 39m thick including the characteristic shale member and the Craig Member, an informal sub-unit that is carbonate rich. The lowermost portion of the Rogersville Shale is brownish grey and composed of mudstones that become interbedded with fining-upward subarkosic siltstones (Haase et al. 1985). Glauconite pellets are common in these siltstone intervals and can constitute up to 10 – 30% of an individual siltstone interval. Moving up section within the Rogersville Shale the next interval is reddish brown, massive to thinly bedded mudstone that serves as a marker for the top portion of the unit (Haase et al. 1985). Unique to the region around the bore-hole location, the Craig Limestone Member is a 3m thick interval of upward-coarsening carbonate situated on top of the shale member (Haase et al. 1985).

Maryville Limestone

In the vicinity of Oak Ridge National Laboratory, the Maryville Limestone is 140m thick (Haase et al. 1985) although the reported thickness may be somewhat overestimated due to possible borehole inclination and because of several severely deformed intervals. The Maryville Limestone can informally be subdivided into a lower and an upper member (Haase et al. 1985). The lower

member is composed of thinly bedded to thickly laminated. The beds and lamination are of calcareous mudstones interlayered with upward coarsening cycles of pelloidal wackestones and packstones, calcarenites and calcareous siltstones (Haase et al. 1985). Glauconite pellets are common within the upper portions of upward-coarsening cycles. The upper member is characterized by a flat pebble conglomerate (an intraclastic and locally oölitic packstone) which may account for 40 to 80% of the upper member. In addition to the flat pebble conglomerate, the upper member contains calcarenites and mudstones, which decrease in abundance from bottom to top (Haase et al. 1985).

Nolichucky Shale

The Nolichucky Shale in the area of the Oak Ridge National Laboratory can be subdivided into three members: the Lower Shale, the Bradley Creek, and the Upper Shale members (Markello and Read 1981; Hasson and Haase 1988). The Lower Shale Member is 140m thick, consists of numerous repeating cycles of massive-to-thinly laminated maroon to red- brown/grey shales/mudstones interbedded with upward-fining calcareous siltstone beds and limestones that consist of silty calcarenites, oölitic packstones, and fossiliferous pelloidal wackestones (Haase et al. 1985). The Bradley Creek Member is a 9m thick medium to dark grey lenticularly to wavy bedded algal wackestone and packstone with interstratified micrite layers and oölitic grain layers (Markello and Read 1981). In the region around the bore hole, the Upper Shale Member is only

18m thick (Haase et al. 1985). It occurs as interstratified wavy-to-evenly laminated dark grey calcareous mudstone with occasional upward-fining siltstone beds and a medium to light grey wavy, ribbon-bedded limestones to laminated micrites, wackestones and packstones (Haase et al. 1985).

Maynardville Limestone

The uppermost formation of the Conasauga Group is the Upper Cambrian Maynardville Limestone; it can be divided into two recognizable members. The 55m thick, Low Hollow Member consists primarily of wavy to evenly bedded calcarenites and micrites alternating with oölitic packstones and grainstones (Haase et al. 1985). The 45m thick, Chances Branch Member, is a medium to thin-bedded, buff to light grey dolostone that has ribbon-bedded stringers of calcarenites, wackestones, and micrites, oölitic packstones, and grainstones (Haase et al. 1985). Ribbon-bedded wackestones and oölitic packstones and grainstones are more abundant in the lower portions of this unit (Haase et al. 1985).

Knox Group

Copper Ridge Dolomite

In the vicinity of the study area, the Upper Cambrian Copper Ridge Dolomite (the basal portion of the overlying Knox Group), overlies the Conasauga Group. The contact between the Copper Ridge Dolomite and the

underlying Conasauga Group is gradational over an interval of approximately 4m.

Within this interval, dolomite increases dramatically and calcite content drops

from over 90 % to nearly 0 (Haase et al. 1985).   About 40 m thick, the Copper

Ridge Dolomite consists of two equally abundant and alternating microlithofacies

(Haase et al. 1985). The first lithology is a thinly bedded to laminated, evenly

parallel stratified dark grey dolostone and micrite that grades into mottled

dolostone (Haase et al. 1985). The second lithology is a medium grey dolostone

with wavy lenticular laminations that grades into ribbon-bedded dolostone with

minor shale stringers (Haase et al. 1985).

Glauconite

The study of glauconite began with Keferstein (1828) and continued with

authors such as Schneider (1927). Modern investigations into the mineral

glauconite continued with Cloud (1955), Burst (1958a & 1958b), Hower (1961),

Bentor & Kastner (1964), Triplehorn (1966), Odin & Rex (1982) and Odin (1988).

These authors described with great detail the conditions that characterize

environments of ancient and modern glauconite formation (i.e.—depth,

temperature, sediment accumulation rates, turbulence and spatial distribution).

P.E. Cloud Jr. (1955) recognized the potential for glauconite to be a useful

tool in paleoecologic investigations as a way to provide clues to the depositional

environment. In his 1955 paper, Cloud discussed the conditions he believed to

be necessary for glauconite formation. He summarized the conditions as stating that "the formation of glauconite appears to require marine waters of near normal salinity, reducing conditions, appropriate source material, high organic content in the sediment in which it forms, low or negative sedimentation rates, and finally a wide but not unlimited range of temperatures and depths"(1955, pp. 484). Cloud (1955, pp.484) explained that it was "this variety of limiting factors combined with the general ease of field recognition make glauconite much more useful in paleoecology than other accessory minerals, which are so far known to provide clues to depositional environments."

Information pertaining to the range of factors that may limit the occurrence of glauconite have been well documented (i.e. –depth, temperature, parental material, and turbulence) (Cloud 1955; Burst 1958a & 1958b; Hower 1961; Bentor & Kastner 1964; Triplehorn 1966; Odin & Rex 1982; Odin 1988). In light of conflicting evidence pertaining to the formation of glauconite, Burst (1958a) suggested that glauconite formation is not strictly controlled by individual factors (i.e.—depth, temperature, parent material, and turbulence).   He suggested that because reports of temperature range, water depth, parent material and turbulence generally vary they probably are not in themselves controlling factors in the glauconitization process. His suggestion puts less weight of physical parameters of an environment and more weight on the chemical conditions necessary for glauconite formation.

Burst (1958a pp. 316) recognized that there are several characteristics that are common to most glauconites, these include "consistent values of iron (20-25%), potassium (5-8%), and $Fe3^+/Fe2^+$ ratio 5/8)". He acknowledged that there must be some set of standardized conditions necessary for glauconite formation because of the consistent values of Fe and K. It appears these conditions may be chemical as opposed to physical.

Burst (1958a) concluded that the formation of glauconite can be simplified as a two step process whereby parent material (argillaceous material) is deposited and collects and is then altered by the surrounding sea-water chemistry (micro-reducing environment).

In the past glauconite has been thought to form under specific physical and chemical conditions, which would have made it an ideal tool to help decipher palaeoenvironmental conditions. Today glauconitic minerals are typically formed in open marine continental shelf and slope environments (Figure 6) (Odin, 1988). In recent years, a number of authors have noted the occurrence of glauconite in palaeoenvironments that are not consistent with a restricted interpretation of glauconite formation (Figure 7).
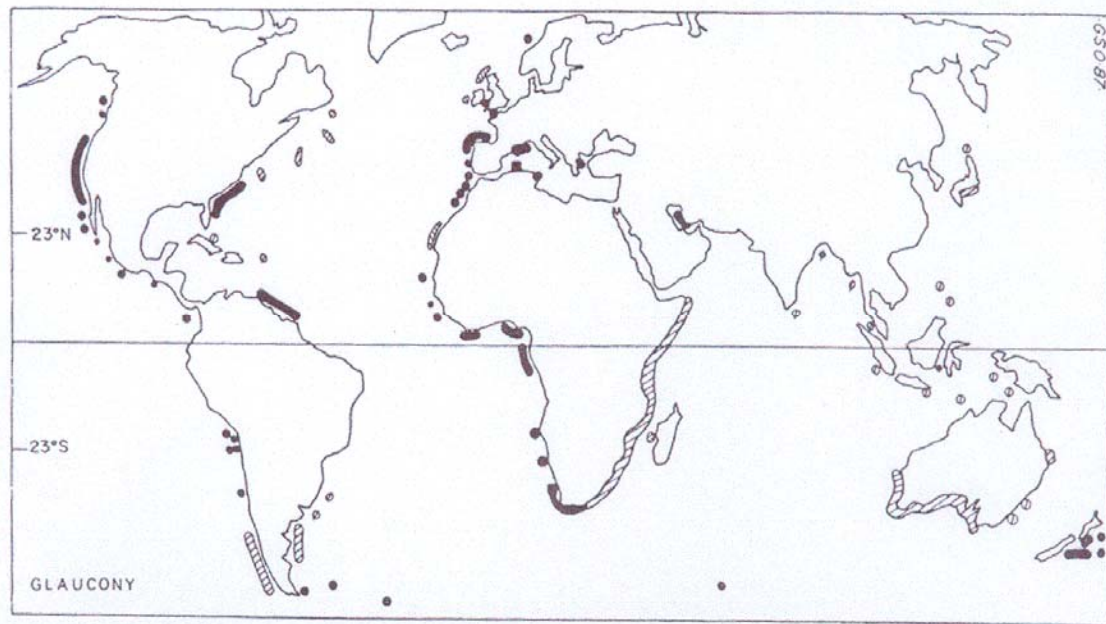
Figure 6. Recent distribution of glauconitic material. Glauconite is forming in open marine settings such as a shelf/slope margins that range from 65° N latitude to 50° S latitude. Black areas represent glauconite deposits and the hachured areas indicate presumed glauconite. This appears to indicate that glauconitic materials today do not have a preferred latitudinal distribution. [From G.S. Odin (1988) "Green Marine Clays" page 325.]

Age	Formation	Location	Environment	Reference
Cambrian	Riley Formation	Central Texas	Estuary, Lagoon tidal channels	Chafetz, 1978
(lower) Riphean	Chitrakut Formation	Central India	Estuary, Lagoon tidal channels	Singh & Kumar, 1978
Eocene	Brackiesham Formation	Hampshire Basin	Estuary, Lagoon tidal channels	Plint, 1983
Lower Cretaceous	(Upper) Mannville Group	Southern Alberta, Canada	Estuary, Lagoon tidal channels	Wood & Hopkins, 1992
Tertiary	-----	Agulhas Banks, South-African Continental Margin	Nearshore (wave-and-storm influenced arenites)	Parker, 1975
Cretaceous	Duwi Formation	Egypt	Nearshore (wave-and-storm influenced arenites)	Glenn & Authur, 1990
Lower Paleocene	Naheola Formation & Porters Creek Formation	Southern Alabama	Nearshore (wave-and-storm influenced arenites)	Mancini & Tew, 1993
Cretaceous (Campanian)	Shannon Sandstone	Wyoming	Nearshore (wave-and-storm influenced arenites)	Walker, Bergman, 1993
-----	-----	Albian near Clars	Inner Shelf (sandwaves and storm layers)	Gebhart, 1982
Mid-Cretaceous	-----	Vocontian Basin Southeast France	Inner Shelf (sandwaves and storm layers)	Breheret, 1991
Cretaceous	-----	-----	Lakes	Triat et al., 1976
Late Jurassic to early Cretaceous	Wealden	Southern England	Rivers	Odin & Rex, 1982
Proterozoic	Pakhal & Sullavia Groups	Pranhita-Godavari Valley	Rivers	Dasgupta et al., 1990
Lower Cretaceous	Purbeckian facies	Northern Aquitaine Basin Southwestern France	Shallow lagoonal	El Albani et al., 2005
Cambrian	Wilberns Formation (Riley Formation), Moore Hollow Group	Central Texas	Very shallow subtidal to intertidal water depth	Chafetz & Reid, 2000
Cambrian	Bliss Formation	Southwestern New Mexico	Very shallow water depth, tidal flat	Chafetz & Reid, 2000
Upper Cambrian	Cap Mountain Limestone Member (Riley Formation)	Central Texas	Tidal-flat to shallow shelf	King & Chafetz, 1983

Figure 7. Reference list for the occurrence of glauconite in a variety of depositional settings [Amorosi, 1997]

Chapter 2

Materials & Methods

This section outlines the material used and the methods followed throughout the duration of this research. A set of 21 thin section samples from the ORNL-Joy2 core have been used extensively in all aspects of this project. This slide set represents the bulk of the examined materials. Methods discussed in this section include petrographic description and analysis of the thin sections, photography and analysis of digital images of Rogersville Shale samples using image analysis and image editing software, and finally maceration of palynologic samples collected from the ORNL-Joy2 core.

Materials

The Core

Samples used in all portions of this investigation were collected from the ORNL-Joy2 core.

Thin sections

After the drilling was complete, a collection of thin sections was prepared from the ORNL-Joy2 core by a commercial laboratory (Baxter, 1989). This set of thin sections was used in the primary core description (Haase et al. 1985) and in several earlier Masters Theses at the University of Tennessee (Baxter, 1989;

Weber, 1988). In all, 21 thin section samples were available from the cored

Rogersville Shale, and although several slides were damaged due to general

degradation over time, all were used in this study. Many thin sections throughout

the core are damaged from bubbles or air pockets where the epoxy no longer

adheres the sample to the glass slide.

Palynologic Samples

Samples for the palynologic portion of this investigation were collected by

Professor P.K. Strother and J. Beck directly from the ORNL-Joy 2 core in

December 2001. However, not all of the palynologic samples correspond exactly

to the location of the thin section samples.

Methods

One of the research tools was to use digital images and image analysis in

the examination of petrographic thin sections. I wanted to know if it were

possible to use more efficient methods such as those commonly associated with

the techniques of image analysis in lieu of the tedious and often time-consuming

methods of traditional petrographic investigation. For example, estimating

mineral percentages by using comparison charts, measuring grain-size with the

reticule, and estimating grain-roundness can all be determined with image

analysis methods. I also applied similar techniques of digital image analysis to

investigation of the biologic activity preserved in the Rogersville Shale. The final

investigation involved the study of the palynologic material contained within the

Rogersville Shale to determine the paleobotanical populations present within the

samples. The methods used in the course of this work are outlined as a flow

chart (Figure 8).

Image Capture
(S1 Shooting Pro
Fuji Digital Camera)

Image enhancement /
Image preparation
(Photoshop)

- Sharpness
- Define grain boundaries
- Color
- Separate into individual components
- Convert to black & white images

Image Processing
(NIH Image / Image J)

- Measure Area
- Length of perimeter
- Pixel count (grain size)
- Orientation of long & short axes
- Roundness vs. eccentricity

Results
Quantitative Measurements

- Spreadsheets

Figure 8. This flow chart outlines the methods used in the course of this research starting with the initial stage of image capture and follows the process through to the end result. Each large box on the right represents a different step in the process and the smaller boxes on the left represent the outcomes of results of each step.

Petrographic Description and Analysis

To begin, it was necessary to complete a detailed petrographic description and analysis on the Rogersville Shale samples (See Appendix I). Each sample was examined to determine mineral content, physical characteristics of grains (such as size and shape), and texture. The extent of bioturbation and overall fabric of the sample was described, a composite sketch of each thin section was made, and a photograph of each slide was taken. Information from the thin section samples were compiled and examined (Appendix I). This information lead to individual descriptions of the microlithofacies present within the Rogersville Shale.

Photography and Digital Image Analysis of Thin sections

Digital image analysis of thin sections was used in this research to examine glauconite grains within the different microlithofacies. Glauconite was analyzed to determine if its presence in the different microlithofacies could relay information about the depositional environment. Was the glauconite contained within the different microlithofacies unique? To answer this question, the percent of glauconite in each thin section was examined. The percentage of glauconite within the thin sections with relation to vertical position in the core was also examined. The size of glauconite grains were measured as area of the image they cover. The grain size numbers were reported as an average area. In

addition, circumference of grains was measured as well as the length of the major axis.

Image Analysis Technique

Quantitative image analysis techniques were pioneered in the 1960's. While examples of quantitative image analysis techniques in the field of geology appear at present to be somewhat limited, the medical health field has long been aware of the many applications for quantitative digital image analysis. Ruzyla (1992) gives perspective as to suggested geologic procedures to follow, common sources of error and limitations of quantitative image analysis. Van den Berg et al. (2002, 2003), Heilbronner (2000, 2002), Ehrlich et al. (1984), Yamaji and Masuda (2005), White et al. (1998), Ruzyla (1992), Francus (1998), and Williams et al. (1998) are just a small subset of recent researchers who have attempted to utilize image analysis software programs to quantitatively analyze digital images of geologic samples. Van den Berg et al. (2002, 2003), Heilbronner, (2000, 2002), White et al. (1998), and Francus (1998) have specifically used NIH Image to characterize physical parameters of grains and in some cases pore space.

NIH Image is a public domain image analysis software program (currently available on the Internet at http://rsb.info.nih.gov/nih-image/) with many scientific applications. The initial version, *NIH Image* was developed by the National Institutes of Health (NIH) to aid in the analysis of digital images for Macintosh

platforms up to versions *OSX*. NIH then developed *Scion Image*, which is

compatible with computers that run on a Microsoft *Windows* platform. In the

following years, *Image J* was created. This version is a *Java* application and will

run on new Mac operating systems and is also compatible with Microsoft

Windows. All three software applications are essentially the same, and all were

used during the course of this research. To avoid confusion, I will refer to all

three programs collectively as *NIH Image* from this point on.

　　The procedures Van den Berg et al. (2002, 2003), Heilbronner (2000,

2002), White et al. (1998), and Francus (1998) used to analyze digital images

were all very similar. Acquire a digital image, edit and prepare the image for

analysis in *Adobe Photoshop*, analyze the image in *NIH Image*, and finally

interpret the data (Figure 8). Using these methods as outlined by Van den Berg

et al. (2002, 2003), Heilbronner (2000, 2002), White et al. (1998), Ehrlich et al.

(1984), and Francus (1998), I had to fine-tune the process for my specific needs.

Determining the most advantageous set-up for acquiring digital images of the

samples, editing and preparing images for analysis, and reporting the data

collected was largely a process of trial and error to decipher what combination of

steps in this process would work best together.

　　Image Capture

　　Beginning with image capture, several different approaches were

attempted before determining what camera setup would work best. Initially a

digital camera back with a macro lens mounted to a copy stand was used. This

proved to be the best scale at which to take the pictures but ultimately the

images were not sharp because of shutter vibration.

The next setup involved using a video camera to capture live images.

This approach made it easy to capture an image of a specific area or feature.

However, the images produced were highly magnified at a scale that was no

longer useful. Also the video camera only produced black and white images

which later proved difficult to manipulate in *Adobe Photoshop.*

The optimal set-up for image acquisition included a Wild M420

macroscope attached to a S1 Fuji digital camera connected directly to a

PowerMac computer running camera controlling software, *S1 Shooting Pro*. This

setup provided a direct link between the digital camera and the computer, and

proved to be ideal for several reasons. Captured images could be viewed

instantly. The means by which the camera was mounted on the macroscope

reduced vibration produced by the camera shutter. This setup produced a sharp,

color, reasonably scaled digital image ready for image editing in *Adobe*

Photoshop.

Editing Digital Images

Although the current camera setup produced optimal images (Figure 9),

digital editing was necessary. With *Photoshop*, colors of the thin section slide

images were adjusted to appear as accurate as possible compared to the

microscope view, add sharpness, and better define individual features (in this case grains) (Figure 10). Once the digital photo is opened in *Photoshop* the first adjustments are made to correct color. Looking individually at the red (R), blue (B), and green (G) color channels of the color image and manually adjusting the associated pixel distribution histograms will ensure a normal distribution of light and dark colored pixels. Adjusting these histograms can sometimes lead to images that are unnatural hues of red, blue and green. A final adjustment of overall color is generally necessary to achieve a natural look for the images. This is done by viewing the RBG color channels simultaneously and correcting the overall histogram for the image. Next, sharpness is added to the image. This helps to better define individual grain boundaries by increasing contrast of adjacent pixels, and focusing soft edges to increase clarity. Adjusting the color and sharpness of an image ultimately makes it easier to distinguish between different mineral grains in the subsequent stages of this process.

Figure 9. Initial image taken from the camera. This image has not been edited.

Figure 10. Digital image that has been adjusted for sharpness and color in *Adobe Photoshop*.

Once an image has easily distinguishable shapes and colors (in this case different mineral grains), it is now ready to be separated into individual mineral components. Because the photographs were taken at a known scale, a new window with the same dimensions is created. In the original photograph, grains are selected based on their color (i.e. pixels of a specified color range can be individually selected) allowing the user to only select mineral grains of interest. Once all the grains of a specific mineral component are selected, they can then be copied, temporally removed from the original photo and pasted into the new window with the same spatial dimensions as the original photo. This process is then repeated until all the mineral components of interest have been removed from the original (Figure 11).

Figure 11. This image is of glauconitic mineral only. They have been selected based on their green color.

There are now several color images (i.e., one for each mineral of interest) these images are now ready to be converted into greyscale images as the final step in *Photoshop* before they can be opened in *NIH Image*. Converting the color images to greyscale, discards the color information associated with each pixel and greatly reduces the file size leaving an 8-bit greyscale image, which can be used for analysis in *NIH Image* (Figure12).
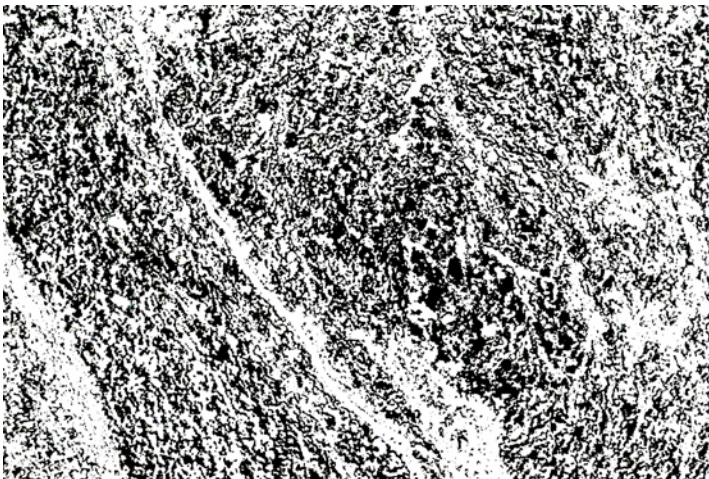
Figure12. The color information of the previous picture has been discarded and only a grey scale image remains.

Image Analysis

Edited and prepared images are now ready to be quantitatively analyzed using *NIH Image*. Upon opening the photos, the first task when quantitatively analyzing images is to set the scale. This was done by taking a photo of a millimeter scale ruler at the same magnification as the thin sections. The image of the ruler can then be opened in *NIH Image* and a scale can be created using the known distance on the ruler. This scale can then be applied to the images of the thin sections allowing one to create real world measurements.

Next, thresholding is done. This is a process whereby an 8-bit greyscale image is changed into a binary image. The pixels of interest (i.e. the grains) are converted to black and the background (i.e. the rest of the pixels) is converted to white.

Limitations of Digital Image Analysis

A significant problem encountered during the course of this research was how to separate grains that are touching. Ruzyla (1992) stated that the touching of particles is a persistent problem with digital images that prevent individual grain analysis. If two or more grains are in contact, the image analysis software will count the touching grains as one, instead of recognizing the individual grains. Measurements and calculations based on the amalgamated grains can have a tendency to skew the results, creating some inaccuracy. To achieve the most

accurate results possible, it was necessary to find a method to separate

amalgamated grains, most preferably by automated means.

Macros written for *NIH Image* are widely available on the Internet, some

have specifically been written to perform the task of separating touching particles

or grains by using different algorithms. Several of these macros, Van den Berg's

Digital Cutting Method (DCM) (2002) and Heilbronner's Lazy Grain Boundary

method (LGB) (2000), have been written specifically in a geologic sense for

separating touching particles. The DCM and LGB macros proved to be difficult to

use, requiring extensive programming skills in order to use them for grain

separation.   A function within the NIH Image program called watershedding

segmentation method (WSM) was found to produce results of a similar quality as

the macros. Van den Berg et al. (2002) found that the DCM and the WSM

"produce a similar amount of erroneous separations…" and (2003) reported the

DCM was "…slightly better than the watershedding method." So the decision to

use the watershedding segmentation method was made because the technique

did not require any additional effort, time or memory and produced reasonable

results that were consistent with other separation methods that are considered by

some to be more reliable.

The watershedding segmentation method (WSM) works best on slightly

rounded convex particles that do not overlap extensively

(http://rsb.info.nih.gov/nih-image/). It is recommended by Russ (1998) and Van

den Berg et al. (2002) that an erosion and dilation cycle be performed prior to the

WSM. This process smoothes edges and fills interior holes by subtracting

(erosion) or adding (dilation) pixels to the grains. This process may create slight

changes in the grain boundaries, but ultimately will not significantly change grain

morphology. Using the binary image that has undergone thresholding, WSM

begins by generating a Euclidian distance map (EDM) with Ultimate eroded

points (UEP) (Figure13a and Figure13b). An UEP represents the center point of

a particle, and the EDM is the area around the UEP (i.e. the area of the grain

within the grain boundary) represented as a decreasing grey value as distance

away from the center (UEP) increases (http://rsb.info.nih.gov/nih-image/). NIH

Image then dilates each grain center (UEP) as far as possible until one of two

situations occurs: (1.) the edge or grain boundary is reached, or (2.) another

growing grain center (UEP) is intersected (http://rsb.info.nih.gov/nih-image/). If

the growing UEP is not intersected, and can grow to the full extent of the grain

boundary, no segmentation occurs. If growing UEPs overlap, a segmentation is

made where the EDMs meet (Figure13c) (http://rsb.info.nih.gov/nih-image/).

Thresholded Cells

13a

EDM and UEPs

13b

After Watershed Segmentation
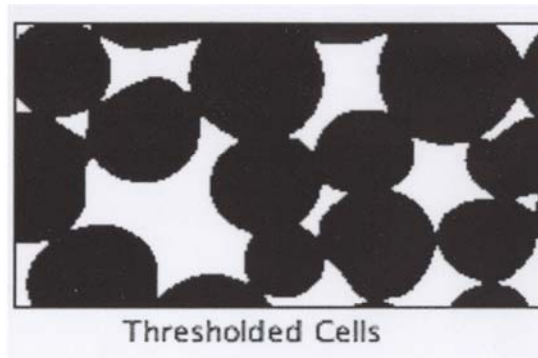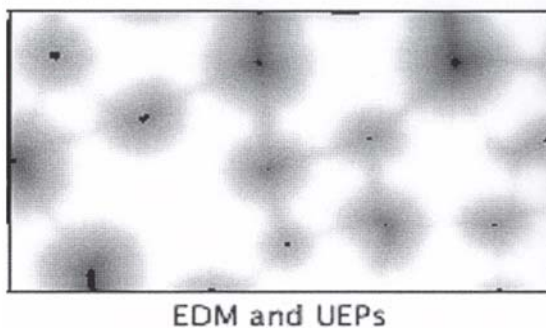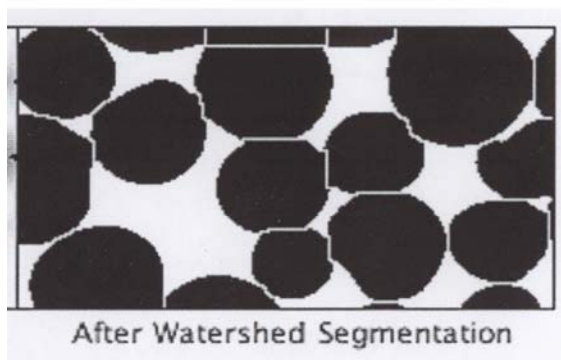
13c

Figures 13a, 13b, and 13c. These images show step wise the procedure for the watersheding segmentation method (WSM). Beginning with 13a, the initial image has many amalgamated grains. The process continues with 13b, as a Euclidian distance map (EDM) and ultimate eroded points (UEP) are produced. The final stage of this process 13c, shows the resulting image in which the grains that were initially amalgamated are now separated and can be recognized as individual grains by NIH Image. [From the National Institutes of Health (NIH) website http://rsb.info.nih.gov]

Measurements

NIH Image can now make quantitative measurements on the thin sections. For the final preparations prior to making the measurements, the parameters the program will need to measure must be constrained. To do so, several pull-down style menus are accessed from the tool bar, here the operator must specify a size range to be measured which is entered as a minimum and maximum particle size in number of pixels, how the data will be displayed, and finally the user must specify what measurement *NIH Image* should make. For this, I requested measurements of area of particles, length of the perimeters, length of major axis (of a best fitting ellipse), length of minor axis (of a best fitting ellipse), angle of particle orientation measured away from bedding, and number of particles present within the field. Once the measurements are made, *NIH Image* reports the data in a spreadsheet format that can be easily exported to Microsoft *Excel* or *MatLab* for further analysis. Utilizing the quantitative measurements generated by *NIH Image* one can obtain estimates of grain size, grain shape, orientation of grains relative to a bedding plane, and number of grains within a field of view.

To ensure the image analysis techniques were correct and the measurements produced by *NIH Image* were accurate a test case was created using an image of grains with known grain size, length of major and minor axes, orientation of the long axis, and percent composition. These parameters were determined by conventional methods involving taking measurements, point counting, and visual estimation. These measurements were compared with the

results of those produced by *NIH Image*. Although amalgamated grains still produce some amount of inaccuracy, the measurements done by *NIH Image* are sufficiently accurate for grains that are not in extensive contact with each other.

Analysis of Bioturbation

Can the effects of bioturbation be responsible for producing recognizable differences in the microlithofacies contained within the Rogersville Shale? To answer this question the difference between sediment that was bioturbated (i.e. sediment contained within a cross-sectional burrow) was compared to other randomly chosen samples, and finally to samples that were believed to have been bioturbated but not contained within a cross-sectional burrow.

Identifying cross-sectional burrows and characterizing the fabric they contain was the first step in analyzing bioturbation. Cross-sectional burrows were preferentially selected and images of these burrows went through the same process as previously outlined (refer back to Figure 4). Mineral components were identified, grain-size was measured, and percent composition (expressed as a percent of the total area that the mineral covered) were analyzed; this information was compiled and averaged. These characterizations were then compared to observations from the petrographic investigation to see if the amount of organic matter decreased and the amount of quartz increased with varying degrees of bioturbation.

In the final stage of this investigation, the data collected on the burrows was compared to the fabric that was believed to have been affected by biologic activity but was not contained within a cross-sectional burrow. By comparing the three types of fabric samples, I was able to determine if a sample had been affected by biological activity by looking for a distinctive fingerprint. If a sample of the fabric that was believed to have been bioturbated was found to be similar to a sample that is known to have been bioturbated (i.e. the fabric is contained within a cross-sectional burrow) this provides a better indication that the sample had indeed undergone some amount of biological reworking.

Palynologic Investigation

The palynologic portion of this research was conducted by Professor P.K. Strother. He examined the thin section samples as well as samples he collected from the ORNL-Joy2 core in an effort to characterize the acritarch and cryptospore populations. Researching the palynologic populations contained within the ORNL-Joy2 core samples has lead to a determination of where the depositional site was located in relation to the paleoshoreline.

Maceration of the samples collected directly from the ORNL-Joy2 core was necessary to release the paleobotanical material. The samples were processed using a sequence of different acids (HCl, HF, and HNO_3) to dissolve the rock material and leave behind organic material (Strother et al., 2004). Organic material, dissolved rock material, and a supersaturated solution of $ZnCl_2$

are then centrifuged so that the organic residue can be decanted off from the rest

of the liquid. At this stage in the process the palynologic samples were isolated

and mounted onto glass slides using glycerin gel. Others samples to be used for

the scanning electron microscope (SEM) were mounted onto aluminum stubs

that are used in the SEM. These images were scanned using 15 or 20 KeV on

an Amray 1600 SEM at Weston Observatory and the images were captured on

Fuji S1Pro digital camera. From the point of image acquisition, the images were

then edited and converted into greyscale images in *Adobe Photoshop* to ready

them for analysis.

Chapter 3

Results

Characterizing the lithologic microlithofacies of the Rogersville Shale will ultimately help to decipher the palaeoecologic conditions existing in this region during the Middle-to-Late Cambrian. Detailed descriptions of the individual microlithofacies, morphologic forms of glauconite contained within the samples, effects of biologic activity evident from the trace fossils present, and palynomorphs within the Rogersville Shale will be presented in this section. Studies of the petrographic, ichnologic, and palynological aspects of the microlithofacies of the Rogersville Shale help to constrain how and where the sediments were formed.

Microlithofacies Descriptions

The five lithofacies of the Rogersville Shale may be more accurately described as microlithofacies. These microlithofacies exist on a small scale and are only clearly visible in thin section. Five different microlithofacies of the Rogersville Shale were distinguished: a homogenous unlaminated mudstone, laminated mudstone, siltstone, bioclastic siltstone, and a limestone. The descriptions of each microlithofacies follows. Please note individual sample numbers in the text and in the appendix such as 1523 refer to down hole footage.

Microfacies I: Homogenous Unlaminated Mudstone

The first microfacies can be characterized as a homogenous unlaminated mudstone (Figure 14). Grain size is largely in the mud/ clay range and the clay particles appear to be oriented. This mudstone contains a detrital fraction (approximately 17%), which consists of matrix supported, angular to sub-angular white quartz grains ranging from 0.023 mm to 0.17 mm. Red-brown and grey-brown to occasionally very dark brown (this may be due to an increase in organic material and opaque minerals) in color when viewed in thin section, this microfacies can exhibit a wide range of colors. Generally homogenous, the mudstone itself contains no discernable laminations, although several small-scale discontinuous laminations of detrital material are present within this microfacies. These discontinuous laminations usually consist of very fine-grained white quartz grains, white to very pale green and brown platy mica flakes as well as phosphotized (collophane) lingulid shell fragments and glauconitic material. The glauconitic material and shell fragments exhibit parallel alignment. These discontinuous laminations are generally wavy or lenticular and have undulatory surfaces. This microfacies also contains diffusely dispersed amounts of organic material and opaque reduced minerals, such as pyrite and hematite, which appear to have been formed secondarily. This microfacies contains evidence of bioturbation in the form of cross-sectional burrows that are easily identified but are not abundant. These burrows have a higher concentration of densely packed angular to sub-angular white detrital quartz grains than the

surrounding mud and clay material. This higher concentration of quartz grains appears to be due to the removal of the matrix (i.e., the clay) by the burrowing animals and later infilling.
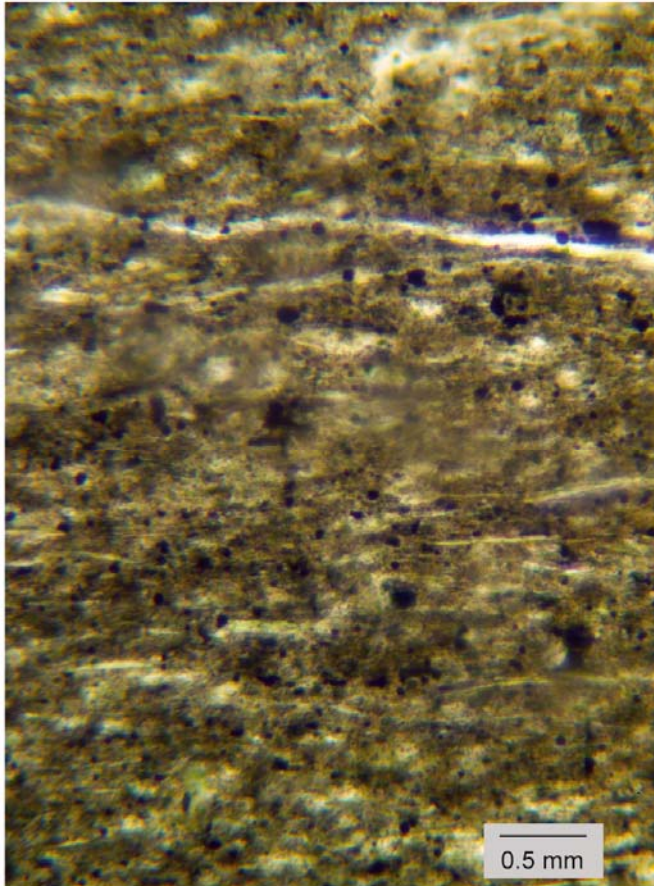
Figure 14. Microfacies I, Homogeneous Unlaminated Mudstone. This photograph is of a portion of sample number ORNL-J2-1523. Defining characteristics of this Microfacies include lack of distinct laminations, oriented clays, and diffusely dispersed pyrite and organic matter.

Table 1: Mode Table for Microfacies I

Microfacies I. Homogenous Unlaminated Mudstone Average	
Grain Type	Modal Grain Size (mm)
Quartz	0.049
Pyrite	0.027

**Note—The clay fraction of Microfacies I was not analyzed for modal grain size.

Microfacies II: Laminated Mudstone

Brown-beige to medium-red-brown in color when viewed in thin section, the mudstone of this microfacies can typically exhibit a variation in the color range (Figure 15). The mudstone within this microfacies is like microfacies I, the homogenous unlaminated mudstone. Grain size is again in the clay range. Microfacies II however, also contains nearly 39% detrital grains, consisting of matrix-supported, sub-round to sub-angular, silt sized white quartz ranging in size from 0.065 mm to 0.34 mm. The clay/mud fraction defines laminations that are more or less continuous. Detrital grains occur as isolated pockets of silt. These silty pockets are wavy to lenticular often having undulatory margins. Clays appear to be drape over and in between these detrital pockets. The matrix of this microfacies is largely composed of the mudstone and minor amounts of a "pseudomatrix" which is clay that was (partially) altered into authigenic glauconite. This glauconite-clay intermediate occurs as a very pale green to nearly clear, clay and glauconite intermediates. The pseudomatrix can also occupy an area that was previously void and/or pore space or a glauconite precursor material. This microfacies will generally contain micro-stylolites and sparry calcite veins as features identifiable in thin section. Some of the sparry calcite veins have been replaced by chert and dolomite. In addition, microfacies II contains diffuse organic matter, phosphatic lingulid shell fragments (collophane), and glauconite, which often exhibit parallel alignment to each other. Microfacies II also contains opaque minerals such as pyrite and lesser amounts

of hematite. Some bioturbation is evident although it is apparent that the effects

of the biological activity were not widespread throughout this Microfacies

because the presence of bioturbation is minimal. Cross-sectional burrows and

other trace fossils can be identified by areas of higher concentrations of densely

packed detrital quartz grains, occurring throughout the mudstone of Microfacies

II. Perhaps the feature that most distinguishes the Microfacies I mudstone from

the Microfacies II mudstone is the significant increase in quartz silt and other

detrital material.

Table 2: Mode Table for Microfacies II

Microfacies II. Laminated Mudstone	
Grain Type	Modal Grain Size (mm)
Quartz	0.185
Glauconite	0.11
Pyrite	0.04

**Note—The clay fraction of Microfacies II was not analyzed for modal grain size.

Figure 15. Microfacies II, Laminated Mudstone. This photograph is of a portion of sample number ORNL-J2-1523. Defining characteristics of this microfacies include a mixture of silt and clay material, laminations defined by the clay material, and diffusely dispersed pyrite and organic matter.

0.5mm

Microfacies III: Siltstone

Microfacies II is commonly interbedded to interlaminated with a (subarkosic) siltstone, microfacies III (Figure 16) (See appendix slides 1504 through 1523 and 1535 through 1602 for examples of interlamination). This siltstone is largely made up of the same angular to sub-angular, white quartz grains as found in the mudstones of microfacies I and II, some chert, and much lesser amounts of clays (50% < than microfacies I, and 25% < than microfacies

II) and feldspar. Most quartz grains in the siltstone range from 0.053 mm to 0.345 mm. In addition to the quartz grains, other less common grains, include feldspar, mica flakes, chert, detrital glauconite (ranging from 0.11 – 1.621 mm), pyrite framboids (ranging in size 0.0391 – 1.42 mm), hematite, sparry calcite, and dolomite rhombs. The detrital grains of this siltstone are surrounded by a clay matrix, which is very similar to the clay/mudstone of microfacies I and II. This microfacies generally appears white to very light beige to sometimes pale brown in thin section with increasing amount of clay contained within the matrix. As percentage of clays increases, from nearly 20% to approximately 40%, the resulting color takes on a more brownish hue overall. Contained within the siltstone are discreet laminations of phosphatic lingulid shell fragments (collophane) and autochthonous glauconite pseudomorphs of the phosphatic shell fragments (Figure 23). The glauconite and shell fragment lamination occur as sub-parallel to parallel laminations. Bedding typically shows fining upward cycles, with the largest silt laid down first, gradually fining upward through the laminations into the mudstone. Occasionally very thin, more continuous, ribbon-like laminations of the mudstone occur throughout the siltstone. Very dark brown to nearly black in appearance, these ribbon-like laminations appear to contain significantly higher concentrations of organic material and opaque minerals than the surrounding sediment. Other bedding features include small scale, mostly discontinuous cross-beds along with several microfaults. Evidence of bioturbation in this microfacies occurs in the form of cross-sectional and

longitudinal burrows. These burrows occur throughout the siltstone, where they

are easily identified as the areas of considerably less clay or muddy material.
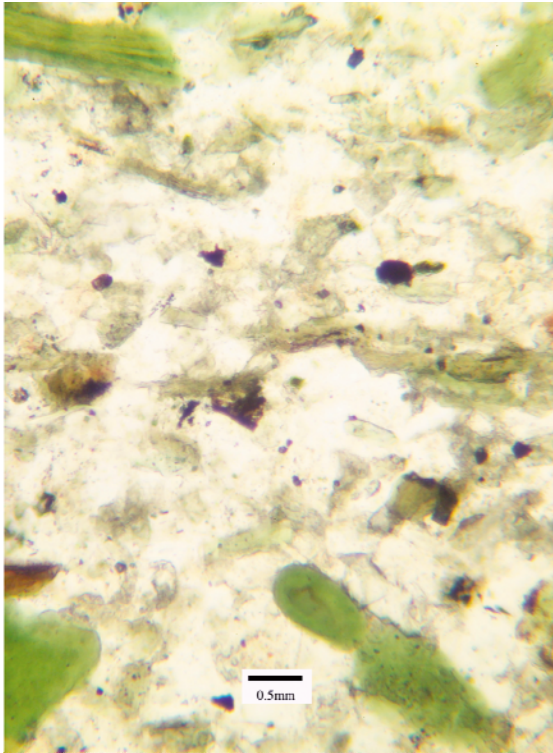
Figure 16. Microlithofacies III, Siltstone. This photograph is of a portion of sample number ORNL-J2-1523. Defining characteristics of this microfacies include a composition of quartz, glauconite, and carbonate grains, the presence of collophane shell fragments, and diffusely dispersed pyrite and organic matter.

Table 3: Mode Table for Microfacies III

Microfacies III. Siltstone	
Grain Type	Modal Grain Size (mm)
Quartz	0.11 and 0.24
Glauconite	0.56
Pyrite	0.07
Shell Fragments	0.18
Carbonate	0.34

** Note—The clay fraction of microfacies III was not analyzed for modal grain

size.

Microfacies IV: Bioclastic Siltstone

Microfacies IV is very similar to the siltstone of microfacies III, although this microfacies contains 4 % more glauconite grains as well as more bioclastic material in the form of phosphatic lingulid shell fragments (Figure 17). Here, lingulid fragments are larger, ranging from 0.21 – 1.57 mm, and can be seen easily with the naked eye. The glauconite grains in this microfacies range from 0.12 to 0.37 mm. The quartz grains are similar in size range to microfacies III. Microfacies IV is consistent with the description of microfacies III with the exception of having a higher concentration of bioclastic material and glauconitic grains.

Table 4: Mode Table for Microfacies IV

Microfacies IV. Bioclastic Siltstone	
Grain Type	Modal Grain Size (mm)
Quartz	0.09
Glauconite	0.21
Pyrite (Framboids)	0.27
Shell Fragments	0.95

** Note—The clay fraction of microfacies IV was not analyzed for modal grain size.
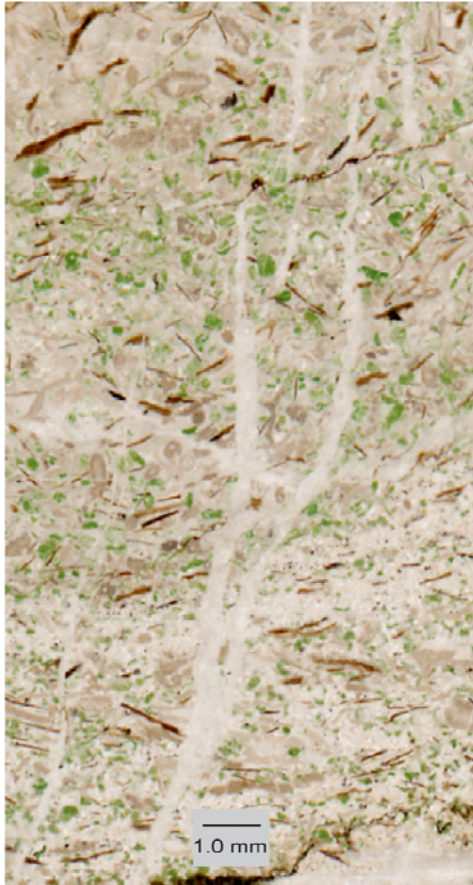
Figure 17. Microfacies IV, Bioclastic Siltstone. This photograph is of a portion of sample number ORNL-J2-1524. The bioclastic siltstone is very similar to the siltstone of microfacies III, with the exception of the amount and size of the collophane shell fragments present. Like microfacies III, this microfacies is composed of quartz, glauconite, and carbonate grains. What distinguishes this microfacies from the other siltstone is the significant increase in the amount and size of the shell fragments present. The phosphatic shell fragments are thought to be *lingulellids*.

Microfacies V: Carbonate (Craig Limestone)

Microfacies V occurs exclusively within the top several meters of the Rogersville Shale as an informal subunit, the Craig member limestone (Figure 18). Aside from the Craig limestone, no other appreciable amounts of carbonate occur within the Rogersville Shale. Off white to buff in color, the carbonate unit occurs as ooids, sparry calcite and tiny rhombs of dolomite. A horizon of carbonate ooids exists within this Microfacies, located on slide number ORNL-Joy2 1486 (Figure 18). The ooids range in size from 0.939 to 1.2992 mm. This Microfacies also contains lesser amounts of clay, organic material, shell

fragments, glauconite and chert. This microfacies represents the transition from the clastic Rogersville Shale to the overlying carbonate Maryville Limestone and the shifting of depositional environments.
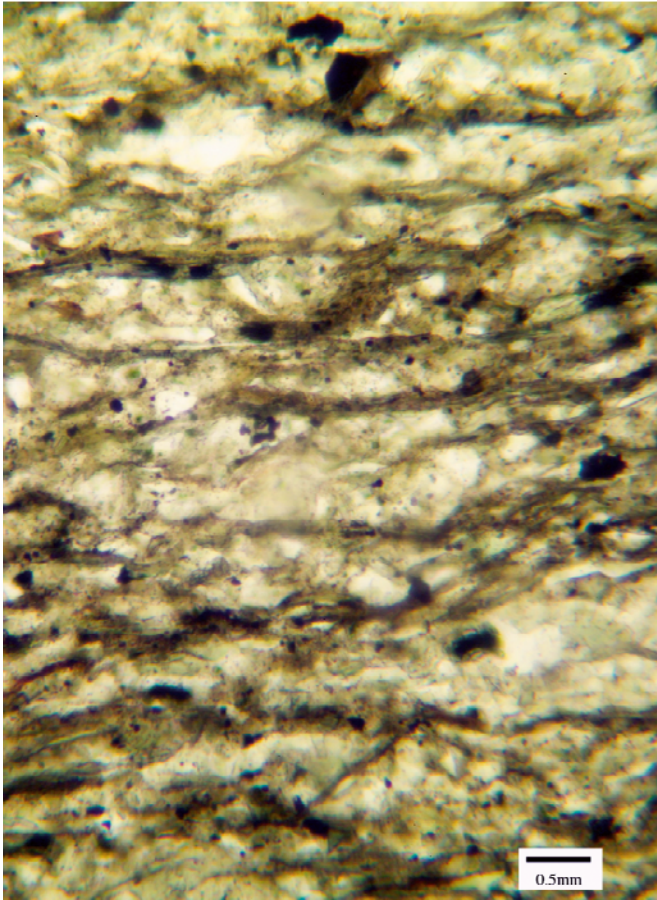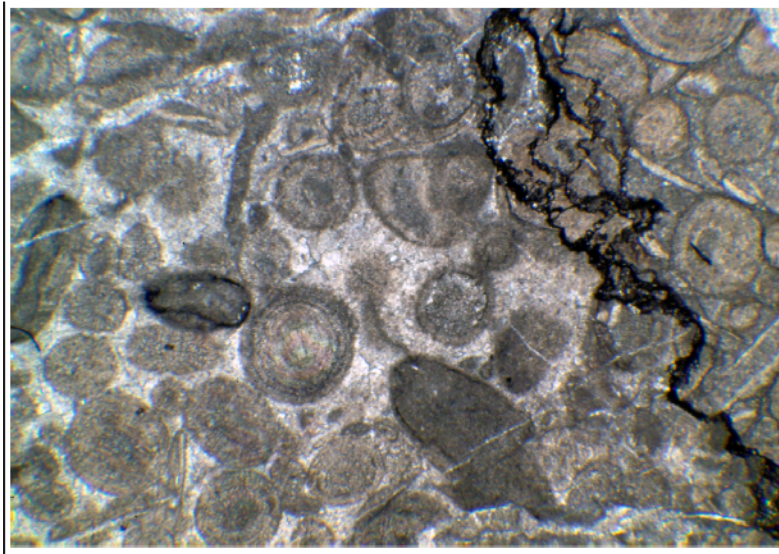

Figure 18. Microfacies V, Carbonate (Craig Limestone). This photograph is of a portion of sample number ORNL-J2-1486. Defining characteristics of this microfacies include ooids.

1.0 mm

Table 5: Mode Table for Microfacies V

Microfacies V. Craig Limestone Member	
Grain Type	Modal Grain Size (mm)
Ooid	0.55

Summary & Discussion

When the ORNL-Joy2 core is viewed macroscopically, slight color variations are visible. These color variations represent the difference between the darker clay-rich layers and the lighter silt-rich layers. Aside from these color variations, most other details are not recognizable at this scale. Not until the thin

sections are viewed microscopically do the fine details of the five microlithofacies become apparent.

Although no formal analysis was done to determine if the five microlithofacies occur in non-random order no patterns are evident at this point. Microfacies thickness can range from approximately less than 1 mm to just over 3 cm. With the exception of the three thin sections (ORNL-J2-1484, ORNL-J2-1486 & ORNL-J2-1524), the rest of the thin sections contain more than one microlithofacies per slide (See appendix slides 1490.5 – 1523 and 1535 – 1602). Table 6 shows what microlithofacies are present per slide (See Table 6). With the exception of the Craig member (Microfacies V) the four other microlithofacies are found closely interlaminated. They vary vertically on a very small scale that is not evident at the macroscopic level. Horizontally most laminations are continuous across the thin section although some discontinuous laminations due occur. The nature of these samples do not lend themselves to determine if the microlithofacies vary laterally beyond the edges of the thin section.

Table 6: Microfacies per Down-hole Footage

Down-hole Footage	Microfacies I	Microfacies II	Microfacies III	Microfacies IV	Microfacies V
1484					X
1486					X
1490.5	X	X			
1496.5	X	X			
1504	X	X	X		
1512.5	X	X	X		
1519.5	X	X	X		
1523	X	X	X		
1524.5				X	
1535	X	X	X		
1541	X	X	X		
1549	X	X	X	X	
1550	X	X	X	X	
1558	X	X	X		
1563	X	X	X		
1572.5	X	X	X		
1581	X	X	X		
1586	X	X	X		
1594	X	X	X		
1599.5	X	X	X		
1602	X	X	X		

The five microlithofacies of the Rogersville Shale exhibit several major

similarities and some important differences. Overall mineral composition is a

good example of a major similarity. Certain minerals are common to all five

microlithofacies although in different proportions; these include quartz,

glauconite, mud-clay, organic matter, chert, pyrite, hematite, collophane, calcite

and dolomite. The more silty microlithofacies are largely composed of the silt-

sized quartz grains (i.e.—the siltstone microfacies III and IV) in contrast to the

higher mud-clay matrix in microfacies I and II. While the mudstone microfacies

are composed mostly of mud and clay material, they also contain smaller amount

of the silt common to microfacies III or IV, though finer. Although the same

minerals occur through the formation, the ratios in which they occur vary widely.

Table 7: Percent Composition for Microlithofacies I through IV

Microfacies	Average % Glauconite	Average % Mud-Clay	Average %Qtz. & Carbonate	Total
I. Homogenous Unlaminated Mudstone	10.7	69.7	17.7	98.1
II. Laminated Mudstone	15	44.8	38.5	98.3
III. Siltstone	23.7	19.4	56.7	99.8
IV. Bioclastic Siltstone	27.5	8.5	63.6	99.6

Glauconite Content

Glauconite is common throughout the Rogersville Shale, however the

percentage of glauconite varies between the microlithofacies although not a great

deal despite significant differences in the silt-clay ratio. For example the

siltstones of microfacies III and IV contain greater proportions of glauconite with

the bioclastic siltstone containing 27.5% (on average) and the siltstone of

microfacies III containing slightly less with 23.7% (on average). Microfacies II

mudstone contains 15% (on average) glauconite and the mudstone of

microfacies I contains 10.7% (on average). The occurrence of glauconite grains

within the carbonate microfacies (microfacies V) is rare and was therefore not

measured. While the percentage of glauconite ranges from 10.7% to 27.5% within the four microlithofacies, the ratio between the silt and clay fractions vary greatly. This is one indicator that glauconite appears to be ubiquitous throughout the Rogersville Shale, i.e., independent of depositional region.

Degree of Bioturbation

Differences arise between the five microlithofacies when the degree of bioturbation is compared. The mudstone of microfacies I exhibits the least bioturbation of all the microlithofacies, it is generally homogeneous and distinct trace fossils are also rare. Microfacies II contains nearly 21% more detrital quartz than microfacies I. This may indicate an increase in the degree of bioturbation. The organisms responsible for producing these trace fossils were likely seeking the organic matter that makes up a large part of the mud-clay matrix (as a food source) and leave behind residual silt. It is reasonable to believe that the decrease in organic material is linked to an increase in bioturbation that can be seen in these microlithofacies. This conclusion also holds true if one examines the microfacies IV. This microfacies exhibits the highest degree of bioturbation and contains the least amount of the mud-clay matrix.

On a larger scale, it appears that there is an inverse relationship between the amount of mud-clay matrix and amount of glauconite present. For example microfacies I contains 69% mud-clay material and 10% glauconite. Whereas

microfacies IV contains 8.5% mud-clay material and 27% glauconite. Also there appears to be a positive correlation between glauconite and bioturbation. For example, microfacies IV contains the most glauconite (27%) and has the most observed evidence of bioturbation. The conditions creating the chemical environment necessary for autochthonous glauconite formation are not found in the homogenous unlaminated mudstone, whereas these conditions abound in the bioclastic siltstone.

Microfacies I contains the least amount of glauconite (8.5%) and very low degree of bioturbation but, has the highest concentration of the mud-clay matrix (69%). Because high concentrations of the mud-clay matrix exist within microfacies I and there is little evidence of bioturbation, one can assume these conditions were not as highly favorable for glauconite formation.   Because bioturbation is nearly absent, the micro-reducing environment necessary for autochthonous glauconite formation was not produced. Conversely the bioclastic siltstone contains the highest degree of bioturbation and consequently the least amount of mud-clay matrix material and the highest concentration of glauconite making it the ideal environment for the formation of glauconite.

Glauconitic Minerals in the Rogersville Shale
Both authigenic and allogenic morphologic forms of glauconite are present within the Rogersville Shale. Authigenic glauconite forms include glauconite/clay intermediates, replacement of shell fragments and detrital grains, and some

vermiform or zebra grains. Allogenic glauconite forms include pelloidal, platy, and potentially some vermiform or zebra grains. All the aforementioned morphologic types of glauconite will be described in detail later in this chapter.

Grain morphology is thought to be an indicator of the physical and chemical history of glauconite grains (Warshaw (1957); Ellmann et al. (1963); Triplehorn (1966)).   Warshaw (1957) suggested that there is an apparent connection between physical appearance, degree of crystalline order (internal structure), extent of mixed layering in clays, and occurrence of glauconite. Ellmann et al. (1963) determined that it was likely that observations based on the physical appearance of glauconite may provide information similar to that obtained by more complex physical and chemical measurements. Triplehorn (1966) recognized the potential of different glauconite forms being useful for stratigraphic correlation and environmental determination.

I applied these ideas to the glauconite grains within the Rogersville Shale to differentiate whether they were formed authigenically or allogenically.   In addition, differences in the physical and chemical properties exhibited by glauconite grains provided clues about the palaeoenvironmental conditions that prevailed during the deposition of the Rogersville Shale.

Morphologic Forms of Glauconite

    Pelloidal

    Spheroidal or ovoidal glauconitized pelloids are generally larger (on the order of medium to coarse sand) than the surrounding quartz or clay matrix. Glauconitic pelloids are common in the Rogersville Shale, but are most prevalent in the siltstone and bioclastic siltstone Microfacies. Pelloids can be whole or occur as broken fragments. Broken pelloidal fragments may be evidence of grain transport. Most pelloids appear to have a randomly oriented internal structure (Figure 19). Pelloids are found both as constituents of the burrow fill within the mudstone and as larger component within the siltstone and the bioclastic siltstone (Figure 17). A likely precursor for these glauconite grains is that of fecal pellets of the organisms that produced the burrows. The burrows these grains are contained within almost certainly would have provided the locally reducing microenvironment necessary for glauconite formation. Remnants of the organic material, algal cysts and cryptospores these organisms sought can still be seen within some of the pelloids (Figure 19). Within the pellet, it appears that the clay or fecal material has undergone the glauconitization process, leaving some refractory organic matter unchanged. Due to the shape of these pellets it is clear to see that they would be easily transported.
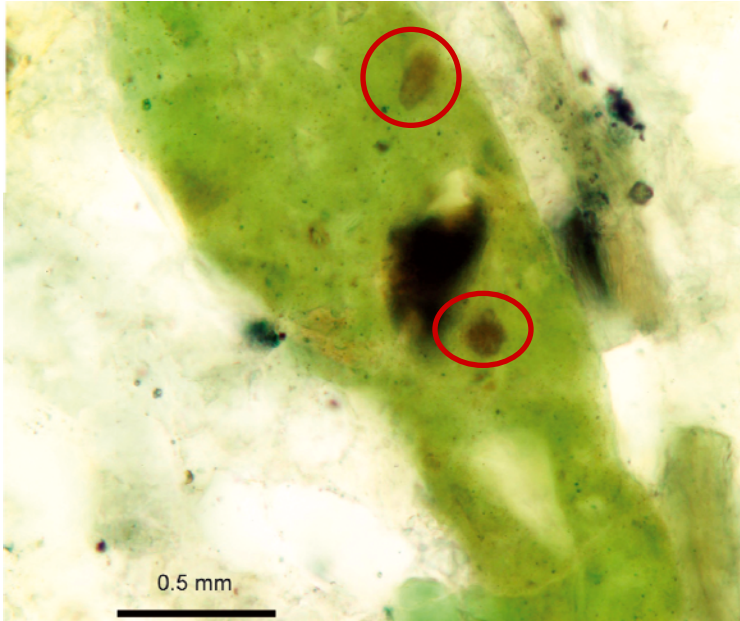
Figure 19. Pelloidal glauconite. This photograph depicts a pelloidal glauconite grain. This grain was likely a fecal pellet prior to undergoing the glauconitization process. This grain is quite unique in that is still contains preserved organic matter and cryptospores. Sample Number ORNL-J2-1523.

Clay / Glauconite Intermediates

An intermediate form of glauconite within the Rogersville Shale has a structure that is transitional between glauconite and its clay precursor (Figure 20). The clastic grains within the siltstones of Microfacies III and IV are surrounded by mud/clay mixtures. Clays in this matrix may partially undergo the glauconitization process. The clay-glauconite intermediates are generally barely green to very pale green. Incomplete glauconitization of the clay matrix seems to indicate that physical and/or chemical conditions may have changed or shifted during early phases of the glauconitization process.   Due to the nature of these grains, the glauconite-clay intermediates were interpreted to have formed in place. Thus, they are autochthonous.
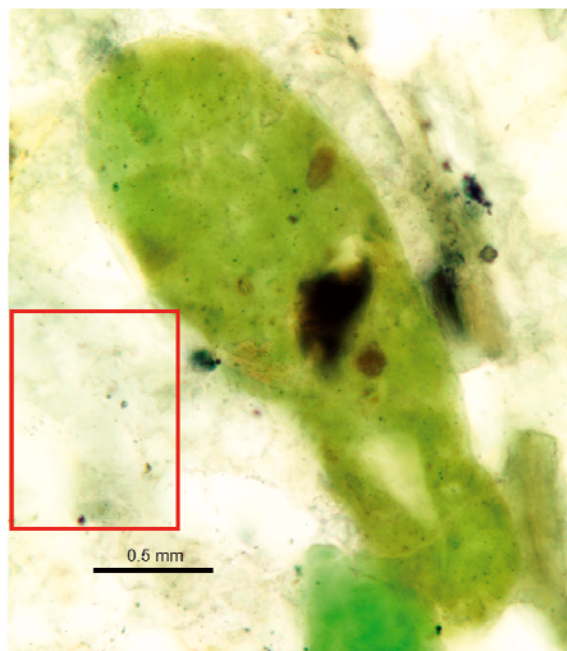
Figure 20. Clay-Glauconite Intermediate. Contained within the box on the left side of the photograph is an example of the clay-glauconite intermediate morphologic form. This form of glauconite generally occurs in between detrital grains and is very pale green in color. Sample Number ORNL-J2-1523

Platy Grains

These grains have a length that far exceeds their thickness and internal layering, most closely resembling pages of a book (Figure 21). The book-like appearance of these grains can be attributed to cleavage planes on precursor micas or thin clay lamina. Platy grains are generally found as a constituent of the siltstone and the bioclastic siltstone of Microfacies III and IV, but also occur (in lesser amounts) within the mudstones of Microfacies I and II. Although their form sometimes appears somewhat delicate, some of these grains appear to have been transported.
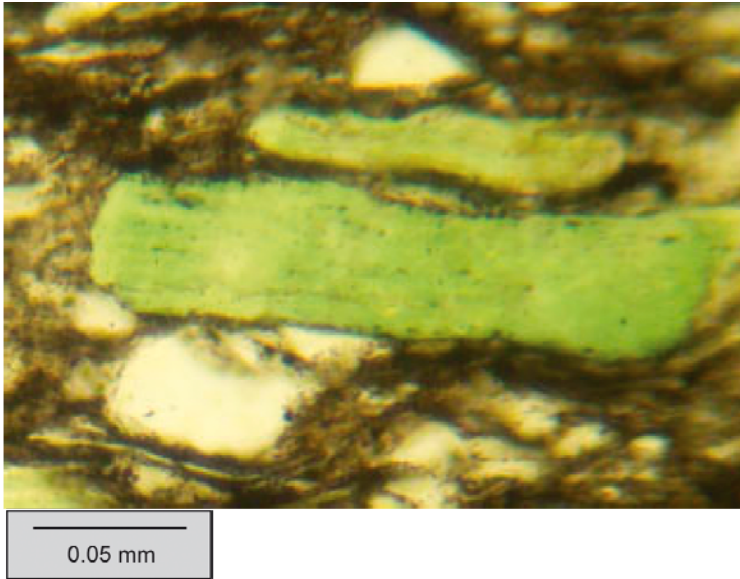
Figure 21. Platy Glauconite. This glauconite grain has a length that far exceeds the thickness, which is characteristic of all platy grains. Sample Number ORNL-J2-1549.

0.05 mm

Vermiform or Zebra Grains

These grains have "zebra-like" stripes, especially when viewed under cross-nicols (Figure 22). Galliher (1935) saw this morphologic form of glauconite as evidence of direct derivation from a micaceous parent material, more specifically biotite. Zebra-like grains alternate layers of ordered internally structured glauconite with unordered (random) internally structured glauconite (Burst 1958b). This appearance may be related to the micaceous cleavage planes which are now perpendicular to the longest axis of the grains (Triplehorn, 1966). Not only does the mica flake appear to gradually transform into (ordered internal structure) glauconite, but glauconite seems to form (with random or unordered internal structure) in between the sheets (Triplehorn, 1966). The zebra grains generally exhibit a slight curvature of the long axis; some grains appear almost crescent-shaped. Triplehorn (1966) suggested that these grains

form in place because the micaceous structure of the grains is not known to be

suitable for transport. Since whole zebra-like grains are quite common in the

siltstones of Rogersville Shale, this may be evidence that glaucony was forming

quite locally during sediment accumulation. Broken fragments of zebra-like

grains also exist within the Rogersville Shale, which may also suggests some

degree of transport was involved subsequent to glaucony formation (Figure 22).

Figure 22. Vermiform or Zebra Grains. These grains have the characteristic appearance of having zebra-like stripes. This characteristic is especially apparent when viewed under cross-nicols. Another feature common to this type of grain is a slight curvature to the long axis of the grain. This feature is apparent on the grain on the left. Sample Number ORNL-J2-1549.
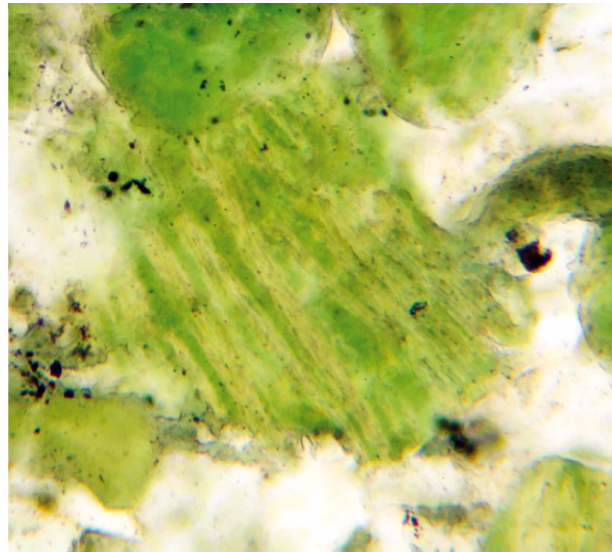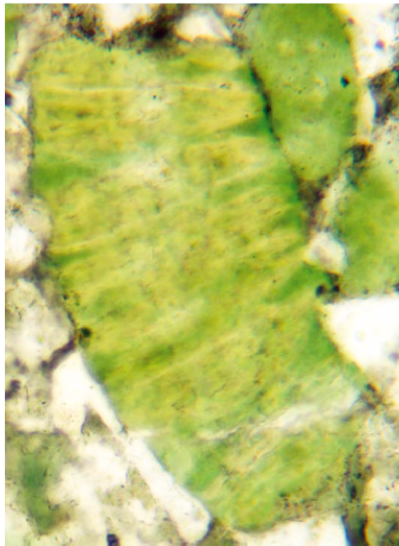
0.05 mm

Same scale for both images.

Replacement of Shell Fragments and Detrital Grains

Authigenic replacement of organic material, shell fragments (Figure 23) and other detrital grains is another morphologic form for the glauconitic material contained within the Rogersville Shale. Replacement of the original or parent material by glauconite seems to be a reasonably common occurrence in the Rogersville Shale, as it is one of the more prevalent morphologic forms for glauconite to take. Replacement of a parent material is generally easily determined by simply looking at grain in question. For example shell fragments have a characteristic elongate or platy appearance. Shell fragments also have a unique texture. Glauconitic material takes the form of the parent material such as the phosphatic shells that it replaces (Figure 23). The glauconite in Figure 23 has replaced the phosphatic shell material. The original texture of the shell is preserved in the glauconite.
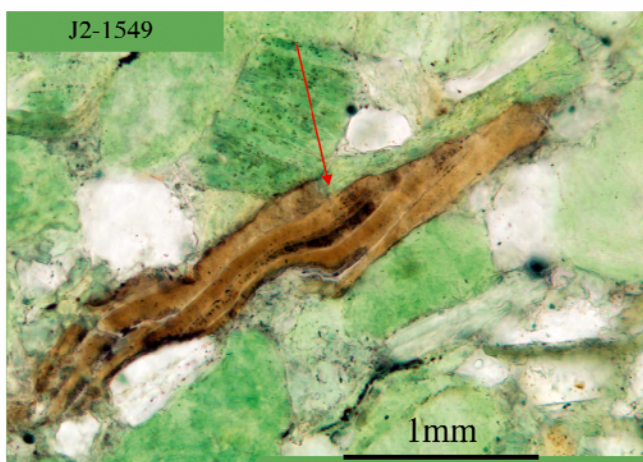
Figure 23. Replacement of a collophane shell fragment. The arrowhead in this photograph shows the point where the shell fragment changes in glauconitic material. The glauconite has retained the morphologic form of the shell fragment that it has replaced. This is an example of authigenic glaucony. Sample Number ORNL-J2-1549.

Location and Distribution of Glauconite Grains

The occurrence of glauconite appears to be ubiquitous throughout the siltstone and the bioclastic siltstone microfacies of the Rogersville Shale. Glauconite is present, but far less prevalent, in the homogenous unlaminated mudstone, the laminated mudstones microlithofacies and the Craig Limestone Member. However, unequal distribution of glauconite among the different microlithofacies may be evidence of a thorough reworking of the siltstone and bioclastic siltstone Microfacies due to biological activity, whereas the mudstones of Microfacies I and II may be areas that have experienced lesser to no biological reworking. The clay/mud material was likely removed or consumed during the processes associated with bioturbation in Microfacies III and IV. Because glauconite is more prevalent in the siltstone and bioclastic siltstone microfacies, there may be a connection between biologic activity and conditions favorable for glauconite formation or accumulation. A less likely possibility to explain the variable glauconite distributions would be geochemical/ geologic conditions that may have alternated between being favorable or not favorable for glauconite formation throughout the duration of deposition of the Rogersville Shale. This would suggest that geochemical conditions or sedimentation regions that prevailed during the deposition of fine particulate matter were significantly different from those during deposition of the larger clasts, but the microfacies scale of this variation would make this less likely. Graph 1 show the vertical distribution of glauconite throughout the ORNL-Joy2 and thin section samples.

Graph 1. The percent of glauconite per slide vs. down hole footage (slide#).

Percentage Glauconite
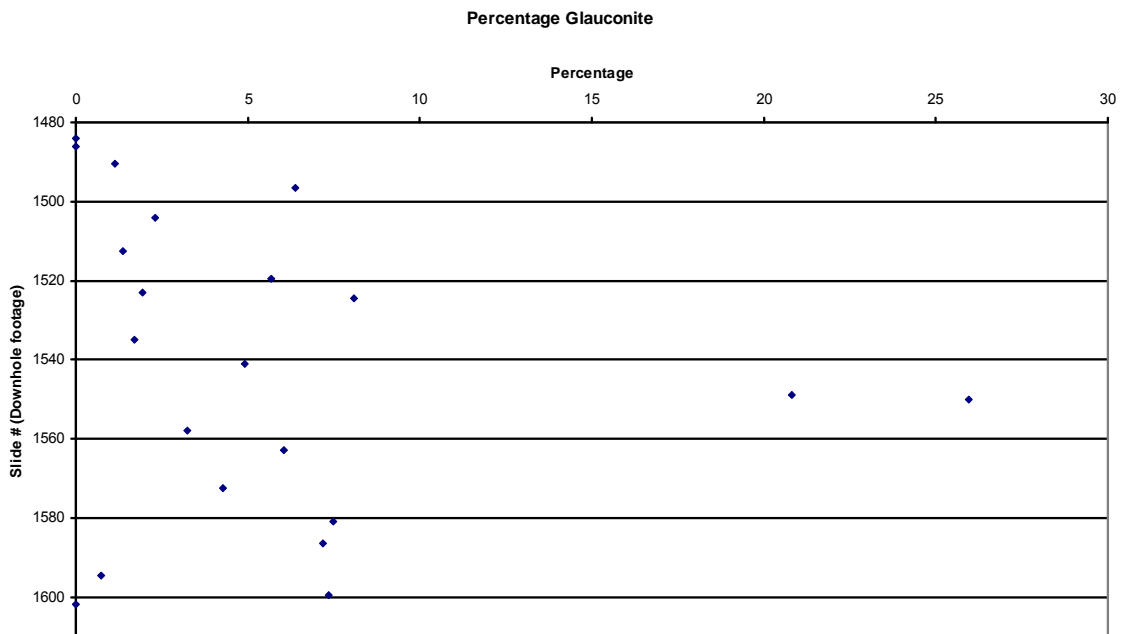
Summary & Discussion

In early work, glauconite was seen as a deep marine indicator associated

with distal shelf and slope deposits. Glauconite occurs in many different kinds of

sedimentary facies not associated with distal shelf/ slope deposits, but, because

of this assumption made early on, it was generally considered allochthonous

when found elsewhere (Figure 24).   Many researchers (Figure 7) are now

questioning this classic view (Chafetz 1978; Chafetz & Reid 2000; Baldwin et al.

2004; el Albani et al. 2005; Rose 2003).   More recent studies still attribute

glauconite to a marine origin, although there appears to be a significant landward

shift in the environment for glauconite formation, most notably during the

Cambrian and Ordovician.
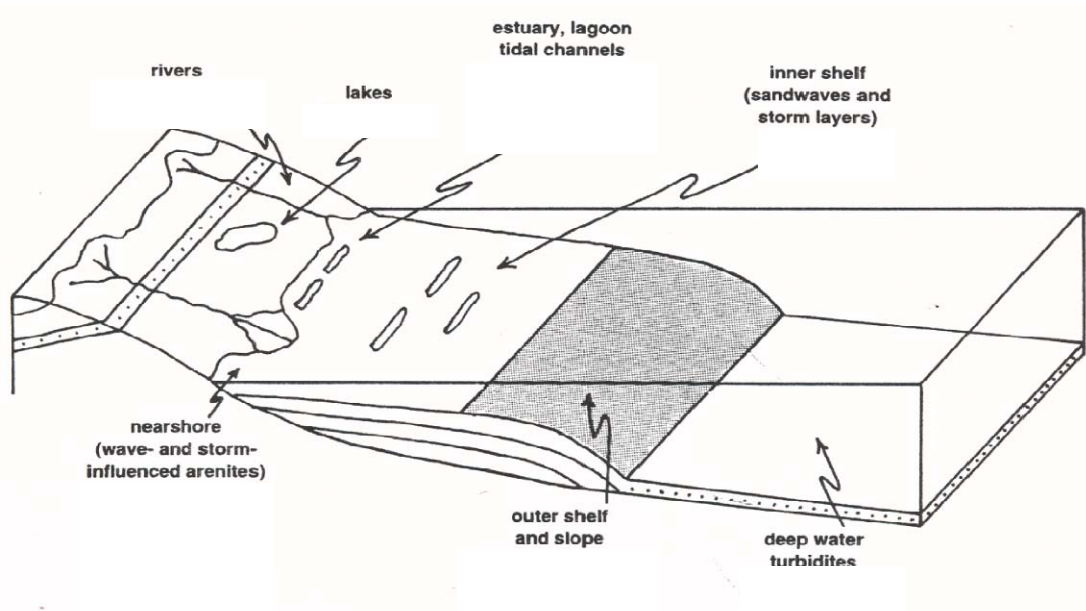
Figure 24. This cross-sectional diagram shows the different environments in which glauconitic materials have been found. The grey area represents where autochthonous glauconite was classically thought to have been capable of formation. Under that assumption, glauconite found elsewhere was thought to be allochthonous. Recent studies of glauconite have found this mineral capable of forming in a wide range of depositional environments. [Amorosi, 1997, page 136]

Evidence of glauconitic minerals forming in shallow water has emerged

from different localities spanning several different time periods (Figure 7).   The

Middle Cambrian margins of Laurentia have produced shallow water glauconite

deposits, two of which will be discussed here the Bright Angel Shale of the

eastern Grand Canyon region (Rose (2003); Baldwin et al. (2004)), and the

Rogersville Shale of eastern Tennessee. New geochemical, mineralogical, and

paleontological evidence has shown that the Bright Angel Shale formed in a restricted estuarine environment (Rose (2003); Baldwin et al. (2004)), rather than the open marine environment previously suggested by McKee & Resser (1945) and Martin (1985). Based on similar sedimentologic and paleontological aspects, the Rogersville Shale of eastern Tennessee is believed to have had a shallow estuarine or lagoonal environment for deposition as well.

Evidence of Cambrian Shallow Water Glauconite

Chafetz (1978) provides evidence of shallow water glauconite deposition in a tidal inlet and associated lagoon in the Cambrian Riley Formation of central Texas. He found both autochthonous and allochthonous glauconite deposited as part of transgressive-regressive shifts in the location of the environment of deposition.

Chafetz & Reid (2000) revisited the Cambrian-Ordovician glauconitic formations of central Texas, reviewing the Moore Hollow Group containing the previously examined Riley Formation and the Ordovician Wilberns Formation. The upper part of the Riley Formation accumulated as part of the lateral migration of a tidal inlet complex associated with a barrier bar / lagoonal system. They suggested that the Wilberns Formation was deposited in an environment that was very shallow, subtidal to intertidal water depths (Chafetz & Reid, 2000). Chafetz & Reid (2000) also studied the glauconite containing Cambrian Bliss

Formation of southwestern New Mexico, which formed under very shallow-water to tidal flat conditions.

El Albani et al. (2005) reported a Lower Cretaceous glauconite-containing formation resulting from a shallow lagoon and brackish water estuary from the Aquitaine Basin in southwestern France. They found evidence of autochthonous glauconite forming in two distinct shallow water environments: (1) An argillaceous dolomitic sediment from a saline shallow lagoon, and (2) a marl-limestone alternation deposited in a brackish water estuary. In addition to the alternating lithologies, there is the rare occurrence of ripples and other high energy sedimentary structures in this formation and marcasite crystals in the carbonate matrix. This team also found fossils typically of eurhaline and freshwater environments, with little to no other fossils present.

Rose (2003) and Baldwin et al. (2004) investigated the Bright Angle Shale (BAS) of the eastern Grand Canyon. The BAS contains lithologies and pelloidal glauconite which are similar to those of the Rogersville Shale. The BAS was also found to have a minimal marine influence due to the lack acritarchs found within the sediment. The abundance of cryptospores suggests a freshwater environment of formation. This idea is further supported by the lack of fossils except for the rare *Linguella* which is generally viewed as a brackish water indicator.

The glauconite within the Rogersville Shale is consistent with other shallow water glauconite deposits of the Middle to Late Cambrian and

Cretaceous (Chafetz 1978; Chafetz & Reid 2000; El Albani et al. 2005; Rose 2003; Baldwin et al. 2004). The presence of glauconite indicates that the environment in which it formed would have been slightly reducing in an overall well oxygenated environment. The most likely scenario involves the formation of glauconite just under the surface of the substrate or inside of the burrows. These locations would have been ideal for creating the micro-reducing conditions necessary for glauconite formation. Glauconite found to have formed authigenically within the Rogersville Shale (Figure 23) would indicate the environment would have been mildly reducing (within a micro-reducing environment) in an overall well oxygenated environment. In addition, the sediment the glauconitic material is contained within, and its degrees of bioturbation, is consistent with other shallow water deposits such as lagoons and estuaries.

Ichnology

The Rogersville Shale was found to contain abundant and diverse trace fossils. The degree of bioturbation within the Rogersville Shale has helped to characterize the five microlithofacies. Six different types of trace fossils were found to exist within the Rogersville Shale. The abundance and diversity of trace fossils within the Rogersville Shale described by this study is in stark contrast to Walker et al. (1990) who claimed there was a lack of bioturbation within the Rogersville Shale.

Degree of bioturbation

     Several degrees of bioturbation have been found in the microlithofacies of the Rogersville Shale. Intact primary laminations indicate little to no bioturbation (Figure 25). Mixed fabrics preserve both primary laminations and bioturbated laminae (Figure 26). Others are heavily bioturbated (Figure 27), or completely reworked.

Figure 25. Preservation of Primary Laminations. Because the primary laminations of this fabric are clearly visible and well preserved there is little evidence of trace fossils. The effects of burrowing organisms are slight, and therefore the degree of bioturbation is low. Other interesting features in this slide include several surface burrows (circled in red) and fining upward sequences. Sample Number ORNL-J2-1586.

Primary Laminations

Burrows

5.0 mm
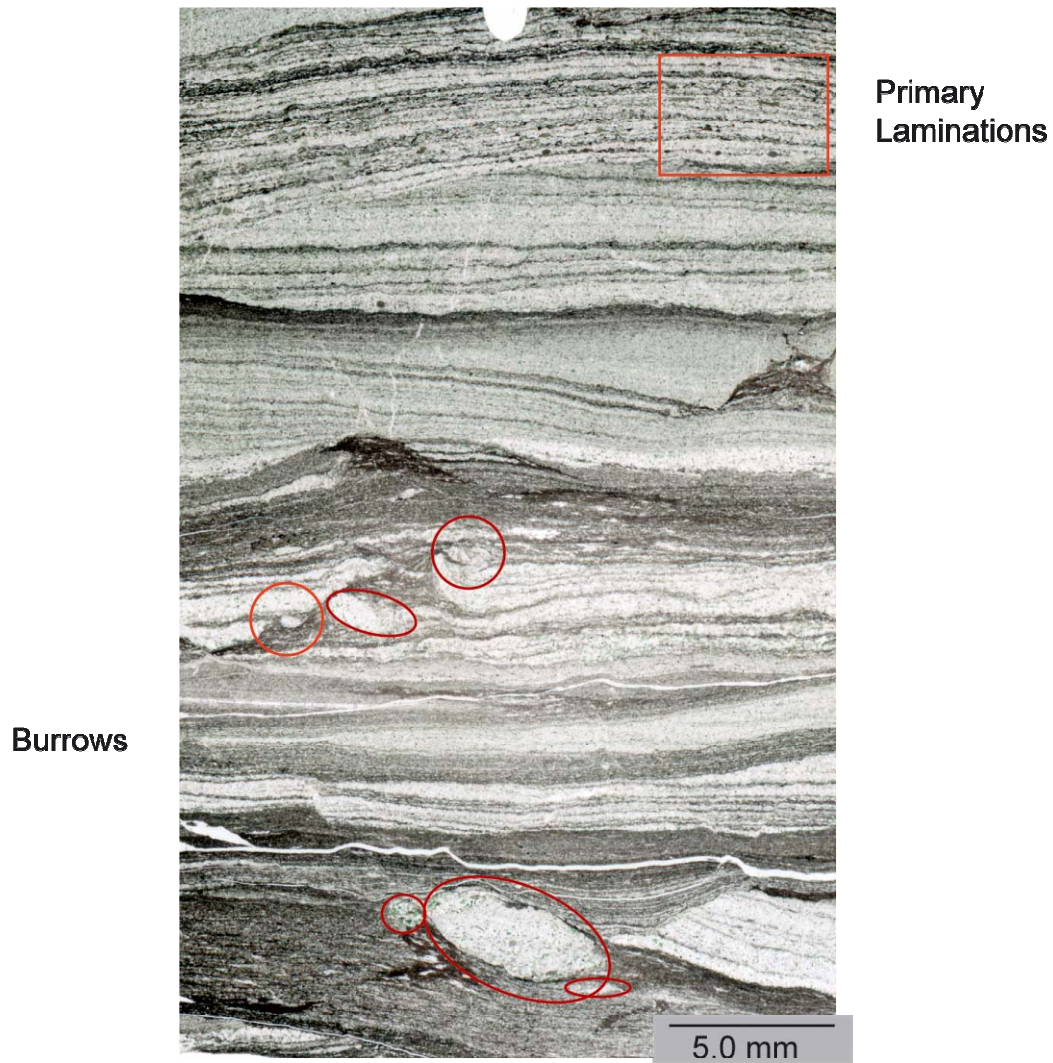
Figure 26. Mixed Fabrics. This photograph depicts an intermediate degree of bioturbation. This sample contains both primary laminations and burrows (circled in red). Sample Number ORNL-J2-1504.

Figure 27. Heavily Bioturbated Fabric. This fabric is characteristic of heavily bioturbated sediment with many preserved burrows and no visible primary laminations. The fabric appears to be nearly completely reworked. Sample Number ORNL-J2-1602.

5.0 mm

The degree of bioturbation preserved within the samples of the Rogersville Shale is a measure of several interrelated factors, such as how prolific the burrowing organisms were, the availability of food, the availability of oxygen and finally the sedimentation and burial rate.

Types of preserved trace fossils

Distinct trace fossils preserved within the thin section samples of the Rogersville Shale include several different types of burrows such as, surface traces, shallow surface burrows, below substrate circular-shaped tubes, evidence of subsurface mining, escape/vertical burrows and "cryptic" burrows. These burrow forms are distinct from one another, and their individual characteristics are discussed below.

Surface traces

Surface traces occur as a small generally semicircular or "U" -shaped depression in an unlithified or unconsolidated substrate or laminae comparable to the clay/mudstones of microlithofacies I and II (Figure 28). These types of traces were most likely produced as burrowing animals made their way through a soupy surface substrate. Quartz silt, (like that of Microfacies III and IV) was subsequently deposited on top of the substrate, filling and preserving the surface trace.
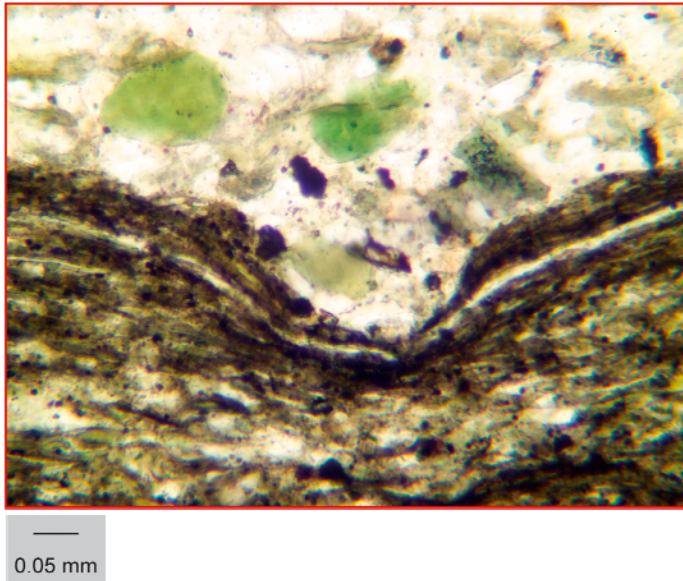
Figure 28. Surface Trace Fossil. This photograph depicts a cross section of a surface trace fossil within the darker mudstone (Microfacies II) and preserved by the lighter colored siltstone (Microfacies III). The burrow is semicircular. This type of burrow is produced by organisms moving through a soupy nonconsolidated substrate.

0.05 mm

Shallow surface burrows

These traces occur as cross-sectional and longitudinal burrows that would have been located (at the time of deposition) within the substrate just below surface (Figure 29). These burrows are generally so shallow that they are barely covered by sediment of the lamina that they are contained within. Depending on how well the traces are preserved within the thin section, some of the burrows retain their roughly circular shape and others become lens-shaped due to subsequent compaction. These burrows generally occur in the mudstones of Microfacies I and II. They contain detrital material similar to the siltstones of Microfacies III and IV, as infillings that are largely free of clay and mud material.
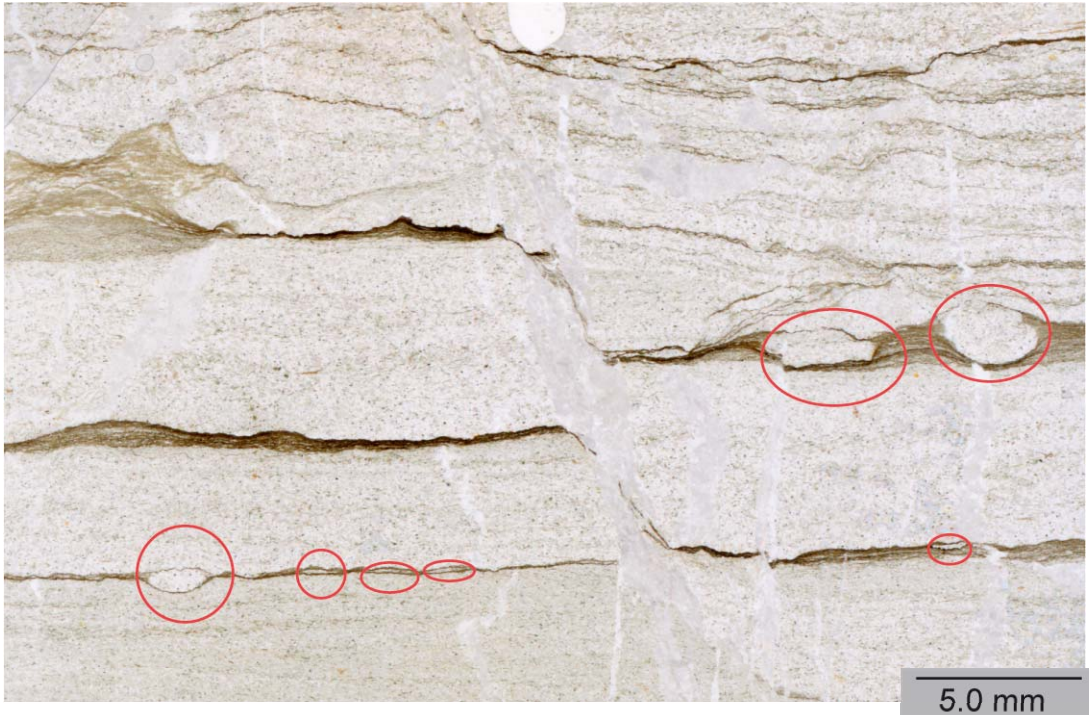
Figure 29. Shallow Surface Trace Fossil. This photograph contains several well preserved examples of shallow surface burrows. The easily identifiable cross sectional burrows are within a mudstone (Microfacies I). Some of the burrows appear to be so shallow that several are barely covered by overlying sediment. Sample Number ORNL-J2-1490.

Below substrate, "Circular" tubes

Burrows that occur in this form are easily identifiable in thin section. They occur as roughly circular cross-sectional burrows, which exhibit a wide range of sizes (Figure 30). The burrows are again contained within the mudstones of microlithofacies I and II, and contain quartz silt like that of Microfacies III and IV, with virtually no clay or mud material as burrow fill. Some of the burrows have taken a more elongate shape, which is likely due to compaction over time, with their shape resembling an eye.
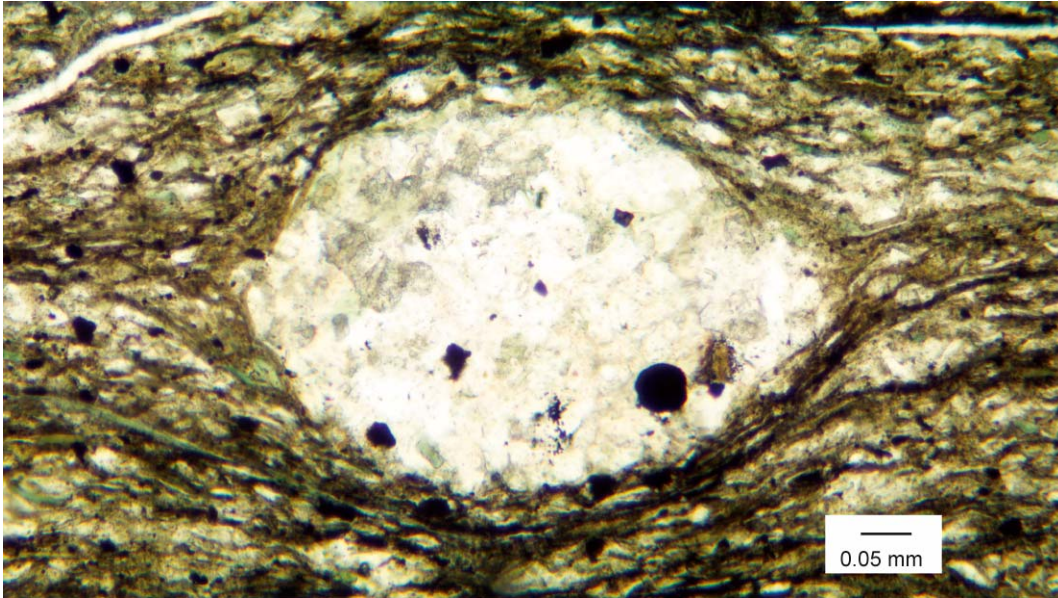
Figure 30. Below Substrate Circular Tubes. This trace is most easily identified as a burrow due to its characteristic shape. This type of burrow occurs in a wide range of sizes. Some burrows have a slightly more elongate shape which may be due to compaction over time. The below substrate circular burrow occur within Microfacies I or II, the mudstones and contain siltstones like Microfacies III and IV as burrow fill. Sample Number ORNL-J2-1523.

Evidence of subsurface mining

Evidence of subsurface mining is present but not abundant within the samples of the Rogersville Shale. Only two such examples were found in thin section, ORNL-Joy2 1496 (Figure 31) and ORNL-Joy2 1541. The shape of these traces is unique. Unlike the other burrows, this trace is more spread out. They are not contained within lamina as they generally occur in massive sediment. These trace fossils are seen within the homogenous unlaminated mudstone (Microfacies I). Another characteristic that distinguishes these traces from other burrows within the Rogersville Shale is that the burrow fill material has a fair to

considerable amount of clay or mud material still contained within it. This may be

a sign of incomplete bioturbation.
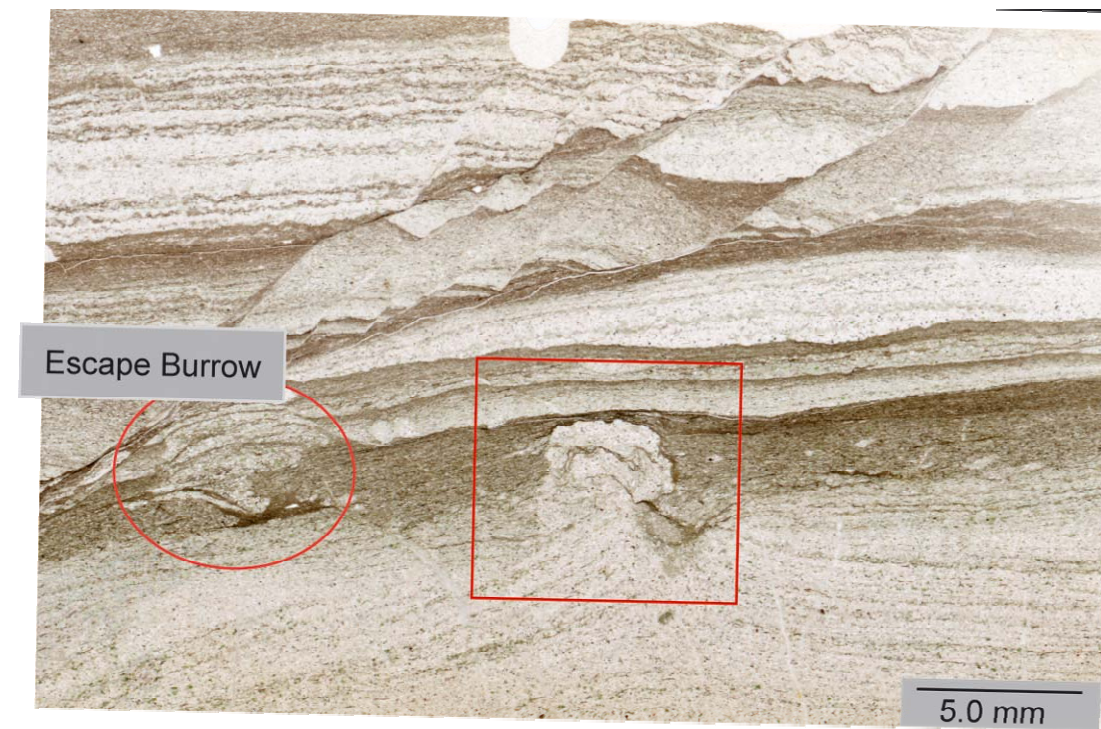
Figure 31. Evidence of Subsurface Mining. This type of trace is unique with only two such examples within the Rogersville Shale. The Shape of this trace is different in that it is very spread out compared to other burrow shapes. This burrow occurs in Microfacies I. An additional interesting feature on this slide is an escape burrow. Sample Number ORNL-J2-1496.

Escape / Vertical disruptions

A feature unique to the escape burrow is their vertical nature (Figure 32),

the other burrows contained within the Rogersville Shale are almost strictly

narrow and horizontal (Figure 28, Figure 29, Figure 30, Figure 31). While the

burrows are not completely vertical, at some point they cease being flat-lying and

the organism that created the burrow appeared to have moved upward. This

may ultimately be an indication of the chemistry in the area of the vertical

disruption. If sediment was continually being deposited, the zone where the

animals lived would also be continually moving upward. Perhaps these burrows

represent a sudden shift in chemical conditions or sedimentation rate from those

that are suitable for sustaining life to those that are not suitable, and the

escape/vertical disruptions represent the organisms burrowing to quickly get out

of these horizons or lamina.
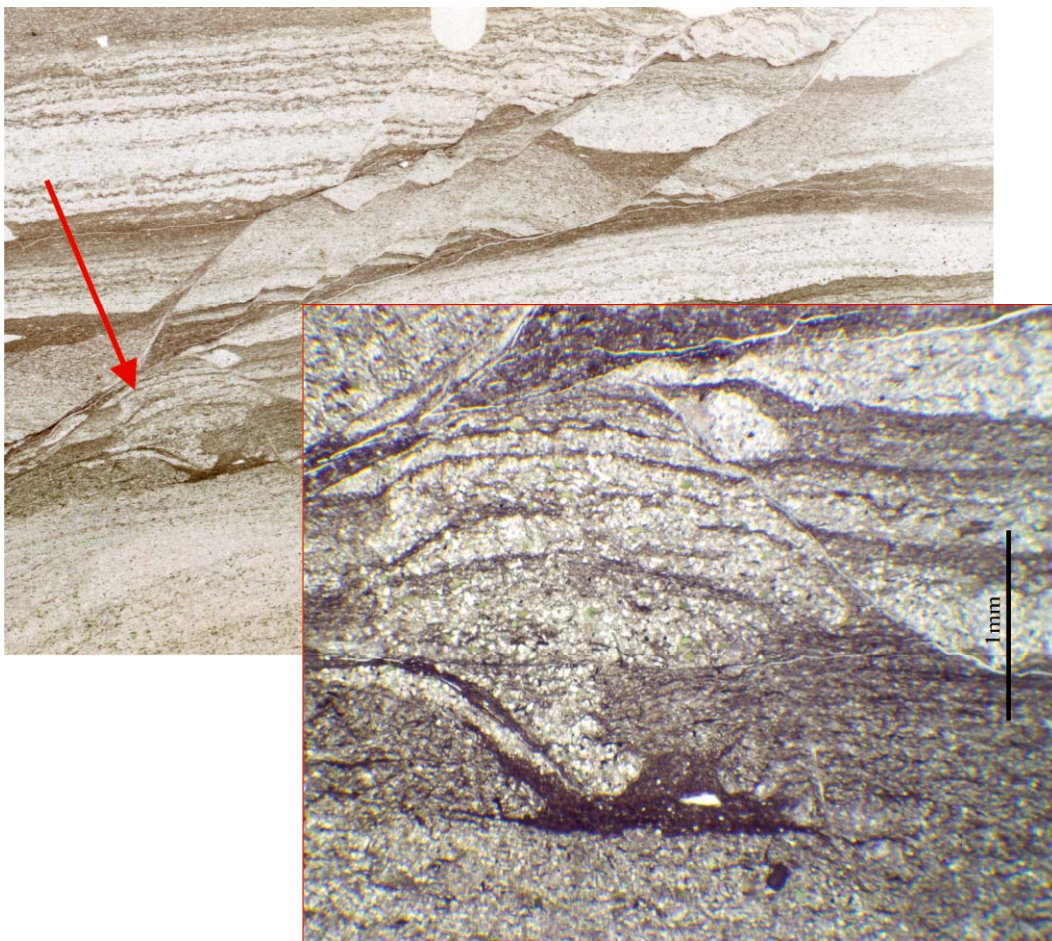
Figure 32. Escape/ Vertical Disruption. A feature unique to this type
of trace is the vertical nature of the burrow. Other burrows are almost
strictly horizontal. Sample Number ORNL-J2-1496.

The escape/vertical disruptions are again confined to the mudstones of Microfacies I and II. The burrow fill material is very much similar to that seen in the surface mining burrows. The burrow fill material contains less clay /mud material than the surrounding material but still contains a considerable amount of fine sediment, which may suggest incomplete bioturbation.

"Cryptic" burrows

The cryptic burrows are the most problematic of the trace fossils found within the microlithofacies of the Rogersville Shale. The problematic nature of these burrows actually lies in determining if they are burrows at all, because the shape of these burrows is generally elongate in cross-section. When viewed longitudinally cryptic burrows look similar to discontinuous lamination of siltstones. The forms of these cryptic burrows are significantly different than that of the other traces fossils found within the Rogersville Shale samples, for this reason the cryptic burrows are generally overlooked as burrows altogether (Figure 33). Such is the case with Walker et al. (1990) who, after their examination of the ORNL cores, state specifically that there is a lack of bioturbation in the Rogersville Shale. In this case one of two possibilities could have occurred: either Walker, Foreman and Srinivasan (1990) were not considering these cryptic burrows as trace fossils and overlooked them, or the Rogersville Shale is variable over its lateral extent.
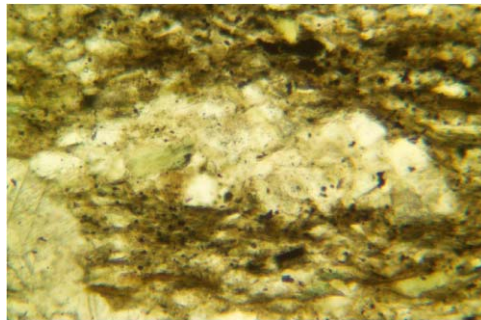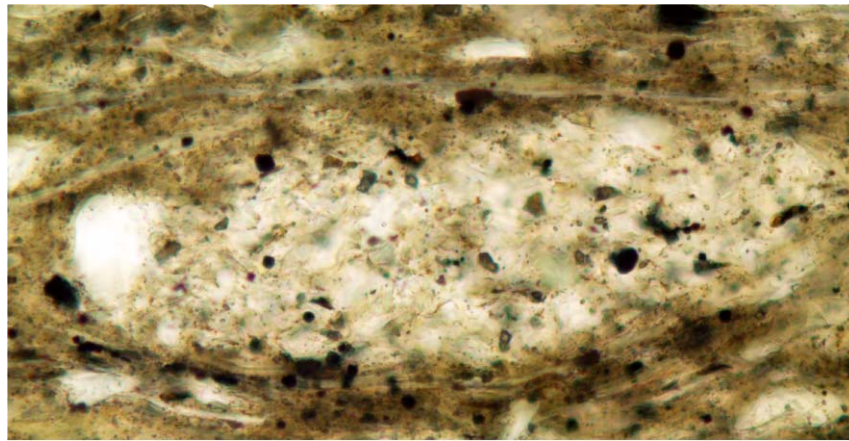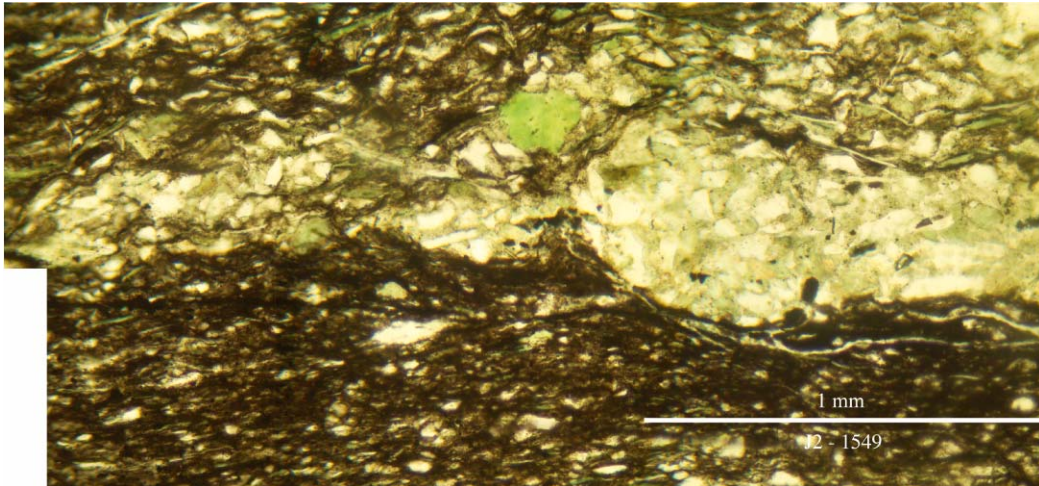
Figure 33. "Cryptic" Burrows. These represent the most problematic trace fossils within the Rogersville Shale. Because the cryptic burrows are not readily identifiable as burrows they may have been overlooked in the past during previous investigations of the Conasauga Group.

Walcott's (1898) *Fossil Medusæ* provides an example of early knowledge of trace fossils existing in the vicinity of the Rogersville Shale in the Middle Cambrian. Illustrations in Plates XXXVI (pg. 177) and XXXVII (pg. 179) of Fossil Medusæ are taken from sections within a 5 mile radius of Rogersville Tennessee, and contain examples of trace fossils. At the time Walcott and others believed these traces to be eophyton or casts of plants (such as seaweed) and imprints of the trailing tentacles of medusa. Through Walcott's investigation we also know that some of them may potentially be casts of burrows.

Summary & Discussion

The types of trace fossils found within the microlithofacies of the Rogersville Shale are characteristic of oxygenated environments. While by themselves the burrows of the Rogersville Shale do not help to constrain the depositional environment, they do help to characterize the different microlithofacies. The burrows indicate that the microfacies of the Rogersville Shale were not anaerobic.

Comparing the findings of this investigation to the investigation done by Walker et al. (1990) has produced some differences with regards to bioturbation. Walker et al. (1990) state that there is a lack of bioturbation within their samples of the Rogersville Shale. A potential reason for this discrepancy may have resulted from the scale at which Walker et al. (1990) investigated the sample of the Rogersville Shale. Walker et al. (1990) may have used hand samples from

the ORNL Joy-2 core and field observation of outcrop samples in their investigation (they made no mention of using thin sections in their paper). Observation of distinct ichnofossils within the samples made at this level may have been difficult. Thus observations made by Walker et al. (1990) about bioturbation were likely based on field observations rather than on a microscopic level of investigation. This difference in the scale at which the samples were investigated could provide a potential explanation as to why Walker et al. (1990) reported an absence of bioturbation in the samples of the Rogersville Shale. However, looking at the same stratigraphic section of the Rogersville Shale in thin section, this investigation was able to differentiate six different styles of trace fossil present in varying degrees in all the microlithofacies.

Rankey et al. (1994) examined the Rogersville Shale as part of a larger investigation of the Conasauga Group, in which they scrutinized different sedimentary fabrics. It seems Rankey et al. (1994) interpreted what we have identified as burrows as an example of fabric-selective dissolution. Figure 7D of Rankey et al. (1994 pg. 307) appears to be a burrow that may have later been subaerialy exposed and subjected to fabric-selective dissolution, the void (or burrow) may have later filled in with equant calcite. This may explain why Rankey et al (1994) also reported finding no evidence of bioturbation within the Rogersville Shale.

Palynology

Characterizing the populations of cryptospores and acritarchs present within the samples of the Rogersville Shale has aided in the determination of the palaeoenvironment of the area during the Middle Cambrian. Cryptospores represent the remains of subaerial plants, as such they should be considered markers of terrestrial influx into the depositional setting. Acritarchs on the other hand represent marine depositional settings. Because cryptospores and acritarchs are believed to indicate distinctly different environments, their presence and proportions in samples have lead to a better understanding of the type of environment that is responsible for producing the microlithofacies of the Rogersville Shale, thereby placing further constraints on paleoenvironmental conditions.

Cryptospores

According to Strother & Beck (2000), "cryptospores are considered to be a class of organic-walled microfossils of probable terrestrial origin, but whose provenance is not necessarily known."   Cryptospores presumably are spore-like remains of early subaerial plants, which lack the trilete mark that characterize vascular plant spores (Strother & Beck 2000). Cryptospores represent the characteristic non-marine palynomorphs from Paleozoic strata (Strother & Beck 2000).

The cryptospore species recovered from the samples of the Rogersville Shale are unlike freshwater algae, and they do not resemble any known alga or plant (Strother et al. 2004). The phylogenetic position of these Middle Cambrian cryptospores is said to be intermediate between the green algae and the vascular plants (Strother et al. 2004). Because cryptospores are of probable terrestrial origin when found in what is thought to be marine sediment, their presence can be considered to be the result of a shallow, near shore lagoonal or estuarine depositional environment, perhaps with a meteoric water input as a source for this probable terrestrial material.

Within the samples of the ORNL-Joy2 core, collected by Strother and Beck, several species of cryptospores have been found (Figure 34). Cryptospore tetrads within the Rogersville Shale have a considerable size range from less than 10 µm to over 30 µm in overall diameter (Strother & Beck 2000). Dyads are also quite abundant within the Rogersville Shale. Because published literature is lacking in information pertaining to cryptospores the taxonomy of many cryptospore species found within the Rogersville Shale is at present still unresolved.
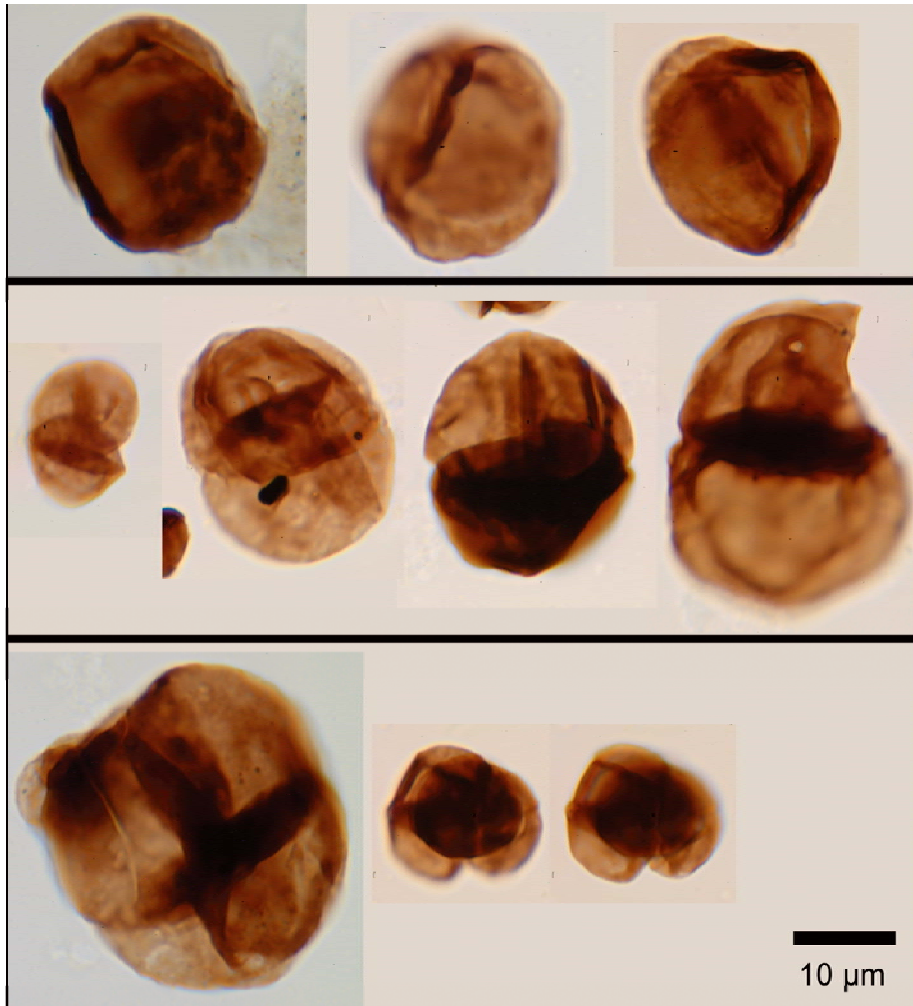
Figure 34. Cryptospores. These images are example of cryptospores populations contained within the Rogersville Shale

Cryptospores have been found largely as a component of the homogenous unlaminated mudstone and laminated mudstone in unbioturbated fabric that contains higher concentrations of mud. The cryptospores are found in the undisturbed material or the material that "escaped" (as it was never subjected to the burrowing) action of the organisms. We can also find a cryptospore in a

fecal pellet that has undergone glauconitization (Figure 19). Whether intentionally ingested or not, the cryptospores made up at least part of the burrowing organisms' diet. This logic works because if the cryptospores were at least part of the burrowing organism's potential food source, they should be more abundant in sediment the organisms have not disrupted (i.e. Microfacies I and II) as opposed to lesser quantities of cryptospores in material that has already been passed through the gut of the burrowing organisms like the siltstone and bioclastic siltstone Microfacies.

Acritarchs

Like cryptospores, acritarchs are organic-walled microfossils that cannot be placed within any existing classification of organisms and again have uncertain origins (Mendelson, 1993). What differentiates the two microfossils is that acritarchs have been consistently recovered from marine sediments (Mendelson, 1993). When acritarchs are found in great abundance within sediment, the sediment can be thought of as having a marine origin. Within the samples of the Rogersville Shale, Strother and Beck have recovered very few species of acritarchs (Figure 35) (Strother, 2006). The acritarchs are far out numbered by the cryptospore population (Strother, 2006).

The presence of the few acritarchs was likely the result of the depositional setting of the Rogersville Shale being temporarily or intermittently inundated with seawater perhaps due to a tidal influence. While the Rogersville Shale was

likely deposited in a shallow water near shore environment with terrestrial input

(probably a restricted estuarine or lagoonal environment), it still may have

received some components of marine waters, which can explain how some

acritarchs are found within the Rogersville Shale.
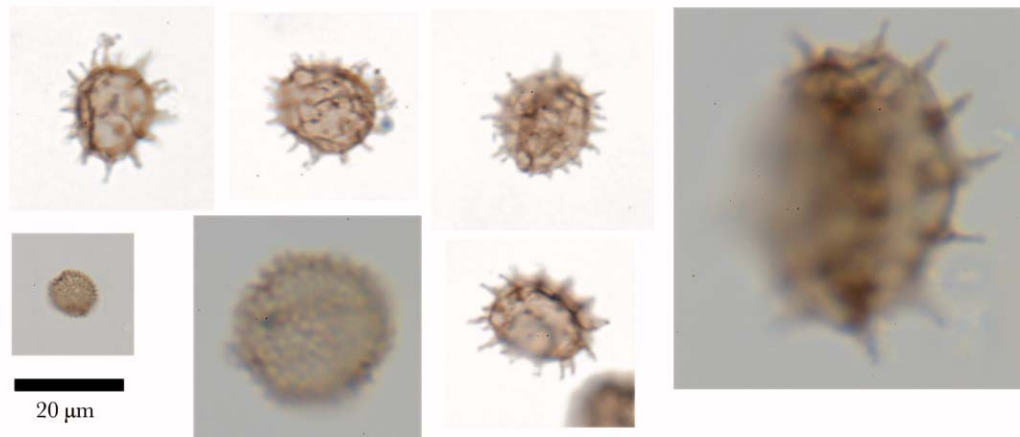
Figure 35. Acritarchs. These images are example of acritarchs populations contained within the Middle to Late Cambrian Rogersville Shale.

Summary & Discussion

Most cryptospore assemblages described to date have come from shallow

marine to paralic sequences (Strother & Beck, 2000). Palynomorphs from the

Rogersville Shale have been valuable in constraining the depositional setting.

Based on the amount of cryptospores within the microlithofacies of the

Rogersville Shale the palaeoenvironment was determined to be the result of a

shallow water, near-shore environment with input of terrestrial waters rather, than

that of a deeper marine setting previously associated with the deposition of the Rogersville Shale. Estuarine or lagoonal environments existed throughout the Middle to Late Cambrian along the margins of Laurentia.

There are many parallels between the Rogersville Shale and the Bright Angel Shale (Baldwin et al., 2004). The Bright Angel Shale of the eastern Grand Canyon region was at one time assumed to be the result of a deep marine palaeoenvironment (McKee and Resser, 1945). McKee and Resser (1945) based their ideas on the presence of thinly laminated shale layers. But when revaluated with additional information, such as trace fossils and palynomorph data, views of the formation changed. The Bright Angel Shale is now generally accepted as being a shallow nearshore marine environment (Baldwin et al., 2004).

The large number of cryptospores and a general lack of acritarchs within the microlithofacies of the Rogersville Shale has indicated a palaeoenvironment that is more closely associated with fresh water and land plants than previously thought. Palynology suggests the depositional environments for the microlithofacies of the Rogersville Shale were more heavily influenced by the terrestrial input and presumably located in a near shore, in a shallow estuary or lagoon.

Conclusion of Results

The Rogersville Shale of the Conasauga Group is a complex intermixing of mudstones and siltstones that, like the Conasauga Group itself, represents sea levels that fluctuated throughout the Middle Cambrian. The suite of minerals in the mudstones of Microfacies I and II are basically the suite of minerals that make up the siltstone and bioclastic siltstone of Microfacies III and IV. The ratio between the different materials changed, resulting in the different microlithofacies present within the Rogersville Shale.

The occurrence of glauconite in the Rogersville Shale has helped to constrain the range of palaeoenvironmental conditions that were responsible for producing these rocks. Because several glauconite grains were observed to have grown in situ (Figure 17) it can be inferred that the chemical environment would have been locally micro-reducing in an overall well oxygenated environment that could support an active subsurface fauna.

The organisms that created the wide variety trace fossils present in the Rogersville Shale may have also been responsible for creating the chemical environment necessary for glauconite formation. The micro-reducing condition in an overall well oxygenated environment needed for glauconite formation may have resulted from organisms burrowing through initially oxygenated sediment. As the organisms moved through the sediment and they were buried, the chemical environment transitioned from being well oxygenated to being slightly reducing. As the organisms passed through the sediment they used up the

oxygen in the sediment during respiration and created microenvironments with reducing conditions within the burrows.

The presence of abundant cryptospores within the Rogersville Shale indicate that deposition occurred in close proximity to the palaeoshoreline. Cryptospores are believed to be non-marine in origin, they must have been transported by water with terrestrial origins. Because cryptospores out number acritarchs within the Rogersville Shale, it is reasonable to believe the deposition occurred in a shallow near shore palaeoenvironment.

Chapter 4

Summary and Conclusions

Summary

The following conclusions about the Middle to Late Cambrian Rogersville Shale of the Conasauga Group in eastern Tennessee were ascertained from this research. Each conclusion helped to constrain the depositional setting for the Rogersville Shale.

Glauconite

Glauconite is abundant in the Rogersville Shale, and is enriched in the siltstone and bioclastic siltstone microfacies (average 5 – 8% respectively). The chemical environment in which glauconite is formed is consistent with the environment produced by the biologic activity within the Rogersville Shale. The micro-reducing environment the burrowing organisms created would have been the ideal location for the formation of glauconite (and pyrite). By knowing that at least some of the glauconite grains within the Rogersville Shale are autochthonous, it has helped determine the local environment below the water surface as reducing.

Trace Fossils

Abundant trace fossils within the Rogersville Shale indicate the substrate would have had adequate oxygen with an ample food supply. Burrowing organisms (that produced the biologic activity) may have chemically altered the environment in which they lived. As the organisms respired and eventually expire and decomposed, they would have used up the available oxygen, creating micro-reducing conditions within the burrows. These reducing conditions allowed for organic preservation, glauconite and pyrite formation.

Lingulid Shell Fragments

Some shell fragments within the siltstone and bioclastic siltstone facies have been identified as lingulids. The presence of lingulid fossils is another environmental indicator. According to Strother and Beck (2004), lingulids have long been viewed as a species that is considered to indicate very shallow water depth. Rudwick (1970, p.158) indicated that "Lingulids may well have tolerated brackish conditions, so that an estuarine setting for *Linguella* is by no means out of the question". The presence of lingulid fragments and the virtual absence of other shelly fossils is a clear indication that the environment of deposition of the Rogersville Shale most certainly would have been that of a shallow restricted marine setting or estuary that was heavily influenced by terrestrial runoff.

Cryptospores

Cryptospores contained within the Rogersville Shale indicate that the depositional environment was influenced by terrestrial runoff, and was not greatly influenced by deep marine conditions. Because acritarchs are rare within the Rogersville Shale it seems likely that the environment was not greatly influenced by marine conditions. Instead the influence is shifted to that of the terrestrial runoff that must have been entering the environment. This runoff contained cryptospores that are found throughout the Rogersville Shale.

Conclusions

	Environmental Indicator	**Conclusion**
Glauconite	• Autochthonous glauconite indicates that the environment of formation was mildly reducing but over all well oxygenated • Burrows would have been the ideal location for glauconite formation • Glauconite is nearly 20% more abundant in siltstone microfacies than in mudstone microfacies	Glauconite most likely formed within or adjacent to burrows where the chemical environment would have been mildly reducing These burrows are believed to be characteristic of shallow water near shore environments
Presence of Cryptospores	• Are abundant in the Rogersville Shale • Indicates a depositional environment that is more heavily influenced by terrestrial runoff • Greatest numbers are found in the Homogenous Unlaminated Mudstone and Laminated Mudstones	The abundance of cryptospores within the Rogersville Shale indicates the depositional environment was likely near shore

	Environmental Indicator	**Conclusion**
Lack of Acritarchs	- There is a general lack of acritarchs within the Rogersville Shale - Acritarchs indicate a depositional environment that is heavily influenced by marine waters	The lack of acritarchs within the Rogersville Shale indicates that the depositional environment was greatly influenced by marine waters
Abundant Trace Fossils	- Indicates the depositional environment would have been adequately oxygenated and contained an ample food supply - As burrowing organisms respired they would have used up available oxygen creating mildly reducing condition where by preserving organic material and allowing for glauconite formation	The activity of burrowing organisms would have likely provided the ideal condition for the formation of glauconite
Lingulid Shell Fragments	- Lingulids indicate very shallow water depth - May have tolerated brackish water (terrestrial runoff) - Virtual absence of other shelly fossils	The presence of Lingulid shell fragments and general lack of other fossils indicates the environment would have likely been very shallow and possibly had terrestrial runoff

While individually the different components of this investigation may not resolve the questions of its origin and environment, in combination they produce major constraints on the environment during the time of its deposition. The picture is one of a near-shore shallow water probable restricted estuarine or lagoonal environment that had a component of terrestrial runoff (and likely contained brackish waters) that existed on the margins of Laurentia during the Mid-to-Late Cambrian.

References

Aitken, J.D., 1978, Revised models for depositional grand cycles, Cambrian of the southern Rocky Mountains, Canada: Bulletin of Canadian Petroleum Geology, v. 26, p. 515-542.

Amorosi, A., 1997, Detecting compositional, spatial, and temporal attributes of glaucony: a tool for provenance research: Sedimentary Geology, v. 109, p. 135-153.

Baldwin, C.T., Strother, P.K., Beck, J.H., and Rose, E., 2004, Palaeoecology of the Bright Angle Shale in the eastern Grand Canyon, Arizona, USA, incorporating sedimentological, ichnological and palynological data, *in* McIlroy, D., ed., The Application of Ichnology to Palaeoenvironmental and Stratigraphic Analysis: London, The Geological Society, p. 213-236.

Baxter, P.M., 1989, Clay mineral diagenesis in the Pumpkin Valley Shale, Oak Ridge, Tennessee [Ph.D. thesis]: Baton Rouge, LA, Louisiana State University and Agricultural and Mechanical College, p. 1-196.

Bentor, Y.K., and Kastner, M., 1965, Notes on the Mineralogy and Origin of Galuconite: Journal of Sedimentary Petrology, v. 35, p. 155-166.

Bond, G.C., Kominz, M.A., and Grotzinger, J.P., 1988, Cambro-Ordovician eustasy: Evidence from geophysical modeling of subsidence in Cordilleran and Appalachian passive margins, *in* Paola, C. and Kleinspehn, K., eds., New Perspectives in Basin Analysis: New York, Springer-Verlag, p. 129-161.

Bond, G.C., Nickeson, P.A., and Kominz, M.A., 1984, Breakup of a supercontinent between 625 Ma and 555 Ma: New evidence and implications for continental histories: Earth and Planetary Science Letters, v. 70, p. 325-345.

Breheret, J.G., 1991. Glauconitization episodes in marginal settings as echoes of mid-Cretaceous anoxic events recorded in Vocontian basin. In: R. Tyson and T. Pearson (Editors), Modern and Ancient Continental Shelf Anoxia. Special Publication Geol. Soc. London, 58: 415-425.

Burst, J.F., 1958a, "Glauconite" Pellets: Their Mineral Nature and Application to Stratigraphic Interpretations: Bulletin of the American Association of Petroleum Geologists, v. 42, p. 310-327.

Burst, J.F., 1958b, Mineral Heterogeneity in "Glauconite" Pellets: The American Mineralogist, v. 43, p. 481-497.

Byerly, D.W., Walker, K.R., Diehl, W.W., Ghazizadeh, M., Johnson, R.E., Lutz, C.T., Schoner, A.K., Simmons, W.A., Simonson, J.C.B., Weber, L.J., and Wedekind, J.E., 1986, Thorn Hill: A classic Paleozoic stratigraphic section in Tennessee, *in* Neathery, T.L., ed., Southeastern section of the Geological Society of America: Boulder, CO, Geological Society of America, p. 131-136.

Chafetz, H.S., 1978, A trough cross-stratified glaucarenite: a Cambrian tidal inlet accumulation: Sedimentology, v. 25, p. 545-559.

Chafetz, H.S., and Reid, A., 2000, Syndepositional shallow-water precipitation of glauconitic minerals: Sedimentary Geology, v. 136, p. 29-42.

Cloud Jr., P.E., 1955, Physical limits of glauconite formation: Bulletin of the American Association of Petroleum Geologists, v. 39, p. 484-492.

Dasgupta, S., Chaudhuri, A.K., and Fukuoka, M., 1990. Compositional characteristics of glauconitic alterations of K-feldspar from India and their implications. Journal of Sedimentary Petrology, 60: 277-281.

deLaguna, W., and et al., 1968, Engineering Development of Hydraulic Fracturing as a Method for Permanent Disposal of Radioactive Wastes: Oak Ridge National Laboratory, Report ORNL-4259.

Department of Energy, Oak Ridge National Laboratory, http://www.ornl.gov: 2006.

el Albani, A., Meunier, A., and Fursich, F., 2005, Unusual occurrence of glauconite in a shallow lagoonal environment (Lower Cretaceous, northern Aquitaine Basin, SW France): Terra Nova, v. 00, p. 1-8.

Ellmann, A.J., Hulings, N.C., and Glover, E.D., 1963, Stages of glauconite formation in modern foraminiferal sediment: Journal of Sedimentary Petrology, v. 33 (1), p. 87-96.

Elrich, R., Kennedy, S.K., Crabtree, S.J., and Cannon, R.L., 1984, Petrographic image analysis, I. analysis of reservoir pore complexes: Journal of Sedimentary Petrology, v. 54, p. 1365-1378.

Francus, P., 1998, An image-analysis technique to measure grain-size variation in thin sections of soft clastic sediments: Sedimentary Geology, v. 121, p. 289-298.

Galliher, E.W., 1935, Geology of Glauconite: American Association of Petroleum Geologists, Bulletin, v. 19, p. 1569-1601.

Gebhart, G., 1982. Glauconitic condensation through high-energy events in the Albian near Clars (Escragnolles, Var, SE-France). In: G. Einsele and A. Seilacher (Editors), Cyclic and Event Stratification. Springer-Verlag, New York, N.Y., pp. 286-298.

Glenn, C.R. and Arthur, M.A., 1990. Anatomy and origin of a Cretaceous phosphorite-greensand giant, Egypt. Sedimentology, 37: 123-154.

Glumac, B., and Walker, K.R., 2002, Effects of grand-cycle cessation on the diagenesis of upper Cambrian carbonate deposits in the Southern Appalachians, U.S.A. Journal of Sedimentary Research, v. 72, p. 570-586.

Glumac, B., and Walker, K.R., 1998, A Late Cambrian positive carbon-isotope excursion in the Southern Appalachians: Relation to biostratigraphy, sequence stratigraphy, environments of deposition and diagenesis: Journal of Sedimentary Research, v. 68, p. 1212-1222.

Glumac, B., and Walker, K.R., 2000, Carbonate deposition and sequence stratigraphy of the terminal Cambrian grand cycle in the Southern Appalachians, U.S.A. Journal of Sedimentary Research, v. 70, p. 952-963.

Haase, C.S., Walls, E.C., and Farmer, C.D., 1985, Stratigraphic and Structural Data for the Conasauga Group and the Rome Formation on the Copper

Creek Fault Block near Oak Ridge, Tennessee: Preliminary Results from Test Borehole ORNL-JOY No. 2: U. S. Department of Energy, Report 2392, p. 1-88.

Hasson, K.O., and Haase, C.S., 1988, Lithofacies and paleography of the Conasauga Group, (Middle and Late Cambrian) in the Valley and Ridge province of east Tennessee: Geological Society of America Bulletin, v. 100, p. 234-246.

Heilbronner, R., 2002, Analysis of bulk fabrics and microstructure variations using tessellations of autocorrelation functions: Computers & Geosciences, v. 28, p. 447-455.

Heilbronner, R., 2000, Automatic grain boundary detection and grain size analysis using polarization micrographs or orientation images: Journal of Structural Geology, v. 22, p. 969-981.

Hower, J., 1961, Some factors concerning the nature and origin of glauconite: The American Mineralogist, v. 46, p. 313-334.

Keferstein, C.H., 1828, Deutschland geognonostich-geologisch dargestellt: Bd. 5, p. 508-512.

King Jr., D.T., and Chafetz, H.S., 1983, Tidal-flat to shallow-shelf deposits in the Cap Mountain Limestone Member of the Riley Formation, Upper Cambrian of Central Texas: Journal of Sedimentary Petrology, v. 53, p. 0261-0273.

Lochman-Balk, C., 1971, The Cambrian of the Craton of the United States. In: C.H. Holland (Editor), Cambrian of the New World, Lower Palaeozoic Rocks of the World Volume1. John Wiley and Sons Publ. London, pp. 79-167.

Mancini, E.A., and Tew, B.H., 1993. Eustasy versus subsidence: Lower Paleocene depositional sequences from southern Alabama, eastern Gulf Coastal Plain. Bulletin of the Geological Society of America, 105: 3-17.

Markello, J.R., and Read, J.F., 1981, Carbonate ramp-to-deeper shale shelf transition of an Upper Cambrian intrashelf basin, Nolichucky Formation, Southwest Virginia Appalachians: Sedimentology, v. 28, p. 573-597.

Martin, D.L., 1985, Depositional systems and ichnology of the Bright Angle Shale (Cambrian), eastern Grand Canyon, Arizona [M.S. thesis] [Ph.D. thesis]: Flagstaff, Arizona, Northern Arizona University, p. 311.

McKee, E.D., and Resser, C.E., 1945, Cambrian History of the Grand Canyon Region: v. 563.

Mendelson, C.V., 1993, Acritarchs and prasinophytes, *in* Lipps, J.H., ed., Fossil Prokaryotes and Protists: Boston, Blackwell Scientific Publications, Inc., p. 77-104.

National Institutes of Health, Research Services Branch, http://rsb.info.nih.gov: 2006.

Odin, G.S. and Rex, D.C., 1982. K-Ar dating of washed, leached, weathered and reworked glauconies. In: G.S. Odin (Editor), Numerical Dating in Stratigraphy. John Wiley and Sons Publ., Chichester, pp. 363-385.

Odin, G.S., 1988, Green marine clays: oolitic ironstone facies, verdine facies, glaucony facies, and celadonite-bearing facies: a comparative study: Amsterdam; New York; New York, N.Y., U.S.A., Elsevier; Distributors for the U.S. and Canada, Elsevier Science Pub. Co., p. 445.

Parker, R.J., 1975. The petrology and origin of some glauconitic and glauco-conglomeratic phosphorites from the south-african continental margin. Journal of Sedimentary Petrology, 45: 230-242.

Plint, A.G., 1983. Facies, environments and sedimentary cycles in the Eocene, Brackiesham Formation of the Hampshire Basin: evidenced for global sea-level change? Sedimentology, 30: 625-653.

Rankey, E.C., Walker, K.R., and Srinivasan, K., 1994, Gradual establishment of Iapetan "passive" margin sedimentation: stratigraphic consequences of Cambrian episodic tectonism and eustasy, southern Appalachians: Journal of Sedimentary Research, v. B64, p. 298-310.

Rose, E., 2003, Depositional Environments and History of the Cambrian Tonto Group, Grand Canyon, Arizona [M.S. thesis] [Ph.D. thesis]: Flagstaff, Arizona, Northern Arizona University, p. 349p.

Rudwick, M.J.S., 1970, Living and Fossil Brachiopods: Hutchinson, London

Russ, J.C., 1998, The Image Processing Handbook: Boca Raton, FL, CRC Press LLC in cooperation wit IEEE Press, p. 771.

Ruzyla, K., 1992, Quantitative image analysis of reservoir rocks: Pitfalls, limitations, and suggested procedures: Geobyte, v. 7, p. 7-20.

Schneider, H., 1927, A story of glauconite: Journal of Geology, v.35, p. 289-310.

Singh, I.B., and Kumar, S., 1978, On the stratigraphy and sedimentation of the Vindhyan sediments in the Chitrakut Area Banda District (U.P.) -- Satna District (M.P.): Journal of the Geological Society of India, v. 19, p. 359-367.

Srinivasan, K., and Walker, K.R., 1993, Sequence stratigraphy of an intrashelf basin carbonate ramp to rimmed platform transition: Maryville Limestone (Middle Cambrian), southern Appalachians: Geological Society of America, Bulletin, v. 105, p. 883-896.

Strother, P. K. 2006. Middle Cambrian Acritarchs from the Conasauga Group, eastern Tennessee, USA. Palaeozoic Palynology in Space and Time. CIMP General Meeting 2006, September 2-6, 2006- Prague, Czech Republic. Book of Abstracts: 51.

Strother, P.K., 2000, Phanerozoic Terrestrial Ecosystems: Cryptospores: The origin and early evolution of the terrestrial flora: The Paleontological Society Papers, v. 6, p. 3-20.

Strother, P.K. and Beck J.H., 2006, Personal communications.

Strother, P.K., Wood, G.D., Taylor, W.A., and Beck, J.H., 2004, *in* Laurie, J.R. and Foster, C.B., eds., Sydney, N.S.W., Australia, Association of Australasian Palaeontologists, p. 99-113.

Sundberg, F.A., 1989, Biostratigraphy of the Lower Conasauga Group a Preliminary Report: Appalachian Basin Industrial Associates, v. 15, p. 166-176.

Triat, J.M., Odin, G.S., and Hunziker, J.C., 1976. Glauconies cretacees remaniees dans le Paleogene continental du bassin d'Apt et Valreas. Bull. Soc. Geol. Fr., 6: 1671-1676.

Triplehorn, D.M., 1966, Morphology, internal structure, and origin of glauconite pellets: Sedimentology, v. 6, p. 247-266.

van den Berg, E.H., Meesters, A.G.C.A., Kenter, J.A.M., and Schlager, W., 2002, Automated separation of touching grains in digital images of thin sections: Computers & Geosciences, v. 28, p. 179-190.

ven den Berg, Elmer H., Bense, V.F., and Schlager, W., 2003, Assessing textural variation in laminated sands using digital image analysis of thin sections: Journal of Sedimentary Research, v. 73, p. 133-143.

Walcott, C.D., 1898, Fossil Medusae: Washington D.C., Government Printing Office, p. 201.

Walker, K.R., Foreman, J.L., and Srinivasan, K., 1990, The Cambrian Conasauga Group of eastern Tennessee: A preliminary general stratigraphic model with a more detailed test for the Nolichucky Formation: Appalachian Basin Industrial Associates, v. 17, p. 184-189.

Walker, R.G. and Bergman, K.M., 1993. Shannon Sandstone in Wyoming: a shelf-ridge complex reinterpreted as lowstand shoreface deposit. Journal of Sedimentary Petrology, 63: 839-851.

Warshaw, C.M., 1957, The mineralolology of glauconite: Dissertation Abstract 17, No. 12, Pennsylvania State University, p.155.

Weber, Lawrence J., Jr., 1988, Paleoenvironmental analysis and test of stratigraphic cyclicity in the Nolichucky Shale and Maynardville Limestone (Upper Cambrian) in Central East Tennessee [Ph.D. thesis]: Knoxville, TN, The University of Tennessee, Knoxville, p. 1-388.

White, J.V., Kirkland, B.L., and Gournay, J.P., 1998, Quantitative porosity determination of thin sections using digitized images: Journal of Sedimentary Research, v. 68, p. 220-222.

Williams, A.T., Wiltshire, R.J., and Thomas, M.C., 1998, Sand Grain Analysis--Image Processing, Textural Algorithms and Neural Nets: Computers & Geosciences, v. 24, p. 111-118.

Wood, J.M., and Hopkins, J.C., 1992, Taps Associated with Paleovalleys and Interfluves in an Unconformity Bounded Sequence: Lower Cretaceous Glauconitic Member, Southern Alberta, Canada: American Association of Petroleum Geologists Bulletin, v. 76, p. 904-926.

Yamaji, A., and Masuda, F., 2005, Improvements in graphical representation of fabric data, showing the influence of aspect ratios of grains on their orientations: Journal of Sedimentary Research, v. 75, p. 514-519.

APPENDIX

Thin Sections

SPECIMEN #	1484' Down Hole Footage	
FORMATION	Rogersville Shale	
MEMBER	Craig Member	
TEXTURE:		
Median GS	0.523 mm	
Sorting	Poor	
Roundness	Subangular → Subround	
Sphericity	Low	
Packing	Dense	

GRAINS:		PRESENT
QUARTZ		X
	Round	
	Broken Round	
	Angular	
	Qtz. Overgrowth	
FELDSPAR		
	K-Spar	
	Plagioclase	
CARBONATES		
	Calcite	X
	Sparry	X
	Micrite	X
	Void Filling	
	Dolomite	X
	Replacement Dolomite	X
GLAUCONITE		
	Pelloidal	
	Clay-Glauconite Intermediate	
	Platy	
	Vermiform or Zebra	
	Replacement	
OTHER MINERALS		
	Phosphatic Material (Collophane)	X
	Chert	
	Clay	X
	Biotite	
	Muscovite	
	Ooids	
	Fecal Pellets	

ACCESSORIES		PRESENT
	Organic Matter	
	Heavy Minerals	
	Ironsulfide (Pyrite?)	X
	Ironoxide (Hematite/Illmenite?)	X
FOSSILS		
	Shell Fragments	X
	Other:	
MICROFOSSILS		
	Cryptospores	
	Acritarchs	
CEMENTS		
	Calcite	X
	Sparry	X
	Micrite	X
	Dolomite	
	Chert	
	Phosphate	
	Clay-Glauconite Intermediate	
	Quartz	
	Clay	
SECONDARY FEATURES:		
	Vugs	
	Stylolites	X
	Soft Sediment Deformation	X
SEDIMENTARY STRUCTURES:	Laminations	
	Finely Laminated	
	Thickly Laminated	
	Wavy Laminated	
	Lenticular Laminated	
	Mud Cracks	
	Cross-Bedding	
	Graded-Bedding	
	Fining Upward	
	Burrows:	
	Surface Trace	
	Shallow Surface Trace	
	Below Substrate Circ Holes	
	Subsurface Mining	
	Escape / Vertical	
	Cryptic	

Hand Lens Observations:		
Glauconite Present?	None	
Laminations:	N/A	
Bioturbation:		
None:	X	
Slight:		
Moderate:		
Extensive::		
Micro-faulting	N/A	
Organic Rich Layers	None	
Facies Present	Limestone (Craig)	
OVERALL LITHOLOGIES	Limestone	
	Mudstone	
	Siltstone	
	Argillaceous Limestone	X
	Calcareous Mudstone	
	Argillaceous Siltstone	
	Dolomite	
	Dolomitic Limestone	
Points of Interest:		

- Micro-spar is present in some of the cements
- Phosphatic shell fragments present
- Soft sediment deformation
- It appears that sparry calcite was formed after the soft sediment deformation
- Calcite overgrowth
- Dolomite replacement
- Minor amounts of pyrite present

Percent Composition:	
Brown	2.5
Grey	46.6
White	51.5
Total	100.6

SPECIMEN #	1486 Down Hole Footage	
FORMATION	Rogersville Shale	
MEMBER	Craig Limestone	
TEXTURE:		
Median GS	0.743 mm	
Sorting	Poor	
Roundness	Subround→ Round	
Sphericity	Moderate	
Packing	Dense	
COLOR:	Brownish Red	
GRAINS:		PRESENT
QUARTZ		
	Round	
	Broken Round	
	Angular	
	Qtz. Overgrowth	
FELDSPAR		
	K-Spar	
	Plagioclase	
CARBONATES		
	Calcite	X
	Sparry	
	Micrite	
	Void Filling	
	Dolomite	
	Replacement Dolomite	X
GLAUCONITE		
	Pelloidal	
	Clay-Glauconite Intermediate	
	Platy	
	Vermiform or Zebra	
	Replacement	
OTHER MINERALS		
	Phosphatic Material (Collophane)	
	Chert	
	Clay	
	Biotite	
	Muscovite	
	Ooids	X
	Fecal Pellets	X

ACCESSORIES		
	Organic Matter	
	Heavy Minerals	
	Ironsulfide (Pyrite?)	
	Ironoxide (Hematite/Illmenite?)	X
FOSSILS		
	Shell Fragments	
	Other:	
MICROFOSSILS		
	Cryptospores	
	Acritarchs	
CEMENTS		
	Calcite	
	Sparry	
	Micrite	
	Dolomite	
	Chert	
	Phosphate	
	Clay-Glauconite Intermediate	
	Quartz	
	Clay	
SECONDARY FEATURES:		
	Vugs	
	Stylolites	
	Soft Sediment Deformation	
SEDIMENTARY STRUCTURES:	Finely Laminated	
	Thickly Laminated	
	Wavy Laminated	
	Lenticular Laminated	
	Mud Cracks	
	Cross-Bedding	
	Graded-Bedding	
	Fining Upward	
	Burrows:	
	Surface Trace	
	Shallow Surface Trace	
	Below Substrate Circular Holes	
	Subsurface Mining	
	Escape / Vertical	
	Cryptic	

Hand Lens Observations:		
Glauconite Present?	N	
Laminations:	N/A	
Bioturbation:		
None:	X	
Slight:		
Moderate:		
Extensive::		
Micro-faulting		
Organic Rich Layers	X	
Facies Present	V	

OVERALL LITHOLOGIES	Limestone	X
	Mudstone	
	Siltstone	
	Argillaceous Limestone	
	Calcareous Mudstone	
	Argillaceous Siltstone	
	Dolomite	
	Dolomitic Limestone	

Öolitic limstone with hematitic and/or phosphatic coating
Concentric ring are visible on many of the grains

Percent Composition:
Brown	N/A
Green	N/A
White	N/A
Total	N/A

Thin Section:

Scale Bar = 1 mm
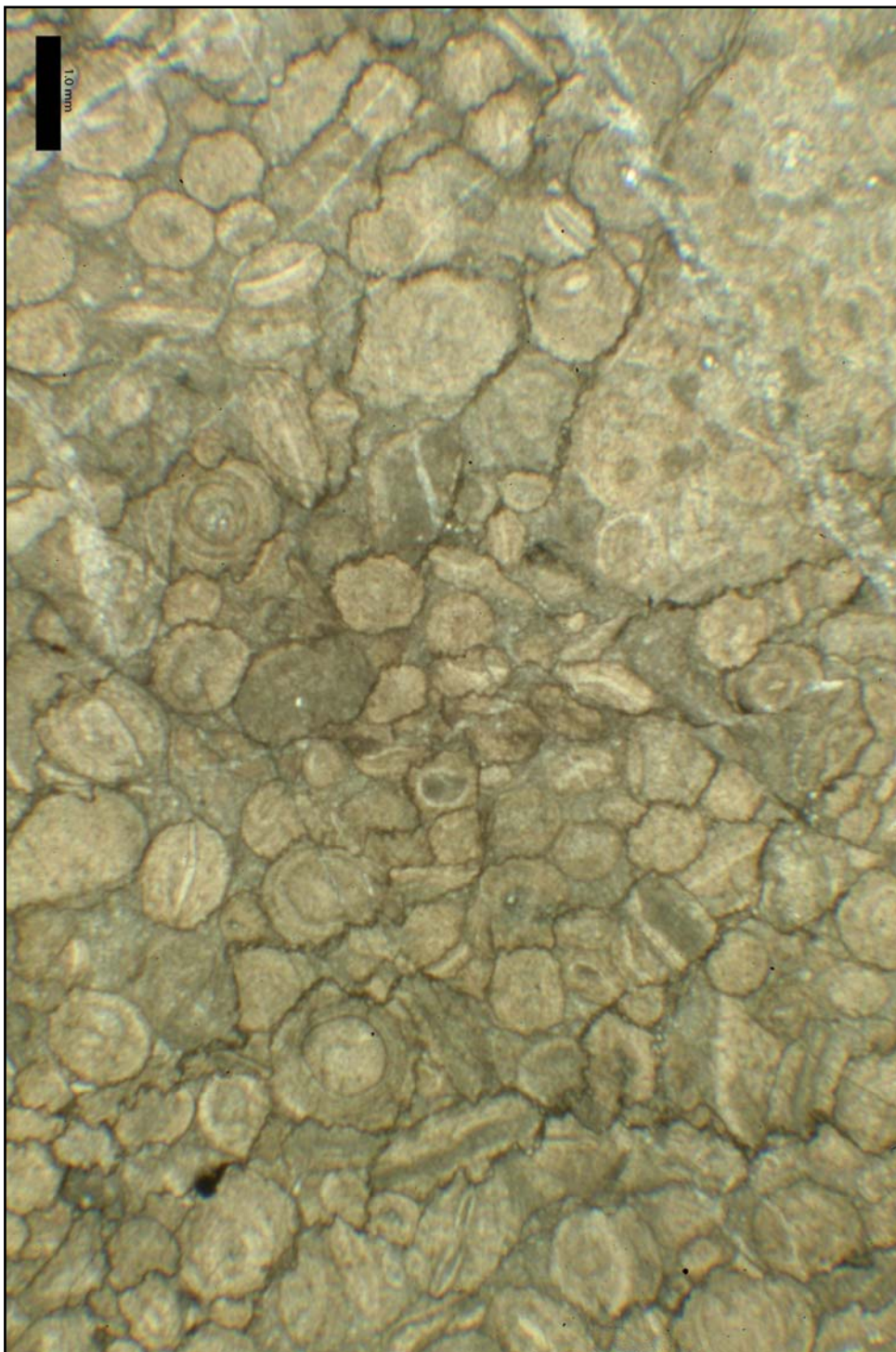
SPECIMEN #	1490.5' Down Hole Footage	
FORMATION	Rogersville Shale	
MEMBER	Craig Limestone	
TEXTURE:		
Median GS	0.0474 mm	
Sorting	Poor	
Roundness	Subangular→ Subround	
Sphericity	Low	
Packing	Dense	
GRAINS:		PRESENT
QUARTZ		X
	Round	
	Broken Round	
	Angular	X
	Qtz. Overgrowth	
FELDSPAR		
	K-Spar	
	Plagioclase	
CARBONATES		
	Calcite	X
	Sparry	X
	Micrite	
	Void Filling	
	Dolomite	
	Replacement Dolomite	
GLAUCONITE		
	Pelloidal	
	Clay-Glauconite Intermediate	
	Platy	
	Vermiform or Zebra	
	Replacement	
OTHER MINERALS		
	Phosphatic Material (Collophane)	X
	Chert	X
	Clay	X
	Biotite	
	Muscovite	
	Ooids	
	Fecal Pellets	

ACCESSORIES		
	Organic Matter	X
	Heavy Minerals	
	Ironsulfide (Pyrite?)	X
	Ironoxide (Hematite/Illmenite?)	
FOSSILS		
	Shell Fragments	
	Other:	
MICROFOSSILS		
	Cryptospores	
	Acritarchs	
CEMENTS		
	Calcite	
	Sparry	
	Micrite	
	Dolomite	
	Chert	
	Phosphate	
	Clay-Glauconite Intermediate	
	Quartz	
	Clay	
SECONDARY	Vugs	
FEATURES:	Stylolites	
	Soft Sediment Deformation	
	Finely Laminated	
SEDIMENTARY	Thickly Laminated	
STRUCTURES:	Wavy Laminated	X
	Lenticular Laminated	
	Mud Cracks	
	Cross-Bedding	
	Graded-Bedding	
	Fining Upward	X
	Burrows:	
	Surface Trace	
	Shallow Surface Trace	X
	Below Substrate Circular Holes	
	Subsurface Mining	
	Escape / Vertical	
	Cryptic	

Hand Lens Observations:		
Glauconite Present?	X	
Laminations:	X	
Bioturbation:		
None:		
Slight:	X	
Moderate:		
Extensive::		
Micro-faulting	X	
Organic Rich Layers	X	
Facies Present	I, II	
OVERALL LITHOLOGIES	Limestone	
	Mudstone	
	Siltstone	
	Argillaceous Limestone	X
	Calcareous Mudstone	
	Argillaceous Siltstone	
	Dolomite	
	Dolomitic Limestone	

Percent Composition:	
Brown	29.2
Green	12.0
White	59.3
Total	100.5

Points of Interest:

Large sparry clacite vein
Wavy lamination is cut by vien

Thin Section:

Scale Bar = 1 mm
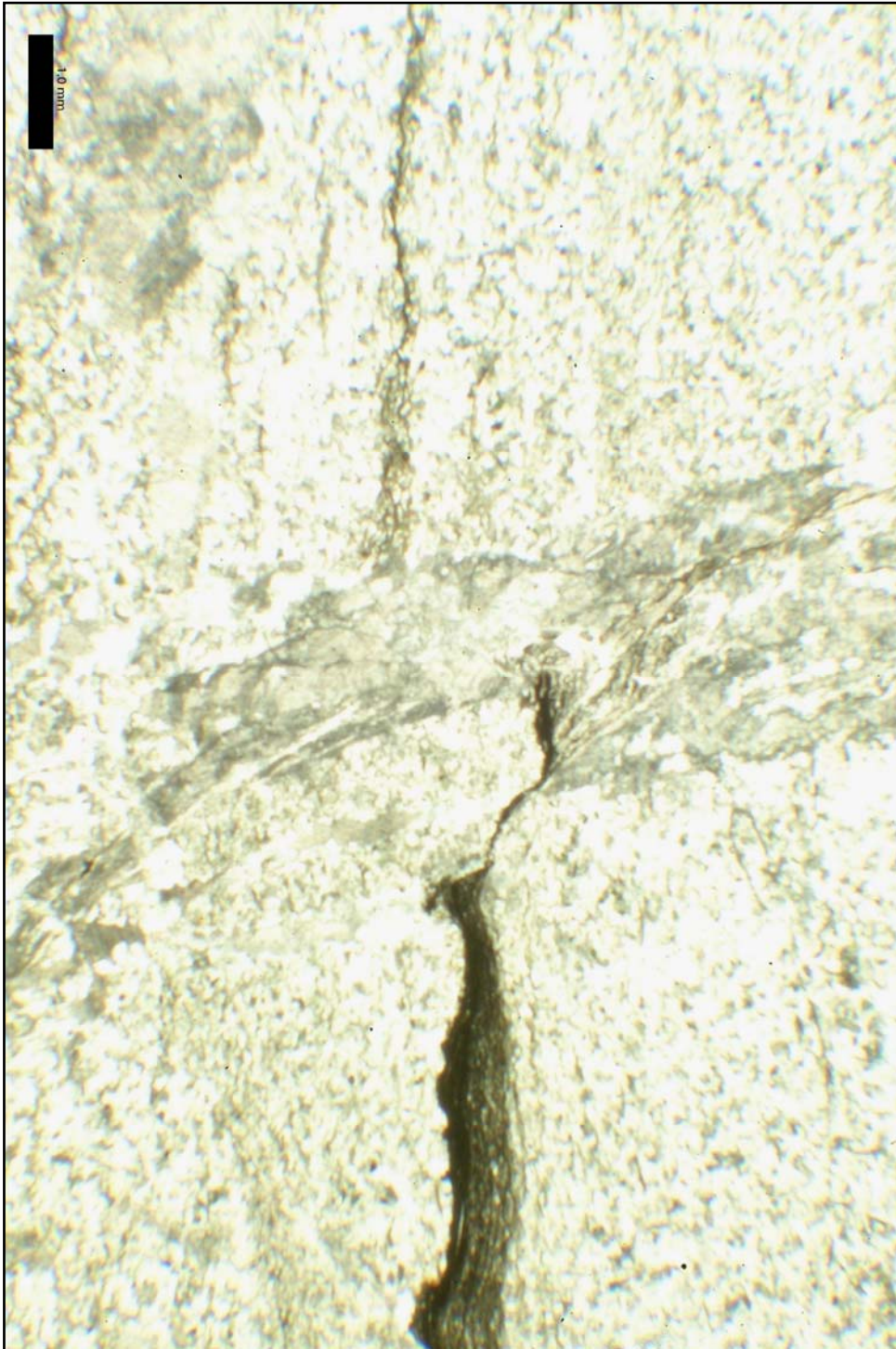
SPECIMEN #	1496.5' Down Hole Footage	
FORMATION	Rogersville Shale	
MEMBER		
TEXTURE:		
Median GS	0.0482 mm	
Sorting	Poor	
Roundness	Subangular→ Angular	
Sphericity	Low	
Packing	Dense	
GRAINS:		PRESENT
QUARTZ		
	Round	
	Broken Round	X
	Angular	X
	Qtz. Overgrowth	
FELDSPAR		
	K-Spar	X
	Plagioclase	
CARBONATES		
	Calcite	X
	Sparry	X
	Micrite	
	Void Filling	
	Dolomite	
	Replacement Dolomite	
GLAUCONITE		
	Pelloidal	X
	Clay-Glauconite Intermediate	X
	Platy	
	Vermiform or Zebra	X
	Replacement	
OTHER MINERALS		
	Phosphatic Material (Collophane)	X
	Chert	X
	Clay	X
	Biotite	
	Muscovite	
	Ooids	
	Fecal Pellets	

ACCESSORIES		
	Organic Matter	X
	Heavy Minerals	
	Ironsulfide (Pyrite?)	X
	Ironoxide (Hematite/Illmenite?)	X
FOSSILS		
	Shell Fragments	X
	Other:	
MICROFOSSILS		
	Cryptospores	
	Acritarchs	
CEMENTS		
	Calcite	X
	Sparry	
	Micrite	
	Dolomite	
	Chert	
	Phosphate	
	Clay-Glauconite Intermediate	X
	Quartz	
	Clay	X
SECONDARY FEATURES:	Vugs	X
	Stylolites	X
	Soft Sediment Deformation	
	Finely Laminated	
SEDIMENTARY STRUCTURES:	Thickly Laminated	
	Wavy Laminated	X
	Lenticular Laminated	
	Mud Cracks	
	Cross-Bedding	
	Graded-Bedding	
	Fining Upward	X
	Burrows:	
	Surface Trace	X
	Shallow Surface Trace	
	Below Substrate Circular Holes	
	Subsurface Mining	
	Escape / Vertical	X
	Cryptic	X

Hand Lens Observations:		
Glauconite Present?	X	
Laminations:	X	
Bioturbation:		
None:	X	
Slight:		
Moderate:	X	
Extensive::		
Micro-faulting		
Organic Rich Layers	X	
Facies Present	I, II	
OVERALL LITHOLOGIES		
	Limestone	
	Silty Mudstone	X
	Siltstone	
	Argillaceous Limestone	
	Calcareous Mudstone	
	Argillaceous Siltstone	
	Dolomite	
	Dolomitic Limestone	

Points of Interest

Micro-hummocky and wavy laminations
Glauconite is very abundant as a psedomatrix with clay
Sparry calcite in veins
some glauconite grains have an oxidation coating

Percent Composition:	
Brown	73.6
Green	12.0
White	14.7
Total	100.3

Thin Section:

Scale Bar = 1 mm
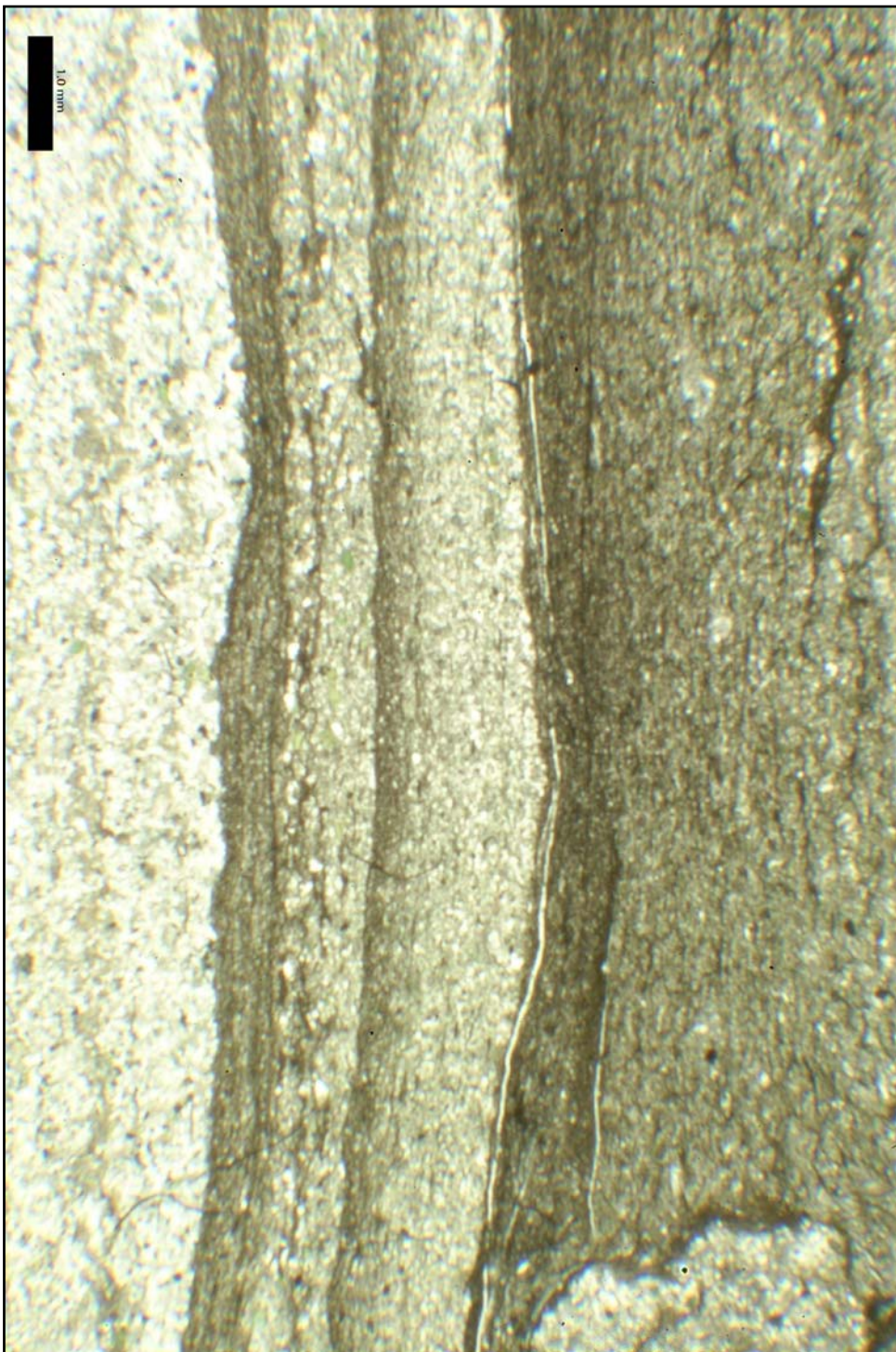
Points of Interest:

Scale Bar = 1 mm

SPECIMEN #	1504' Down Hole Footage	
FORMATION	Rogersville Shale	
MEMBER		
TEXTURE:		
Median GS	0.0251 mm	
Sorting	Poor	
Roundness	Subangular→ Subround	
Sphericity	Low	
Packing	Dense	
GRAINS:		PRESENT
QUARTZ		
	Round	
	Broken Round	X
	Angular	
	Qtz. Overgrowth	
FELDSPAR		
	K-Spar	X
	Plagioclase	
CARBONATES		
	Calcite	
	Sparry	X
	Micrite	
	Void Filling	
	Dolomite	
	Replacement Dolomite	
GLAUCONITE		
	Pelloidal	X
	Clay-Glauconite Intermediate	X
	Platy	
	Vermiform or Zebra	
	Replacement	
OTHER MINERALS		
	Phosphatic Material (Collophane)	X
	Chert	X
	Clay	X
	Biotite	
	Muscovite	
	Ooids	
	Fecal Pellets	X

ACCESSORIES		
	Organic Matter	X
	Heavy Minerals	
	Ironsulfide (Pyrite?)	X
	Ironoxide (Hematite/Illmenite?)	X
FOSSILS		
	Shell Fragments	X
	Other:	
MICROFOSSILS		
	Cryptospores	
	Acritarchs	
CEMENTS		
	Calcite	
	Sparry	
	Micrite	
	Dolomite	
	Chert	
	Phosphate	
	Clay-Glauconite Intermediate	
	Quartz	
	Clay	
SECONDARY FEATURES:	Vugs	
	Stylolites	
	Soft Sediment Deformation	
SEDIMENTARY STRUCTURES:	Finely Laminated	
	Thickly Laminated	
	Wavy Laminated	X
	Lenticular Laminated	
	Mud Cracks	
	Cross-Bedding	
	Graded-Bedding	
	Fining Upward	
	Burrows:	
	Surface Trace	X
	Shallow Surface Trace	
	Below Substrate Circular Holes	
	Subsurface Mining	X
	Escape / Vertical	
	Cryptic	X

Hand Lens Observations:		
Glauconite Present?	X	
Laminations:	X	
Bioturbation:		
None:		
Slight:		
Moderate:	X	
Extensive::		
Micro-faulting	X	
Organic Rich Layers	X	
Facies Present	I, II, III	
OVERALL LITHOLOGIES	Limestone	
	Mudstone	
	Siltstone	
	Argillaceous Limestone	
	Calcareous Mudstone	
	Argillaceous Siltstone	X
	Dolomite	
	Dolomitic Limestone	

Percent Composition:	
Brown	49.9
Green	27.6
White	23.0
Total	100.5

Points of Interest:

Burrow interiors have an increaded chert content and sparry calcite
Laminations are abundant, but vary in width

Thin Section:

Scale Bar = 1 mm
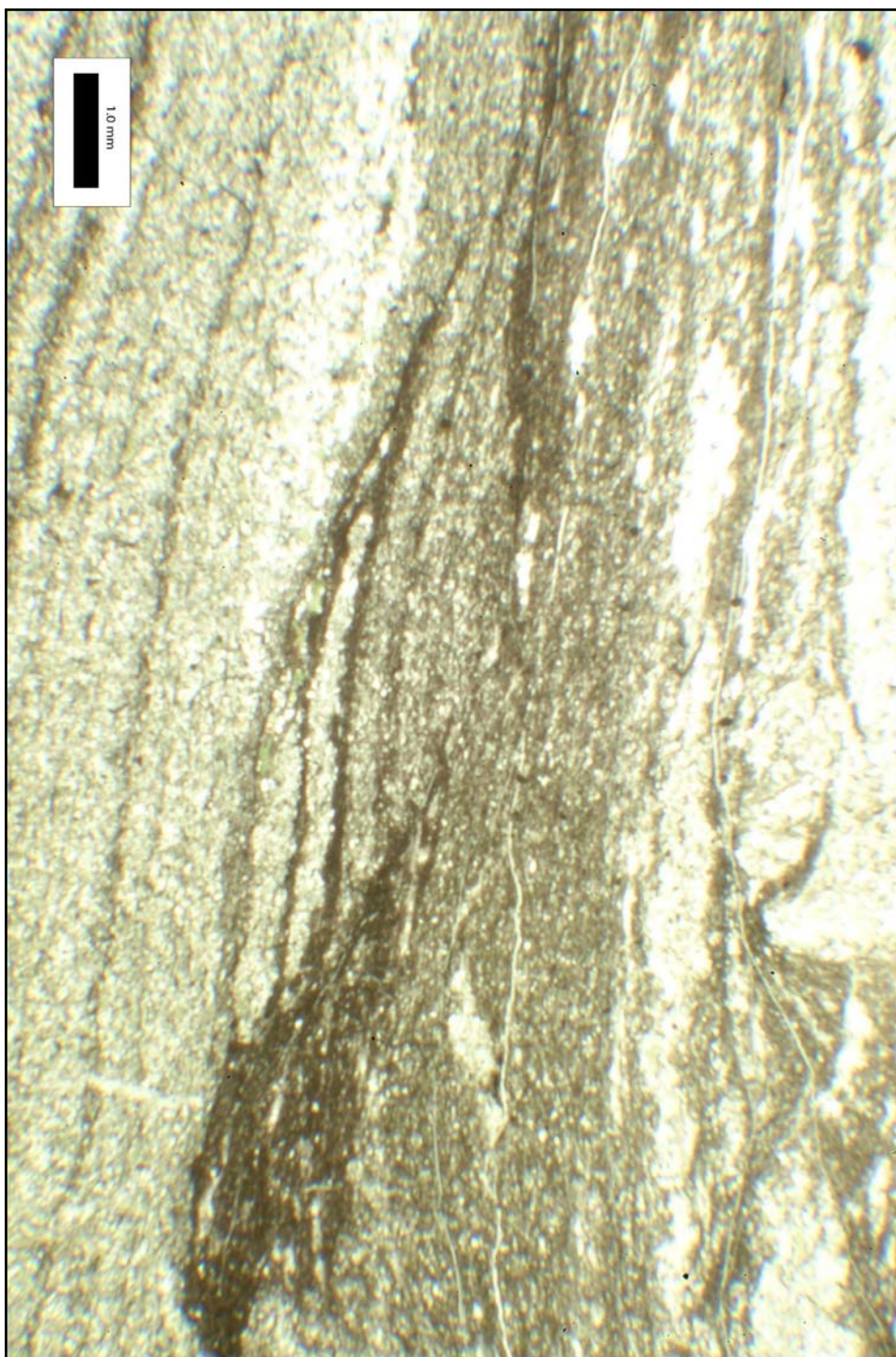
SPECIMEN #	1512.5' Down Hill Footage	
FORMATION	Rogersville Shale	
MEMBER		
TEXTURE:		
Median GS	0.0302 mm	
Sorting	Poor	
Roundness	Subangular→ Subround	
Sphericity	Low	
Packing	Dense	
GRAINS:		PRESENT
QUARTZ		
	Round	X
	Broken Round	X
	Angular	X
	Qtz. Overgrowth	
FELDSPAR		
	K-Spar	X
	Plagioclase	
CARBONATES		
	Calcite	X
	Sparry	
	Micrite	
	Void Filling	
	Dolomite	
	Replacement Dolomite	
GLAUCONITE		
	Pelloidal	X
	Clay-Glauconite Intermediate	X
	Platy	
	Vermiform or Zebra	
	Replacement	
OTHER MINERALS		
	Phosphatic Material (Collophane)	
	Chert	
	Clay	
	Biotite	
	Muscovite	
	Ooids	
	Fecal Pellets	

ACCESSORIES		
	Organic Matter	
	Heavy Minerals	
	Ironsulfide (Pyrite?)	X
	Ironoxide (Hematite/Illmenite?)	X
FOSSILS		
	Shell Fragments	X
	Other:	
MICROFOSSILS		
	Cryptospores	
	Acritarchs	
CEMENTS		
	Calcite	
	Sparry	X
	Micrite	
	Dolomite	
	Chert	
	Phosphate	
	Clay-Glauconite Intermediate	
	Quartz	
	Clay	
SECONDARY	Vugs	
FEATURES:	Stylolites	
	Soft Sediment Deformation	
	Finely Laminated	
STRUCTURES:	Thickly Laminated	
	Wavy Laminated	X
	Lenticular Laminated	
	Mud Cracks	
	Cross-Bedding	
	Graded-Bedding	
	Fining Upward	
	Burrows:	
	Surface Trace	
	Shallow Surface Trace	
	Below Substrate Circular Holes	
	Subsurface Mining	X
	Escape / Vertical	
	Cryptic	X

Hand Lens Observations:		
Glauconite Present?	X	
Laminations:	X	
Bioturbation:		
None:		
Slight:	X	
Moderate:		
Extensive::		
Micro-faulting	X	
Organic Rich Layers	X	
Facies Present	I, II, III	
OVERALL LITHOLOGIES		
	Limestone	
	Silty Mudstone	X
	Siltstone	
	Argillaceous Limestone	
	Calcareous Mudstone	
	Argillaceous Siltstone	X
	Dolomite	
	Dolomitic Limestone	

Percent Composition:	
Brown	39.2
Green	45.1
White	16.0
Total	100.3

Points of Interest:

Sparry calcite vein along a microfault

Thin Section:

Scale Bar = 1 mm
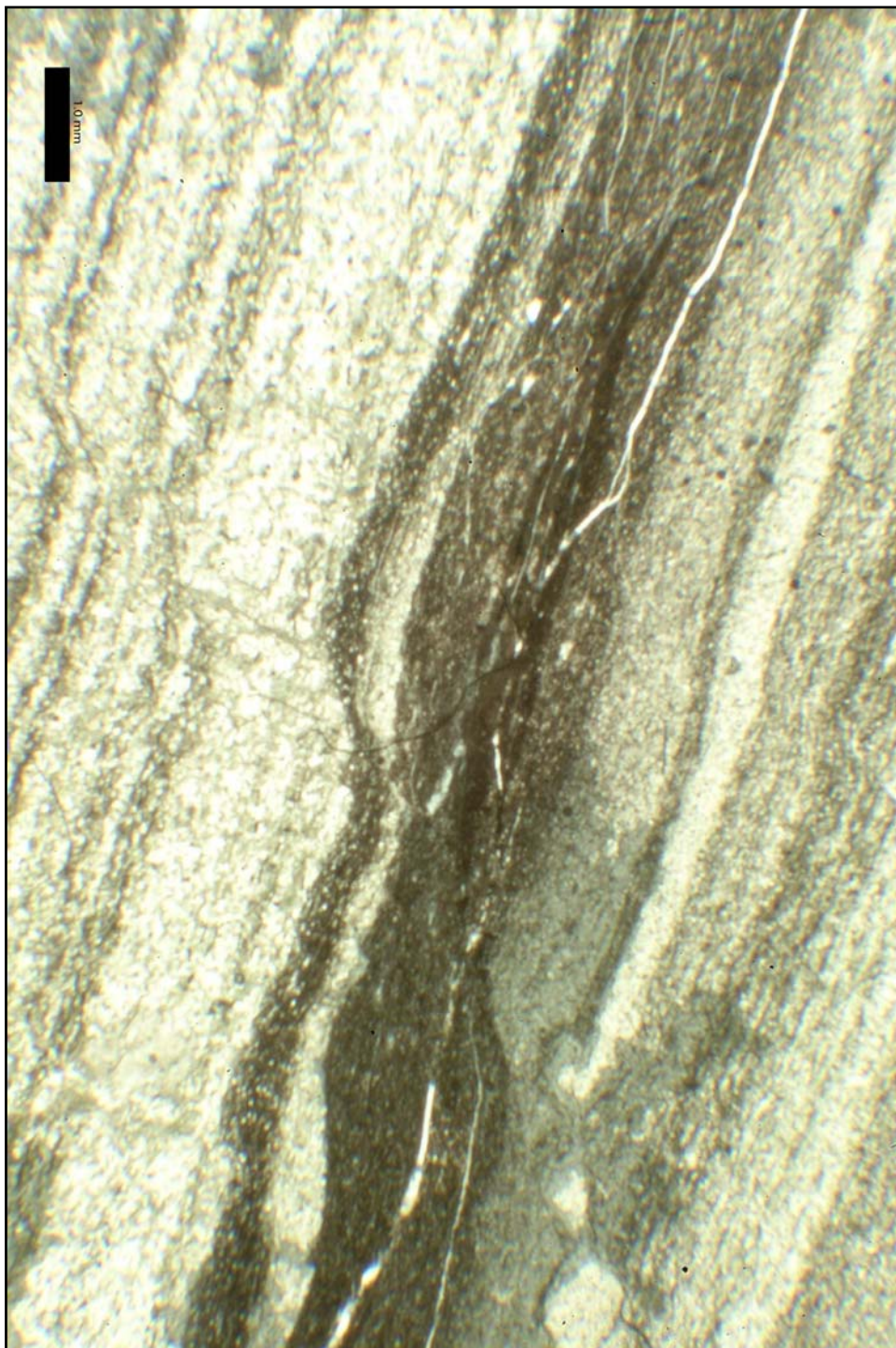
SPECIMEN #	1519.5' Down Hole Footage	
FORMATION	Rogersville Shale	
MEMBER		
TEXTURE:		
Median GS	0.0421 mm Qtz, 0.679 mm Shell	
Sorting	Poor	
Roundness	Angular→ Subround	
Sphericity	Low	
Packing	Dense	
GRAINS:		PRESENT
QUARTZ		
	Round	X
	Broken Round	X
	Angular	X
	Qtz. Overgrowth	
FELDSPAR		
	K-Spar	X
	Plagioclase	
CARBONATES		
	Calcite	
	Sparry	X
	Micrite	
	Void Filling	
	Dolomite	X
	Replacement Dolomite	X
GLAUCONITE		
	Pelloidal	X
	Clay-Glauconite Intermediate	X
	Platy	
	Vermiform or Zebra	
	Replacement	
OTHER MINERALS		
	Phosphatic Material (Collophane)	X
	Chert	X
	Clay	
	Biotite	
	Muscovite	
	Ooids	
	Fecal Pellets	X

ACCESSORIES		
	Organic Matter	
	Heavy Minerals	
	Ironsulfide (Pyrite?)	X
	Ironoxide (Hematite/Illmenite?)	X
FOSSILS		
	Shell Fragments	X
	Other:	
MICROFOSSILS		
	Cryptospores	
	Acritarchs	
CEMENTS		
	Calcite	
	Sparry	X
	Micrite	
	Dolomite	X
	Chert	
	Phosphate	
	Clay-Glauconite Intermediate	X
	Quartz	
	Clay	
SECONDARY FEATURES:	Vugs	
	Stylolites	
	Soft Sediment Deformation	
SEDIMENTARY STRUCTURES:	Finely Laminated	X
	Thickly Laminated	
	Wavy Laminated	
	Lenticular Laminated	
	Mud Cracks	
	Cross-Bedding	
	Graded-Bedding	
	Fining Upward	
	Burrows:	
	Surface Trace	
	Shallow Surface Trace	X
	Below Substrate Circular Holes	
	Subsurface Mining	X
	Escape / Vertical	
	Cryptic	X

Hand Lens Observations:		
Glauconite Present?	X	
Laminations:	X	
Bioturbation:		
None:		
Slight:	X	
Moderate:		
Extensive::		
Micro-faulting		
Organic Rich Layers	X	
Facies Present	I, II, III	
OVERALL LITHOLOGIES	Limestone	
	Mudstone	
	Siltstone	
	Argillaceous Limestone	X
	Calcareous Mudstone	
	Argillaceous Siltstone	
	Dolomite	X
	Dolomitic Limestone	
Points of Interest		

Abundance of dolomite

Several large void spaces cover this slide

Percent Composition:	
Brown	40.9
Green	19.3
White	33.3
Total	93.5

**There is a large void space in this photograph that is not represented in the total of the percent composition which may be a reason for the 6.5 % discrepancy in the total

Thin Section

Scale Bar = 1 mm
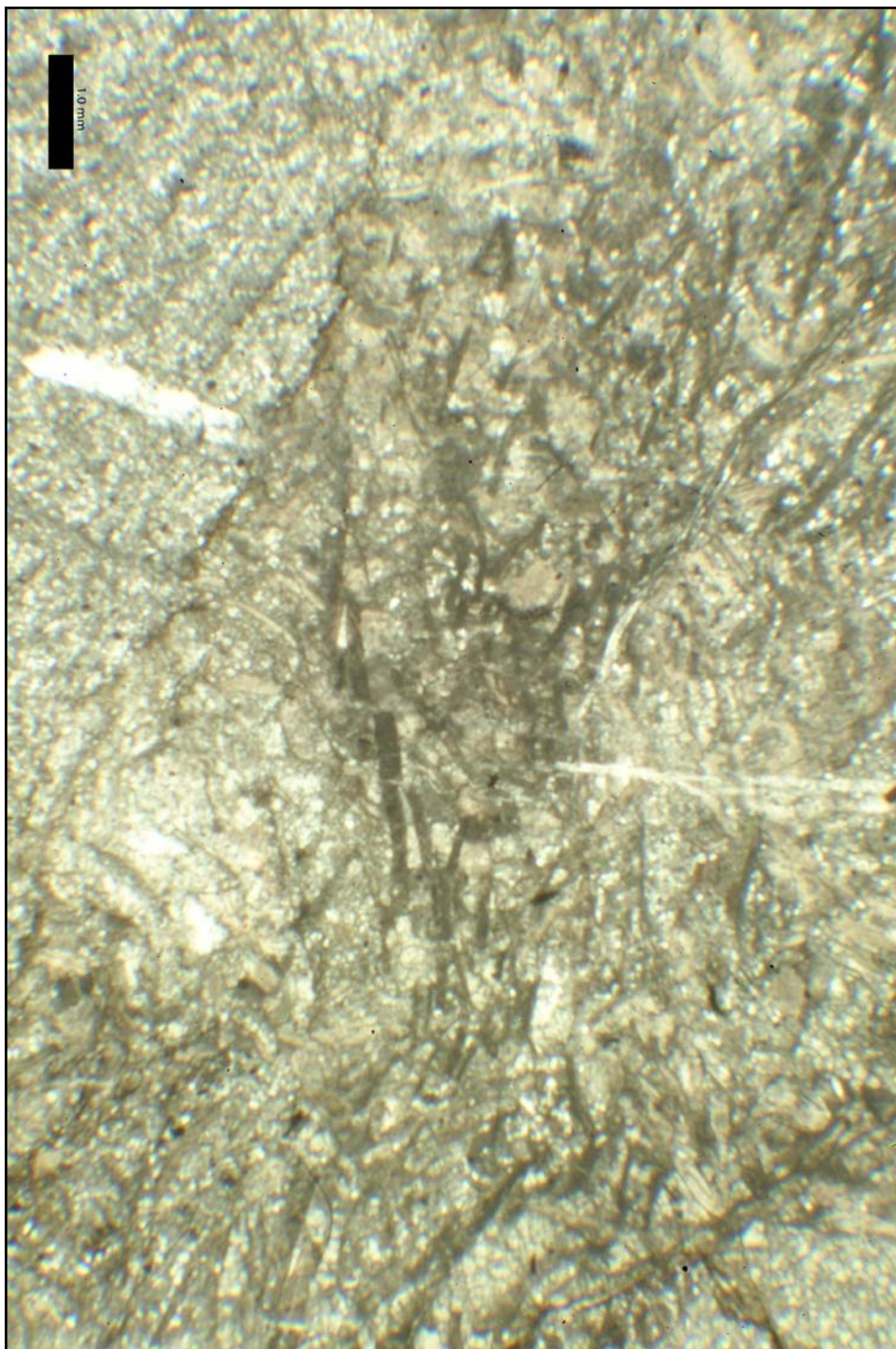
SPECIMEN #	1523' Down Hole Footage	
FORMATION	Rogersville Shale	
MEMBER		
TEXTURE:		
Median GS	0.4495 mm Qtz, 0.155mm Glauc.	
Sorting	Poor	
Roundness	Angular→ Subround	
Sphericity	Low	
Packing	Dense	
GRAINS:		PRESENT
QUARTZ		
	Round	X
	Broken Round	X
	Angular	X
	Qtz. Overgrowth	
FELDSPAR		
	K-Spar	X
	Plagioclase	
CARBONATES		
	Calcite	X
	Sparry	
	Micrite	
	Void Filling	
	Dolomite	
	Replacement Dolomite	
GLAUCONITE		
	Pelloidal	X
	Clay-Glauconite Intermediate	X
	Platy	X
	Vermiform or Zebra	
	Replacement	
OTHER MINERALS		
	Phosphatic Material (Collophane)	X
	Chert	X
	Clay	X
	Biotite	
	Muscovite	
	Ooids	
	Fecal Pellets	X

ACCESSORIES		
	Organic Matter	
	Heavy Minerals	
	Ironsulfide (Pyrite?)	X
	Ironoxide (Hematite/Illmenite?)	X
FOSSILS		
	Shell Fragments	
	Other:	
MICROFOSSILS		
	Cryptospores	
	Acritarchs	
CEMENTS		
	Calcite	
	Sparry	X
	Micrite	
	Dolomite	
	Chert	
	Phosphate	
	Clay-Glauconite Intermediate	X
	Quartz	
	Clay	
SECONDARY FEATURES:	Vugs	
	Stylolites	
	Soft Sediment Deformation	
SEDIMENTARY STRUCTURES:	Finely Laminated	X
	Thickly Laminated	
	Wavy Laminated	
	Lenticular Laminated	
	Mud Cracks	
	Cross-Bedding	
	Graded-Bedding	
	Fining Upward	X
	Burrows:	
	Surface Trace	
	Shallow Surface Trace	X
	Below Substrate Circular Holes	X
	Subsurface Mining	
	Escape / Vertical	
	Cryptic	X

Hand Lens Observations:		
Glauconite Present?	X	
Width of Laminations:	0.7795 mm (median)	
Bioturbation:		
None:		
Slight:	X	
Moderate:		
Extensive::		
Micro-faulting		
Organic Rich Layers	X	
Facies Present	I, II, III	
OVERALL LITHOLOGIES	Limestone	
	Silty Mudstone	X
	Siltstone	
	Argillaceous Limestone	
	Calcareous Mudstone	
	Argillaceous Siltstone	X
	Dolomite	
	Dolomitic Limestone	
Points of Interest:		

Note below substrate circular burrow in lower photograph

Percent Composition:	
Brown	52.5
Green	2.3
White	45.9
Total	100.7

Thin Section
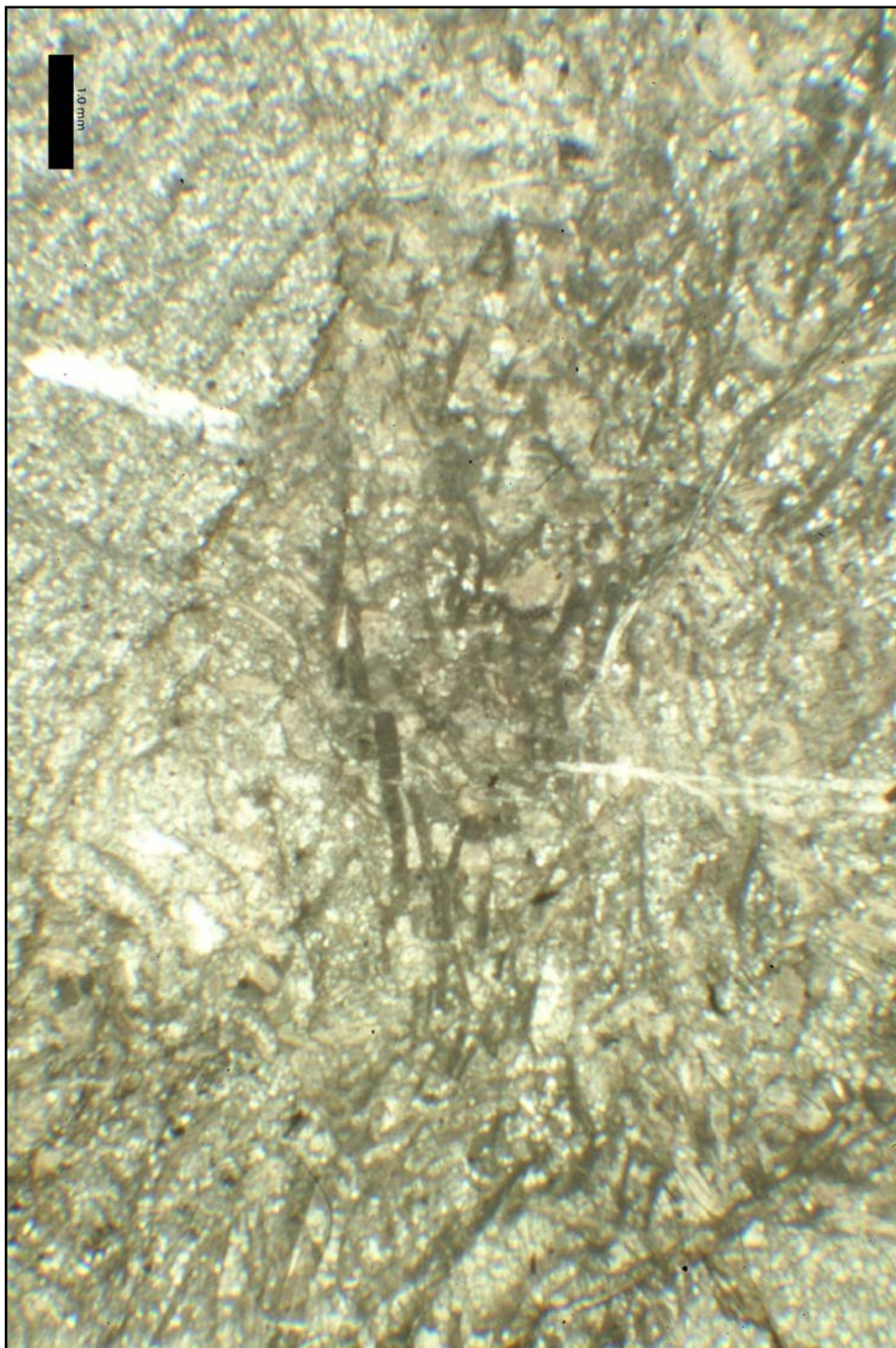
Scale Bar = 1 mm

Points of Interest:

Scale Bar = 1 mm
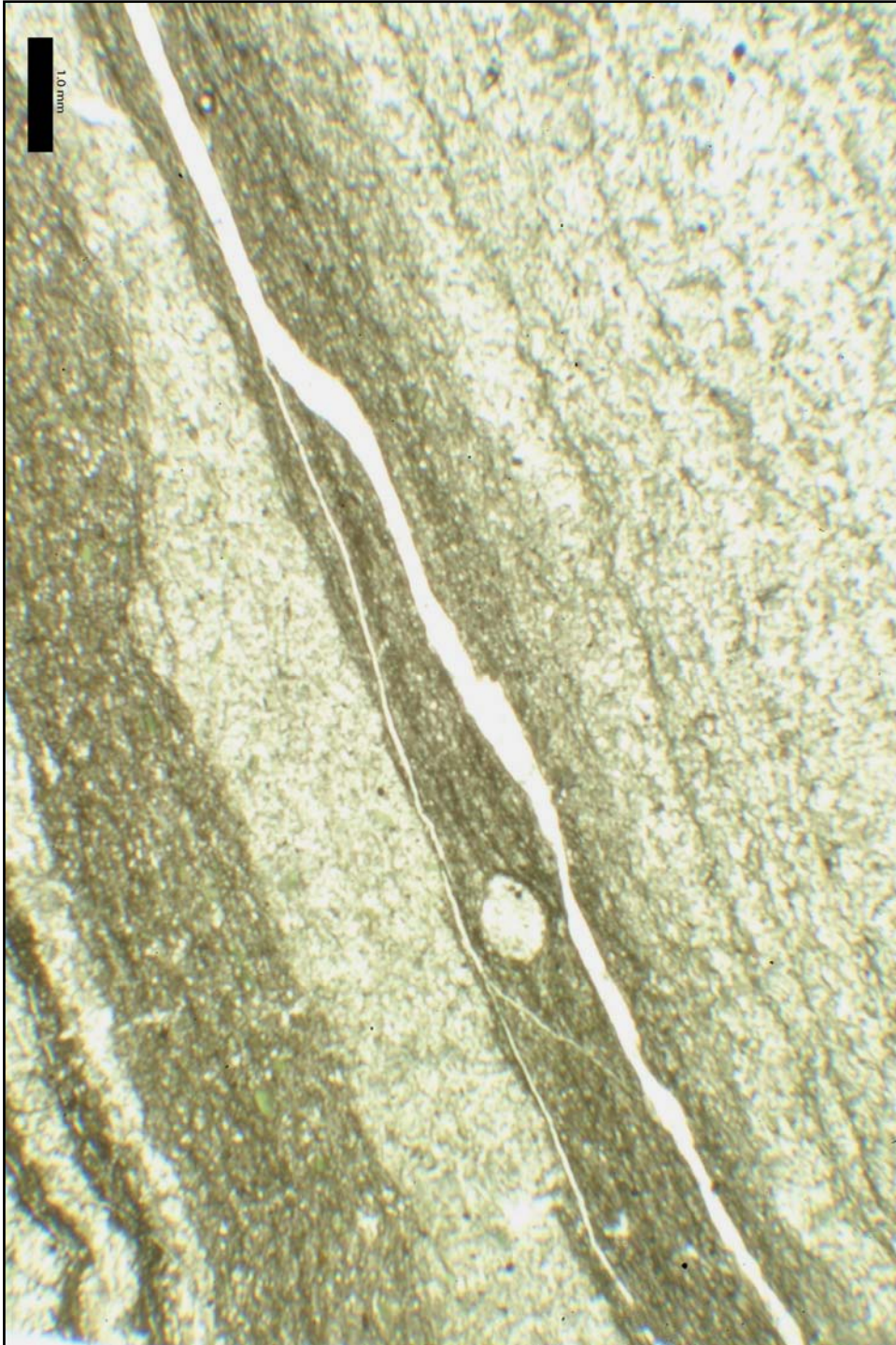
SPECIMEN #	1524.5' Down Hole Footage	
FORMATION	Rogersville Shale	
MEMBER		
TEXTURE:		
Median GS	0.0746 mm Qtz,	
Sorting	Poor	
Roundness	Subangular→ Subround	
Sphericity	Low	
Packing	Dense	
GRAINS:		PRESENT
QUARTZ		
	Round	X
	Broken Round	X
	Angular	X
	Qtz. Overgrowth	
FELDSPAR		
	K-Spar	X
	Plagioclase	
CARBONATES		
	Calcite	X
	Sparry	
	Micrite	
	Void Filling	
	Dolomite	X
	Replacement Dolomite	
GLAUCONITE		
	Pelloidal	X
	Clay-Glauconite Intermediate	X
	Platy	X
	Vermiform or Zebra	X
	Replacement	
OTHER MINERALS		
	Phosphatic Material (Collophane)	X
	Chert	X
	Clay	X
	Biotite	
	Muscovite	
	Ooids	
	Fecal Pellets	X

ACCESSORIES		
	Organic Matter	
	Heavy Minerals	
	Ironsulfide (Pyrite?)	X
	Ironoxide (Hematite/Illmenite?)	X
FOSSILS		
	Shell Fragments	X
	Other:	
MICROFOSSILS		
	Cryptospores	
	Acritarchs	
CEMENTS		
	Calcite	
	Sparry	X
	Micrite	
	Dolomite	
	Chert	
	Phosphate	
	Clay-Glauconite Intermediate	X
	Quartz	
	Clay	X
SECONDARY FEATURES:	Vugs	
	Stylolites	
	Soft Sediment Deformation	
SEDIMENTARY STRUCTURES	Finely Laminated	X
	Thickly Laminated	
	Wavy Laminated	
	Lenticular Laminated	
	Mud Cracks	
	Cross-Bedding	
	Graded-Bedding	
	Fining Upward	X
	Burrows:	
	Surface Trace	
	Shallow Surface Trace	
	Below Substrate Circular Holes	
	Subsurface Mining	X
	Escape / Vertical	
	Cryptic	

Hand Lens Observations:		
Glauconite Present?	X	
Laminations:	X	
Bioturbation:		
None:		
Slight:		
Moderate:	X	
Extensive::		
Micro-faulting		
Organic Rich Layers	X	
Facies Present	IV	
OVERALL LITHOLOGIES	Limestone	
	Mudstone	
	Siltstone	X
	Argillaceous Limestone	
	Calcareous Mudstone	
	Argillaceous Siltstone	
	Dolomite	
	Dolomitic Limestone	
Points of Interest		

Other median grain sizes:
   Pellets replaced by calcite 0.479
   Pellets replaced by glauconite 0.379
   Shell fragments 0.708

Percent Composition:
     Brown   50.6
     Green   40.7
     White   8.3
     Total   99.6

Thin Section

Scale Bar = 1 mm
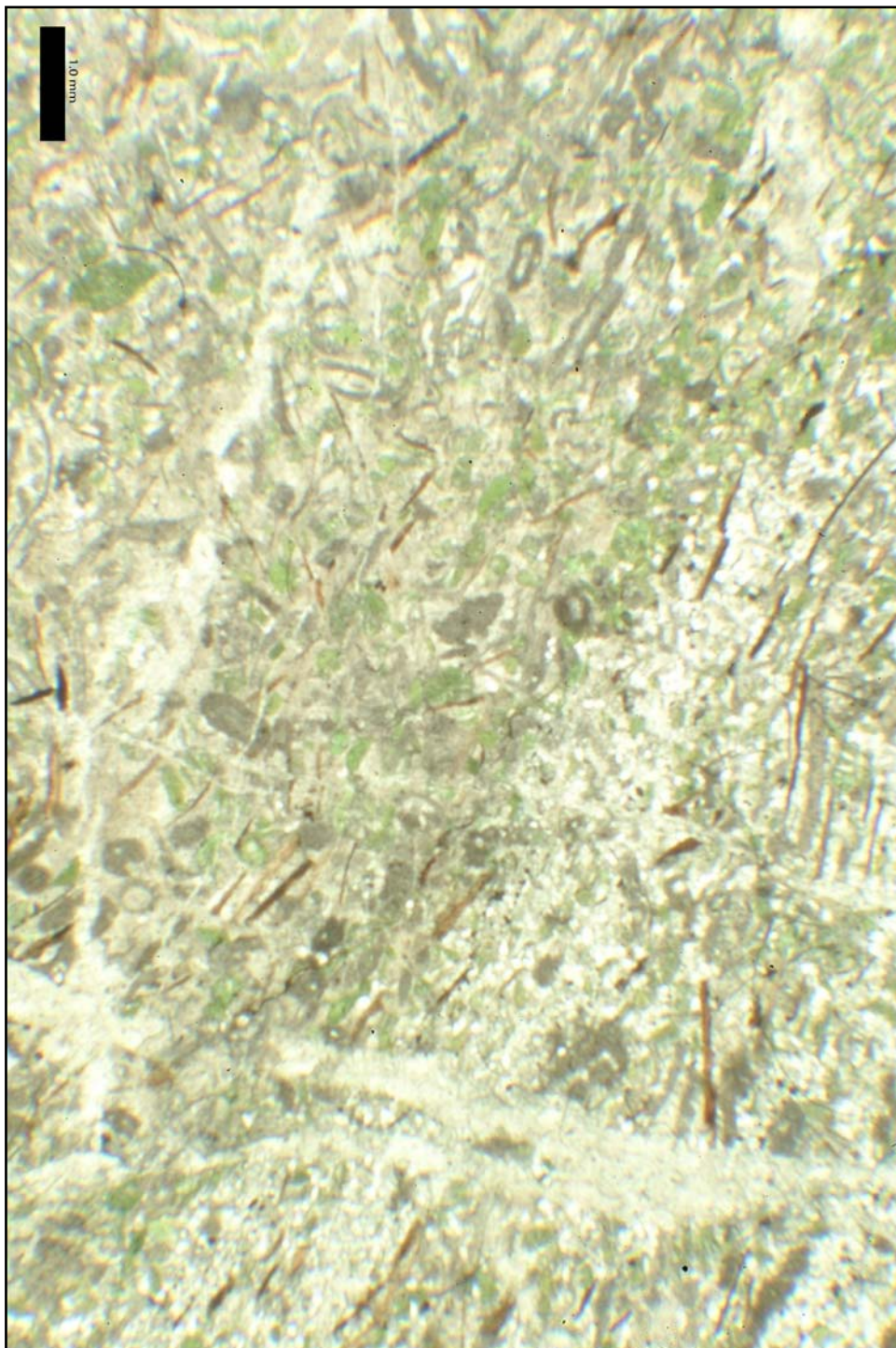
Points of Interest:

Scale Bar = 1 mm
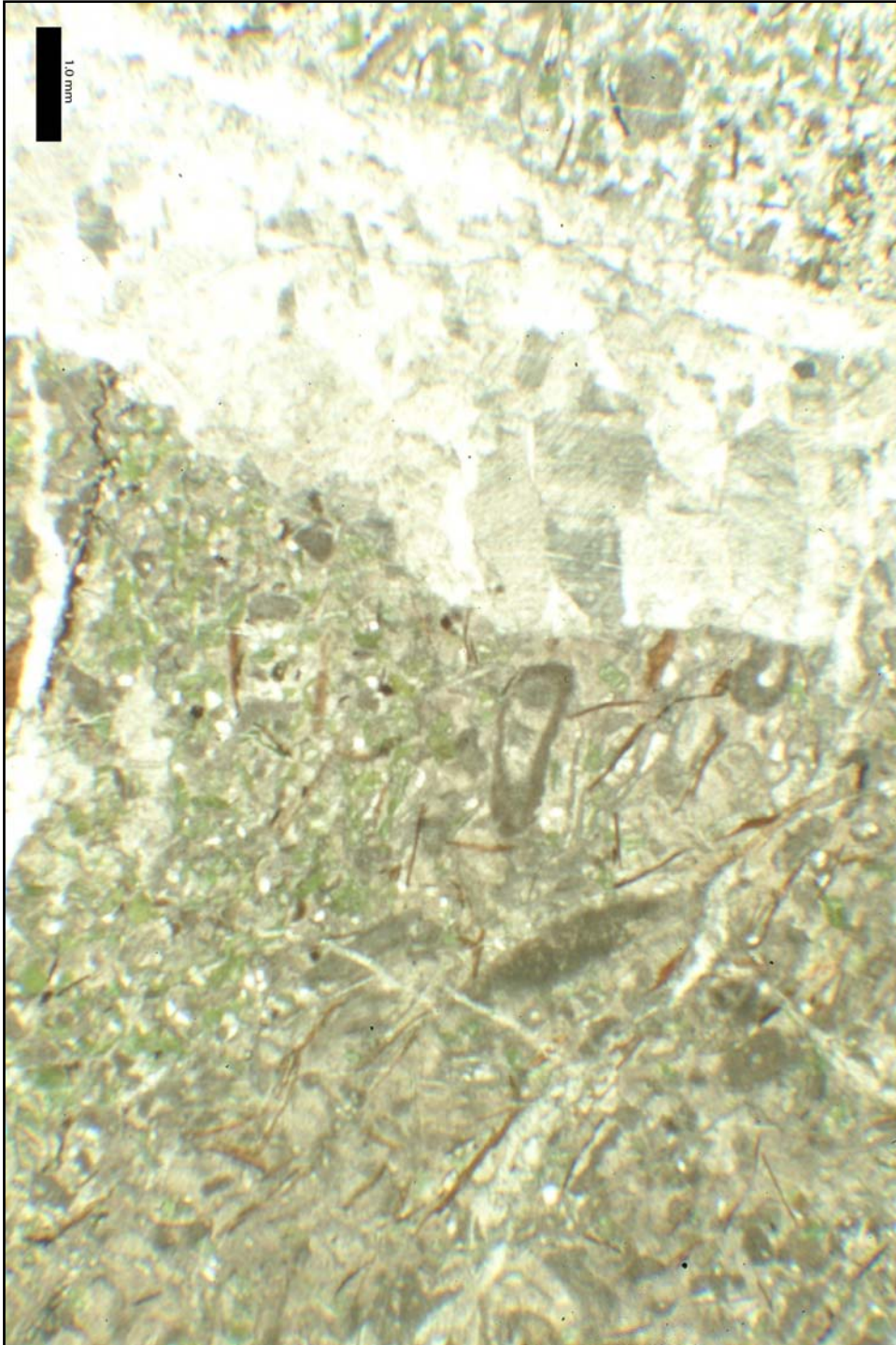
SPECIMEN #	1535 Down Hole Footage	
FORMATION	Rogersville Shale	
MEMBER		
TEXTURE:		
Median GS	0.0443 mm	
Sorting	Poor	
Roundness	Subangular→ Subround	
Sphericity	Low	
Packing	Dense	
GRAINS:		PRESENT
QUARTZ		
	Round	X
	Broken Round	X
	Angular	X
	Qtz. Overgrowth	
FELDSPAR		
	K-Spar	X
	Plagioclase	
CARBONATES		
	Calcite	
	Sparry	X
	Micrite	
	Void Filling	
	Dolomite	
	Replacement Dolomite	
GLAUCONITE		
	Pelloidal	X
	Clay-Glauconite Intermediate	X
	Platy	X
	Vermiform or Zebra	
	Replacement	
OTHER MINERALS		
	Phosphatic Material (Collophane)	X
	Chert	X
	Clay	X
	Biotite	
	Muscovite	
	Ooids	
	Fecal Pellets	

ACCESSORIES		
	Organic Matter	
	Heavy Minerals	
	Ironsulfide (Pyrite?)	X
	Ironoxide (Hematite/Illmenite?)	X
FOSSILS		
	Shell Fragments	X
	Other:	
MICROFOSSILS		
	Cryptospores	
	Acritarchs	
CEMENTS		
	Calcite	X
	Sparry	
	Micrite	
	Dolomite	
	Chert	
	Phosphate	
	Clay-Glauconite Intermediate	X
	Quartz	
	Clay	X
SECONDARY FEATURES:	Vugs	
	Stylolites	
	Soft Sediment Deformation	
SEDIMENTARY STRUCTURES:	Finely Laminated	X
	Thickly Laminated	
	Wavy Laminated	
	Lenticular Laminated	
	Mud Cracks	
	Cross-Bedding	
	Graded-Bedding	
	Fining Upward	X
	Burrows:	
	Surface Trace	
	Shallow Surface Trace	X
	Below Substrate Circular Holes	
	Subsurface Mining	X
	Escape / Vertical	
	Cryptic	

Hand Lens Observations:		
Glauconite Present?	X	
Laminations:	X	
Bioturbation:		
None:		
Slight:		
Moderate:		
Extensive::	X	
Micro-faulting		
Organic Rich Layers	X	
Facies Present	I, II, III	
OVERALL LITHOLOGIES	Limestone	
	Silty Mudstone	X
	Siltstone	
	Argillaceous Limestone	
	Calcareous Mudstone	
	Argillaceous Siltstone	X
	Dolomite	
	Dolomitic Limestone	
Points of Interest:		

Bedding is actually vertical in this slide. Most likely part of a fold

Pyrite is very abundant

Percent Composition:	
Brown	35.4
Green	0.9
White	64.9
Total	101.2

Thin Section

Scale Bar = 1 mm
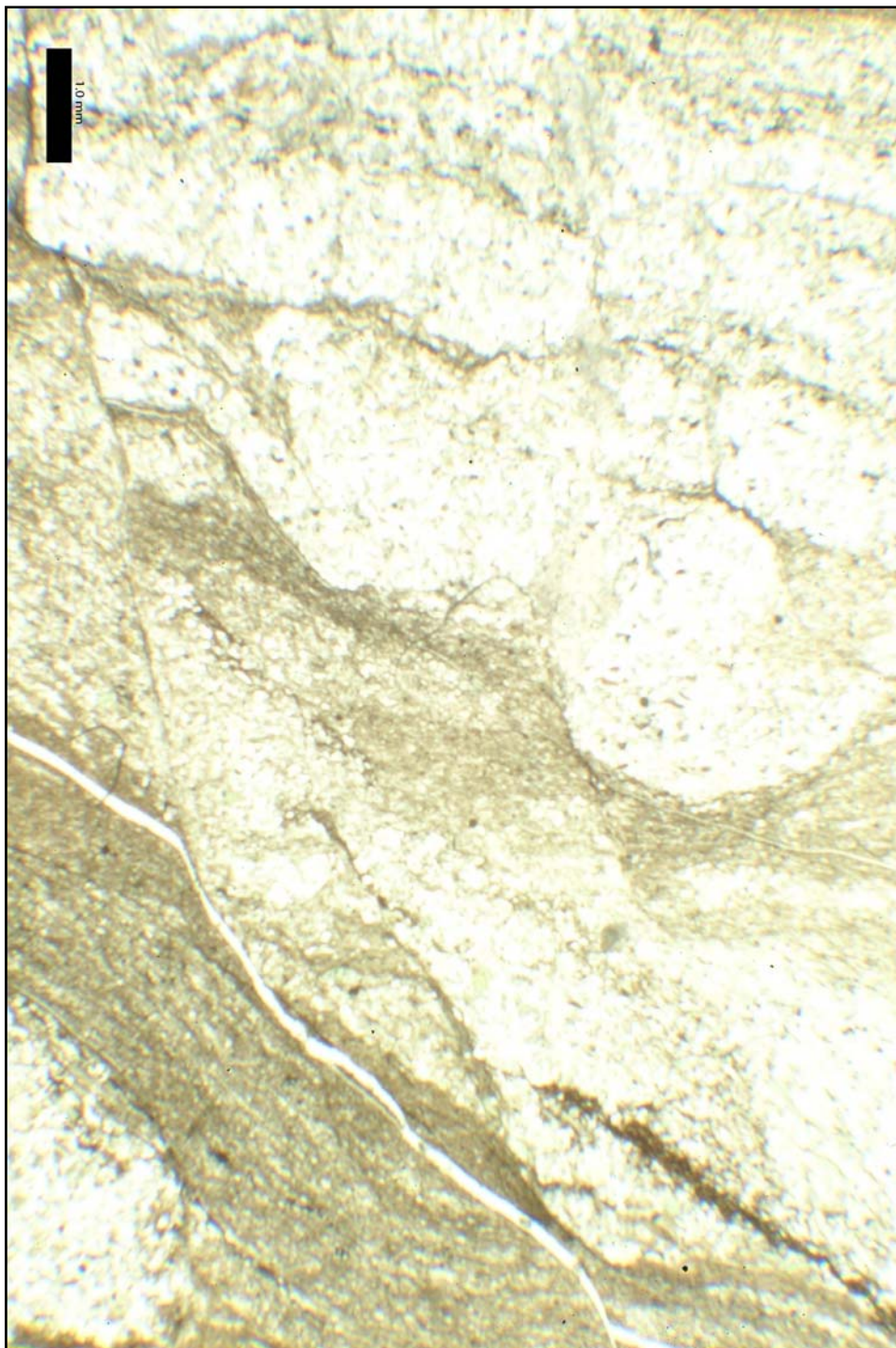
Points of Interest:

Scale Bar = 1 mm
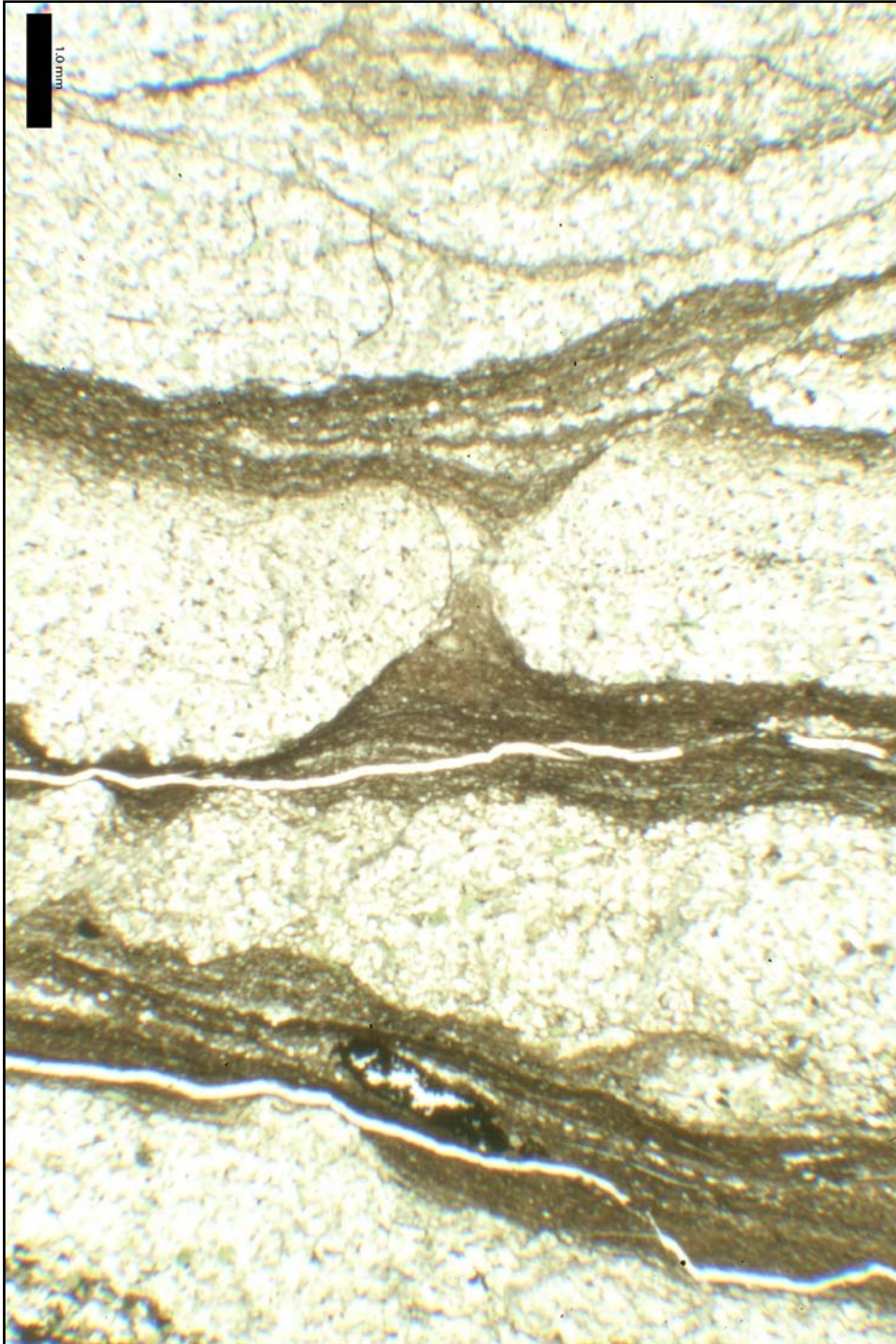
SPECIMEN #	1541' Down Hole Footage	
FORMATION	Rogersville Shale	
MEMBER		
TEXTURE:		
Median GS	0.0365 mm	
Sorting	Poor	
Roundness	Angular→ Subround	
Sphericity	Low	
Packing	Dense	
GRAINS:		PRESENT
QUARTZ		
	Round	X
	Broken Round	X
	Angular	X
	Qtz. Overgrowth	
FELDSPAR		
	K-Spar	X
	Plagioclase	
CARBONATES		
	Calcite	
	Sparry	X
	Micrite	X
	Void Filling	
	Dolomite	
	Replacement Dolomite	
GLAUCONITE		
	Pelloidal	X
	Clay-Glauconite Intermediate	X
	Platy	X
	Vermiform or Zebra	
	Replacement	
OTHER MINERALS		
	Phosphatic Material (Collophane)	X
	Chert	X
	Clay	X
	Biotite	
	Muscovite	
	Ooids	
	Fecal Pellets	X

ACCESSORIES		
	Organic Matter	
	Heavy Minerals	
	Ironsulfide (Pyrite?)	X
	Ironoxide (Hematite/Illmenite?)	X
FOSSILS		
	Shell Fragments	X
	Other:	
MICROFOSSILS		
	Cryptospores	
	Acritarchs	
CEMENTS		
	Calcite	
	Sparry	X
	Micrite	
	Dolomite	
	Chert	
	Phosphate	
	Clay-Glauconite Intermediate	X
	Quartz	
	Clay	X
SECONDARY FEATURES:	Vugs	
	Stylolites	
	Soft Sediment Deformation	
SEDIMENTARY STRUCTURES:	Finely Laminated	X
	Thickly Laminated	
	Wavy Laminated	
	Lenticular Laminated	
	Mud Cracks	
	Cross-Bedding	
	Graded-Bedding	
	Fining Upward	
	Burrows:	
	Surface Trace	
	Shallow Surface Trace	X
	Below Substrate Circular Holes	
	Subsurface Mining	
	Escape / Vertical	
	Cryptic	X

Hand Lens Observations:		
Glauconite Present?	X	
Laminations:	X	
Bioturbation:		
None:		
Slight:	X	
Moderate:		
Extensive::		
Micro-faulting		
Organic Rich Layers	X	
Facies Present	I, II, III	
OVERALL LITHOLOGIES	Limestone	
	Silty Mudstone	
	Siltstone	
	Argillaceous Limestone	
	Calcareous Mudstone	
	Argillaceous Siltstone	X
	Dolomite	
	Dolomitic Limestone	
Points of Interest:		

Interesting feature in lower photograph. Perhaps an unidentified type of burrow.

Percent Composition:	
Brown	52.2
Green	4.2
White	42.2
Total	98.6

Thin Section

Scale Bar = 1 mm
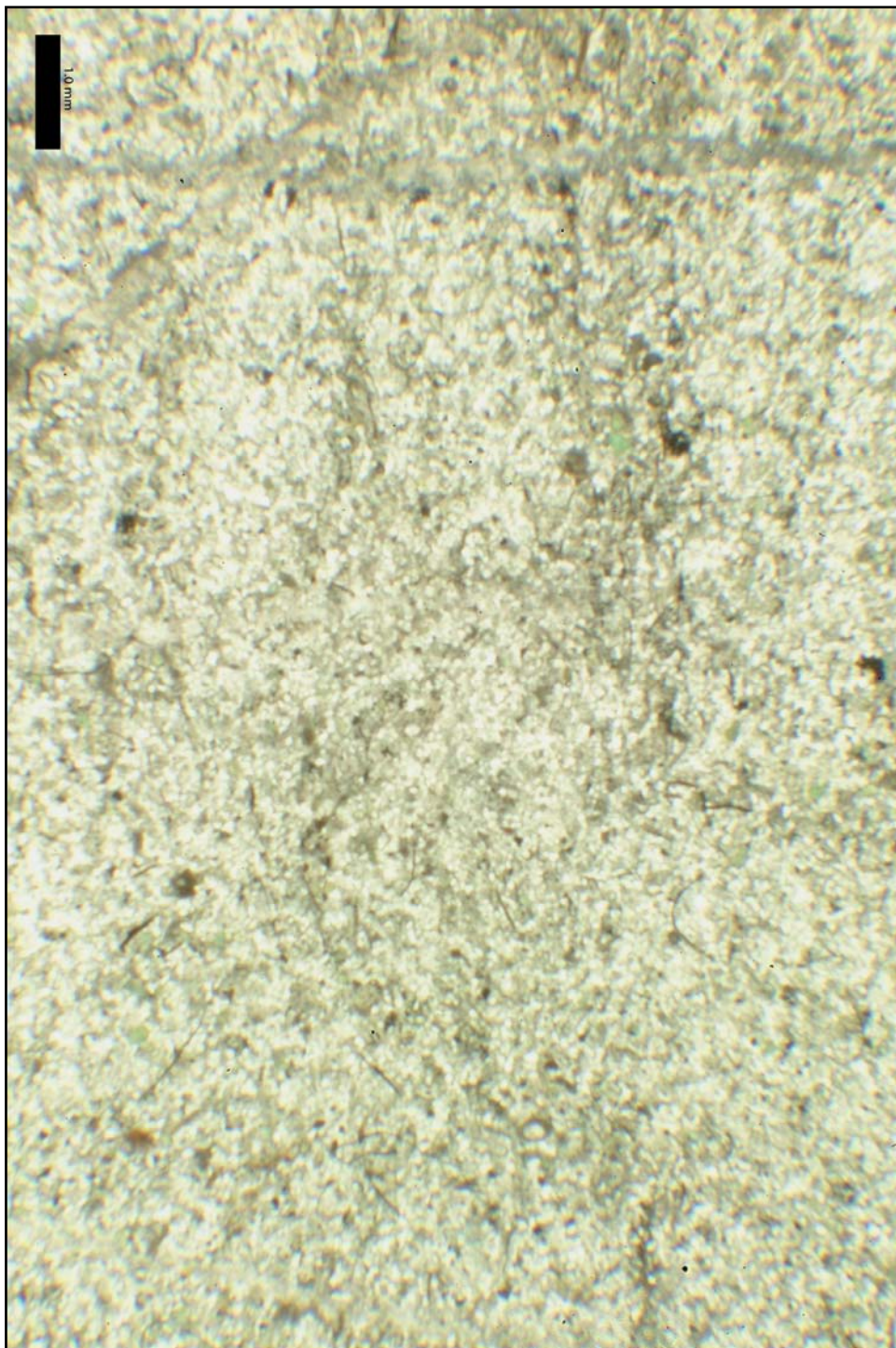
Points of Interest:

Scale Bar = 1 mm

SPECIMEN #	1549' Down Hole Footage	
FORMATION	Rogersville Shale	
MEMBER		
TEXTURE:		
Median GS	0.0519 mm	
Sorting	Poor	
Roundness	Subangular→ Subround	
Sphericity	Low	
Packing	Dense	
GRAINS:		PRESENT
QUARTZ		
	Round	X
	Broken Round	X
	Angular	X
	Qtz. Overgrowth	
FELDSPAR		
	K-Spar	X
	Plagioclase	
CARBONATES		
	Calcite	
	Sparry	X
	Micrite	
	Void Filling	
	Dolomite	
	Replacement Dolomite	
GLAUCONITE		
	Pelloidal	X
	Clay-Glauconite Intermediate	X
	Platy	X
	Vermiform or Zebra	X
	Replacement	X
OTHER MINERALS		
	Phosphatic Material (Collophane)	X
	Chert	X
	Clay	X
	Biotite	
	Muscovite	
	Ooids	
	Fecal Pellets	X

ACCESSORIES		
	Organic Matter	
	Heavy Minerals	
	Ironsulfide (Pyrite?)	X
	Ironoxide (Hematite/Illmenite?)	X
FOSSILS		
	Shell Fragments	X
	Other:	
MICROFOSSILS		
	Cryptospores	
	Acritarchs	
CEMENTS		
	Calcite	
	Sparry	
	Micrite	
	Dolomite	
	Chert	X
	Phosphate	
	Clay-Glauconite Intermediate	
	Quartz	
	Clay	X
SECONDARY FEATURES:	Vugs	
	Stylolites	
	Soft Sediment Deformation	
SEDIMENTARY STRUCTURES:	Finely Laminated	X
	Thickly Laminated	
	Wavy Laminated	
	Lenticular Laminated	
	Mud Cracks	
	Cross-Bedding	
	Graded-Bedding	
	Fining Upward	X
	Burrows:	
	Surface Trace	
	Shallow Surface Trace	X
	Below Substrate Circular Holes	
	Subsurface Mining	
	Escape / Vertical	
	Cryptic	X

Hand Lens Observations:		
Glauconite Present?	X	
Laminations:	X	
Bioturbation:		
None:		
Slight:		
Moderate:		
Extensive::	X	
Micro-faulting		
Organic Rich Layers	X	
Facies Present	I, II, III, IV	
OVERALL LITHOLOGIES	Limestone	
	Mudstone	
	Siltstone	
	Argillaceous Limestone	
	Calcareous Mudstone	
	Argillaceous Siltstone	X
	Dolomite	
	Dolomitic Limestone	
Points of Interest:		

Glauconite and shell fragments are unusually abundant.

One particular shell fragment measured 0.319 mm by 0.753 mm.

Percent Composition:	
Brown	24.8
Green	38.4
White	35.6
Total	98.8

Thin Section

Scale Bar = 1 mm
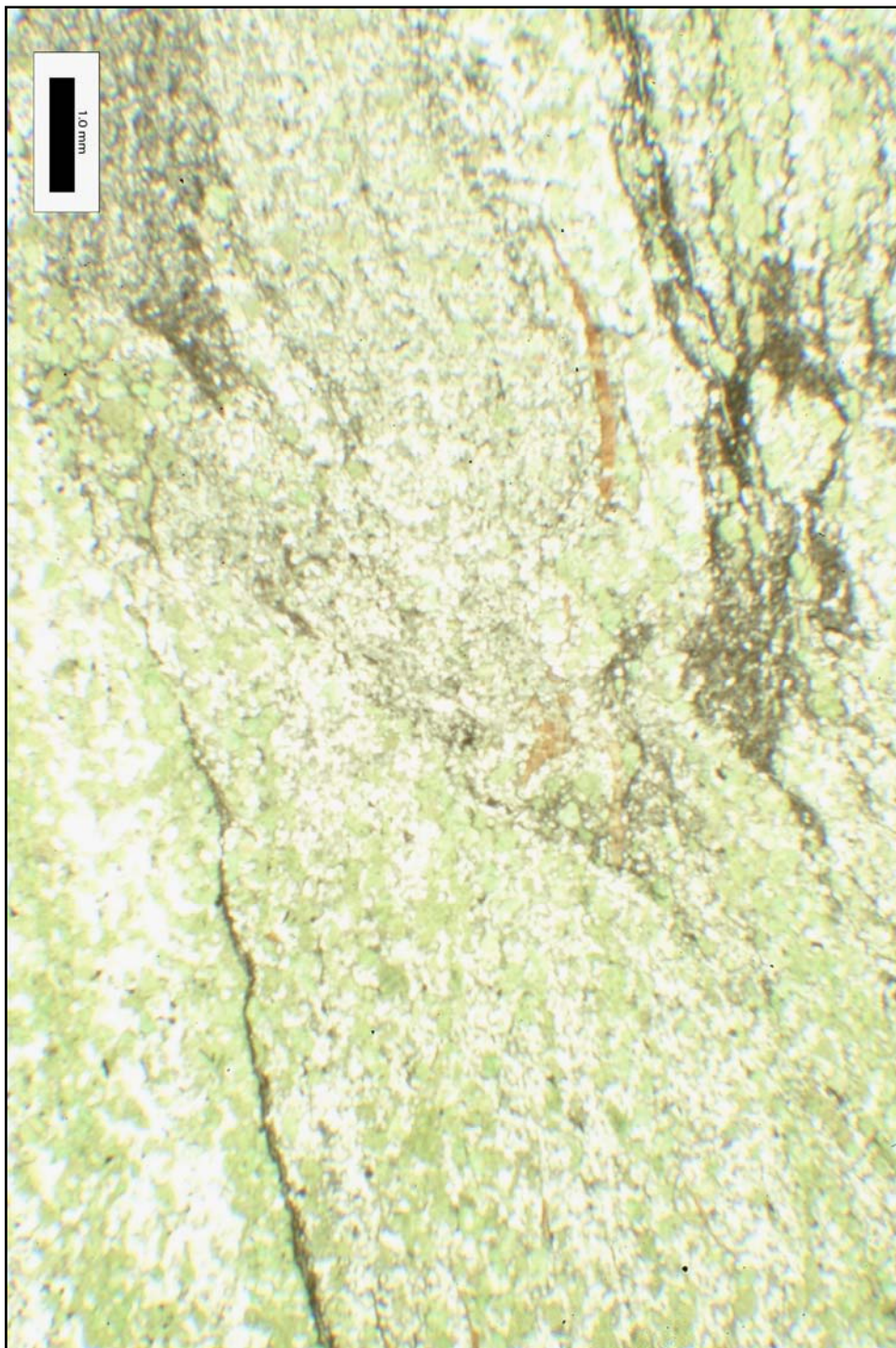
Points of Interest:

Scale Bar = 1 mm
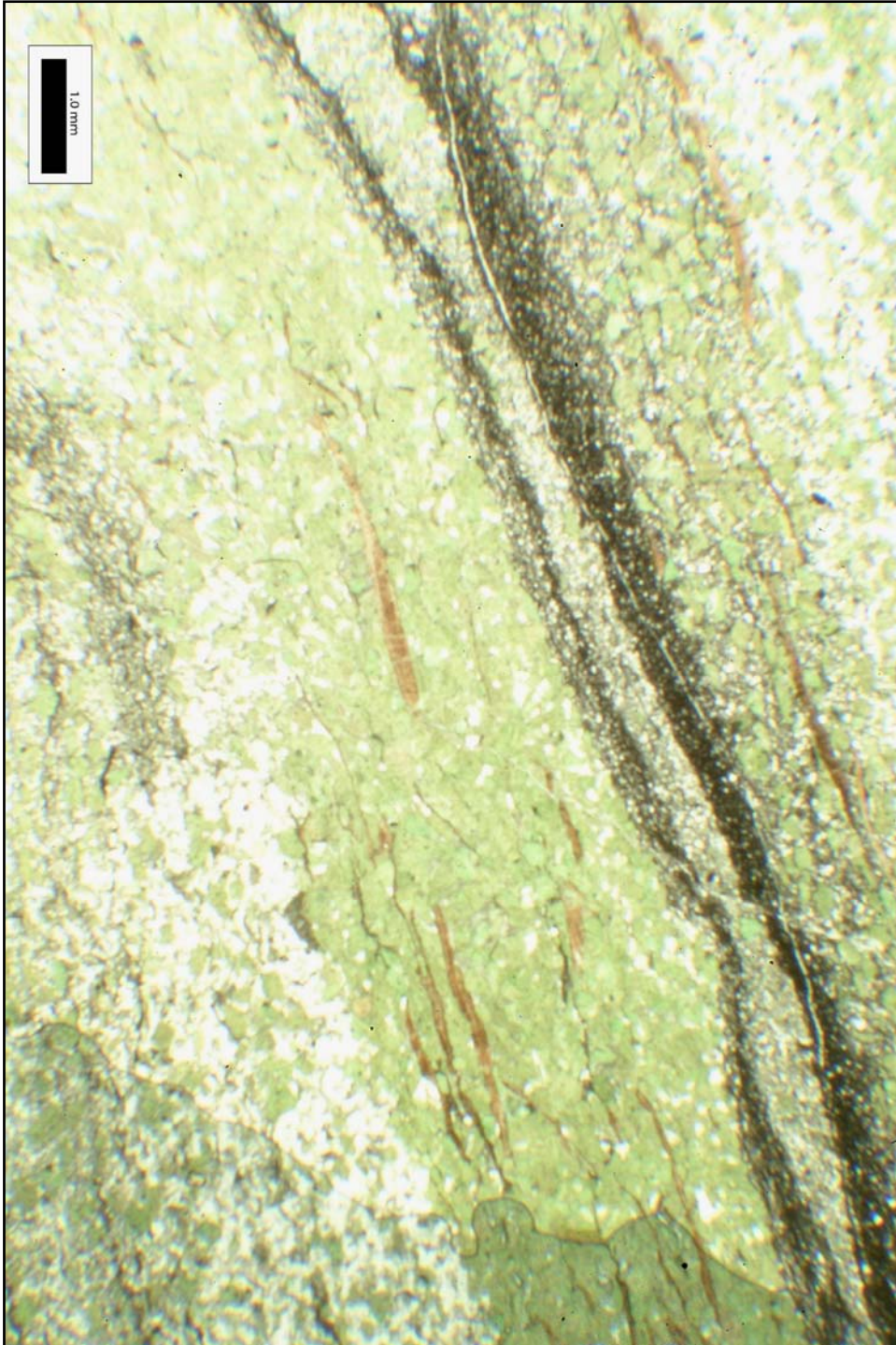
SPECIMEN #	1550' Down Hole Footage	
FORMATION	Rogersville Shale	
MEMBER		
TEXTURE:		
Median GS	0.0284 mm	
Sorting	Poor	
Roundness	Subangular→ Subround	
Sphericity	Low	
Packing	Dense	
GRAINS:		PRESENT
QUARTZ		
	Round	X
	Broken Round	X
	Angular	X
	Qtz. Overgrowth	
FELDSPAR		
	K-Spar	X
	Plagioclase	
CARBONATES		
	Calcite	X
	Sparry	
	Micrite	
	Void Filling	
	Dolomite	X
	Replacement Dolomite	
GLAUCONITE		
	Pelloidal	X
	Clay-Glauconite Intermediate	X
	Platy	X
	Vermiform or Zebra	X
	Replacement	X
OTHER MINERALS		
	Phosphatic Material (Collophane)	X
	Chert	X
	Clay	X
	Biotite	
	Muscovite	
	Ooids	
	Fecal Pellets	X

ACCESSORIES		
	Organic Matter	
	Heavy Minerals	
	Ironsulfide (Pyrite?)	X
	Ironoxide (Hematite/Illmenite?)	X
FOSSILS		
	Shell Fragments	X
	Other:	
MICROFOSSILS		
	Cryptospores	
	Acritarchs	
CEMENTS		
	Calcite	X
	Sparry	
	Micrite	
	Dolomite	
	Chert	
	Phosphate	
	Clay-Glauconite Intermediate	X
	Quartz	
	Clay	X
SECONDARY FEATURES:	Vugs	
	Stylolites	
	Soft Sediment Deformation	
SEDIMENTARY STRUCTURES:	Finely Laminated	
	Thickly Laminated	X
	Wavy Laminated	
	Lenticular Laminated	
	Mud Cracks	
	Cross-Bedding	
	Graded-Bedding	
	Fining Upward	
	Burrows:	
	Surface Trace	
	Shallow Surface Trace	X
	Below Substrate Circular Holes	
	Subsurface Mining	
	Escape / Vertical	
	Cryptic	X

Hand Lens Observations:		
Glauconite Present?	X	
Laminations:	X	
Bioturbation:		
None:		
Slight:		
Moderate:	X	
Extensive::		
Micro-faulting		
Organic Rich Layers	X	
Facies Present	I, II, III, IV	
OVERALL LITHOLOGIES	Limestone	
	Mudstone	
	Siltstone	
	Argillaceous Limestone	
	Calcareous Mudstone	
	Argillaceous Siltstone	X
	Dolomite	
	Dolomitic Limestone	
Points of Interest:		

Unusually glauconite rich.

Other median grain sizes:
   glauconite 0.273 mm

Percent Composition:	
Brown	11.8
Green	76.2
White	10.9
Total	98.9

Thin Section

Scale Bar = 1 mm

Points of Interest:

Scale Bar = 1 mm
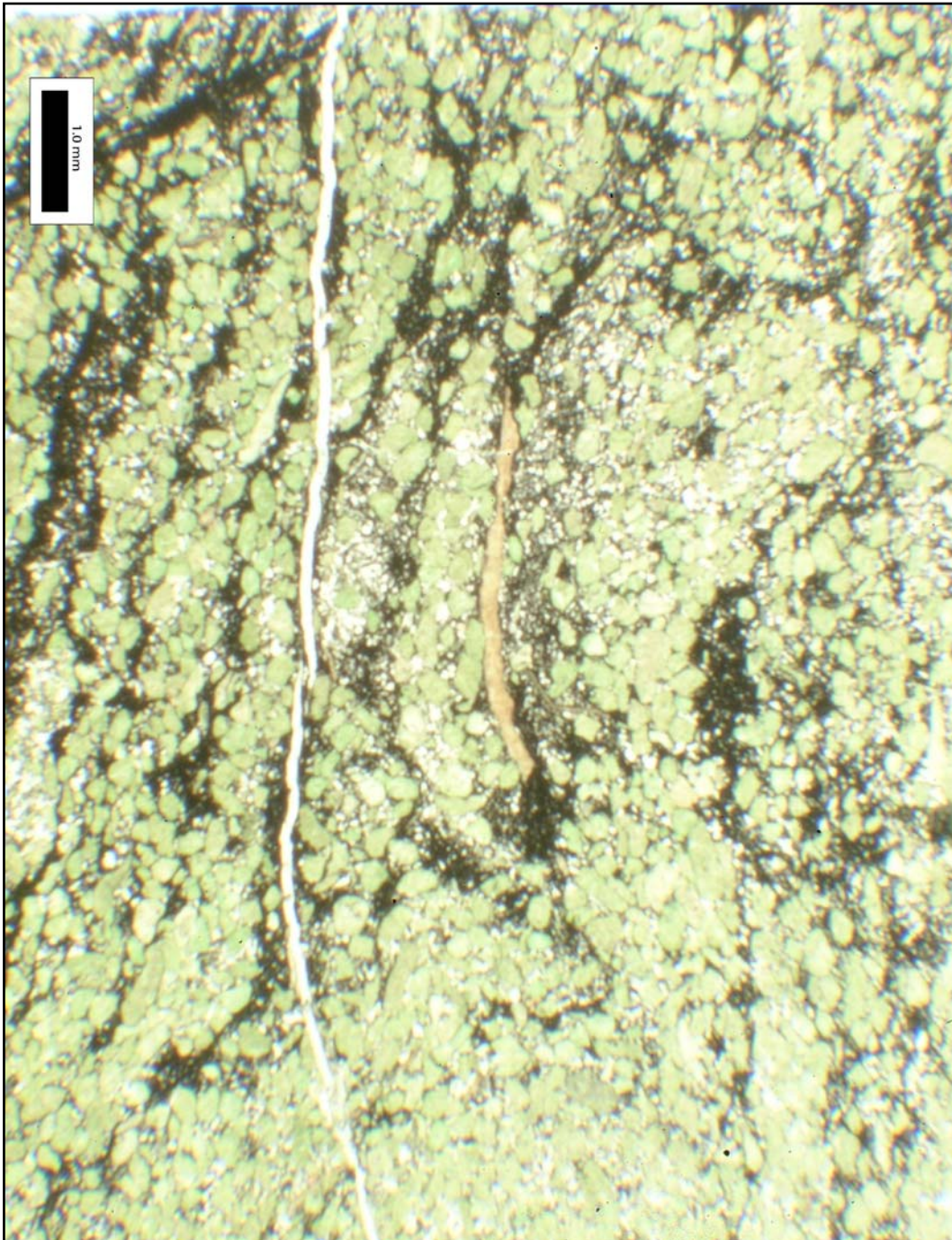
SPECIMEN #	1558' Down Hole Footage	
FORMATION	Rogersville Shale	
MEMBER		
TEXTURE:		
Median GS	0.0367 mm	
Sorting	Poor	
Roundness	Subangular→ Subround	
Sphericity	Low	
Packing	Dense	
GRAINS:		PRESENT
QUARTZ		
	Round	X
	Broken Round	X
	Angular	X
	Qtz. Overgrowth	
FELDSPAR		
	K-Spar	X
	Plagioclase	
CARBONATES		
	Calcite	X
	Sparry	
	Micrite	
	Void Filling	
	Dolomite	
	Replacement Dolomite	
GLAUCONITE		
	Pelloidal	X
	Clay-Glauconite Intermediate	X
	Platy	
	Vermiform or Zebra	
	Replacement	
OTHER MINERALS		
	Phosphatic Material (Collophane)	X
	Chert	X
	Clay	X
	Biotite	
	Muscovite	
	Ooids	
	Fecal Pellets	X

ACCESSORIES		
	Organic Matter	
	Heavy Minerals	
	Ironsulfide (Pyrite?)	X
	Ironoxide (Hematite/Illmenite?)	X
FOSSILS		
	Shell Fragments	X
	Other:	
MICROFOSSILS		
	Cryptospores	
	Acritarchs	
CEMENTS		
	Calcite	X
	Sparry	
	Micrite	
	Dolomite	
	Chert	
	Phosphate	
	Clay-Glauconite Intermediate	X
	Quartz	
	Clay	X
SECONDARY FEATURES:	Vugs	
	Stylolites	
	Soft Sediment Deformation	
SEDIMENTARY STRUCTURES:	Finely Laminated	X
	Thickly Laminated	
	Wavy Laminated	
	Lenticular Laminated	
	Mud Cracks	
	Cross-Bedding	
	Graded-Bedding	
	Fining Upward	
	Burrows:	
	Surface Trace	
	Shallow Surface Trace	X
	Below Substrate Circular Holes	
	Subsurface Mining	
	Escape / Vertical	
	Cryptic	X

Hand Lens Observations:		
Glauconite Present?	X	
Laminations:	X	
Bioturbation:		
None:		
Slight:		
Moderate:	X	
Extensive::		
Micro-faulting	X	
Organic Rich Layers	X	
Facies Present	I, II, III	
OVERALL LITHOLOGIES	Limestone	
	Mudstone	X
	Siltstone	
	Argillaceous Limestone	
	Calcareous Mudstone	
	Argillaceous Siltstone	
	Dolomite	
	Dolomitic Limestone	
Points of Interest:		

Microfaulting appears to have occurred after bioturbation

Percent Composition:	
Brown	48.7
Green	12.7
White	36.6
Total	98.0

Thin Section

Scale Bar = 1 mm
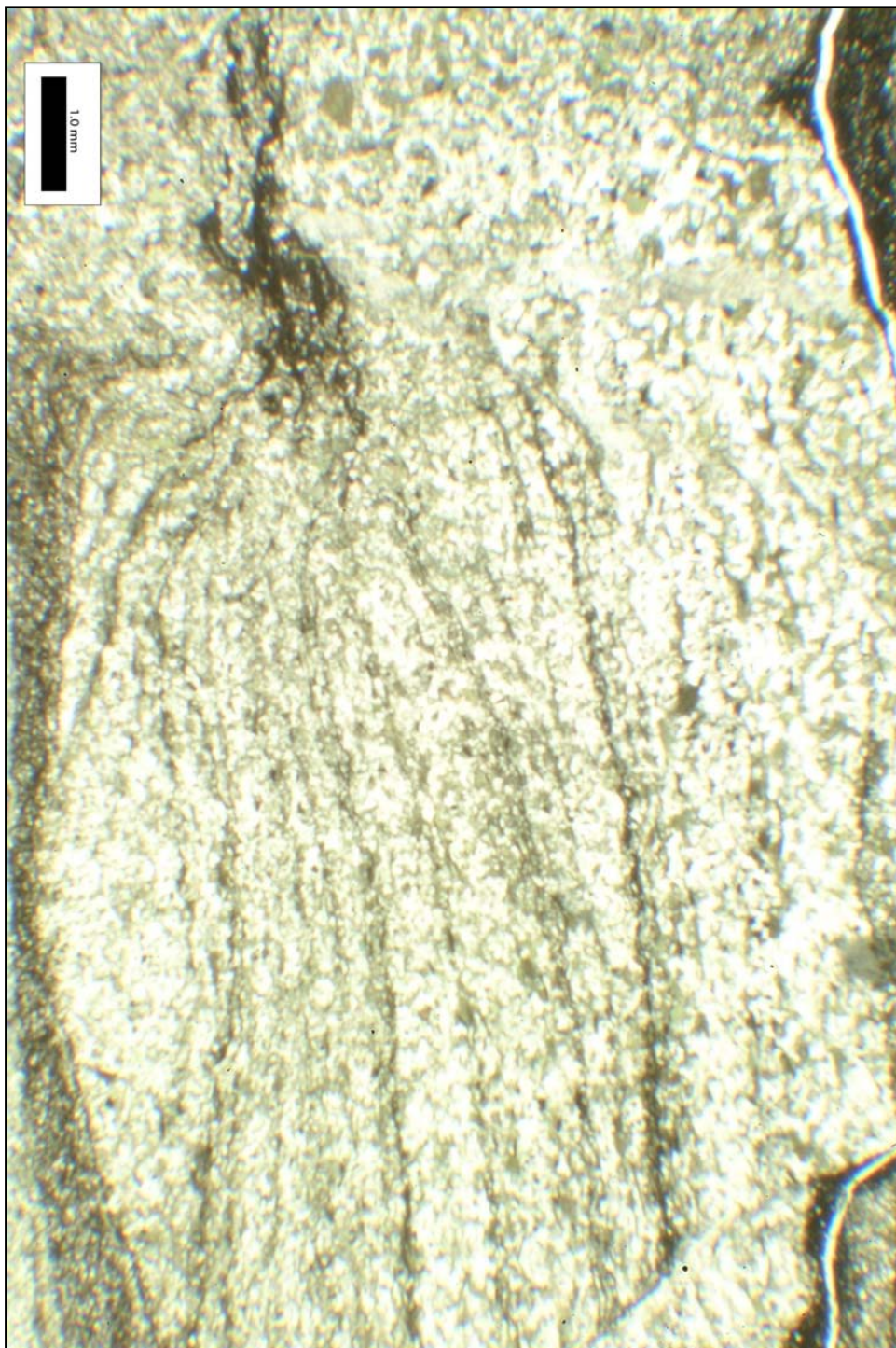
SPECIMEN #	1563' Down Hole Footage	
FORMATION	Rogersville Shale	
MEMBER		
TEXTURE:		
Median GS	0.0364 mm	
Sorting	Poor	
Roundness	Angular→ Subround	
Sphericity	Low	
Packing	Dense	
GRAINS:		PRESENT
QUARTZ		
	Round	X
	Broken Round	X
	Angular	X
	Qtz. Overgrowth	
FELDSPAR		
	K-Spar	X
	Plagioclase	
CARBONATES		
	Calcite	X
	Sparry	
	Micrite	
	Void Filling	
	Dolomite	
	Replacement Dolomite	
GLAUCONITE		
	Pelloidal	X
	Clay-Glauconite Intermediate	X
	Platy	
	Vermiform or Zebra	
	Replacement	
OTHER MINERALS		
	Phosphatic Material (Collophane)	X
	Chert	X
	Clay	X
	Biotite	
	Muscovite	
	Ooids	
	Fecal Pellets	X

ACCESSORIES		
	Organic Matter	
	Heavy Minerals	
	Ironsulfide (Pyrite?)	X
	Ironoxide (Hematite/Illmenite?)	X
FOSSILS		
	Shell Fragments	
	Other:	
MICROFOSSILS		
	Cryptospores	
	Acritarchs	
CEMENTS		
	Calcite	X
	Sparry	
	Micrite	
	Dolomite	
	Chert	
	Phosphate	
	Clay-Glauconite Intermediate	X
	Quartz	
	Clay	X
SECONDARY FEATURES:	Vugs	
	Stylolites	
	Soft Sediment Deformation	
SEDIMENTARY STRUCTURES:	Finely Laminated	X
	Thickly Laminated	
	Wavy Laminated	
	Lenticular Laminated	
	Mud Cracks	
	Cross-Bedding	
	Graded-Bedding	
	Fining Upward	X
	Burrows:	
	Surface Trace	
	Shallow Surface Trace	X
	Below Substrate Circular Holes	
	Subsurface Mining	
	Escape / Vertical	
	Cryptic	X

Hand Lens Observations:		
Glauconite Present?	X	
Laminations:	X	
Bioturbation:		
None:		
Slight:	X	
Moderate:		
Extensive::		
Micro-faulting		
Organic Rich Layers	X	
Facies Present	I, II, III	
OVERALL LITHOLOGIES	Limestone	
	Mudstone	
	Siltstone	
	Argillaceous Limestone	
	Calcareous Mudstone	
	Argillaceous Siltstone	X
	Dolomite	
	Dolomitic Limestone	
Points of Interest:		

Pyrite is vary abundant

Several fecal pellet have been completely replaced by pyrite

Percent Composition:	
Brown	35.9
Green	3.9
White	60.1
Total	99.9

Thin Section

Scale Bar = 1 mm
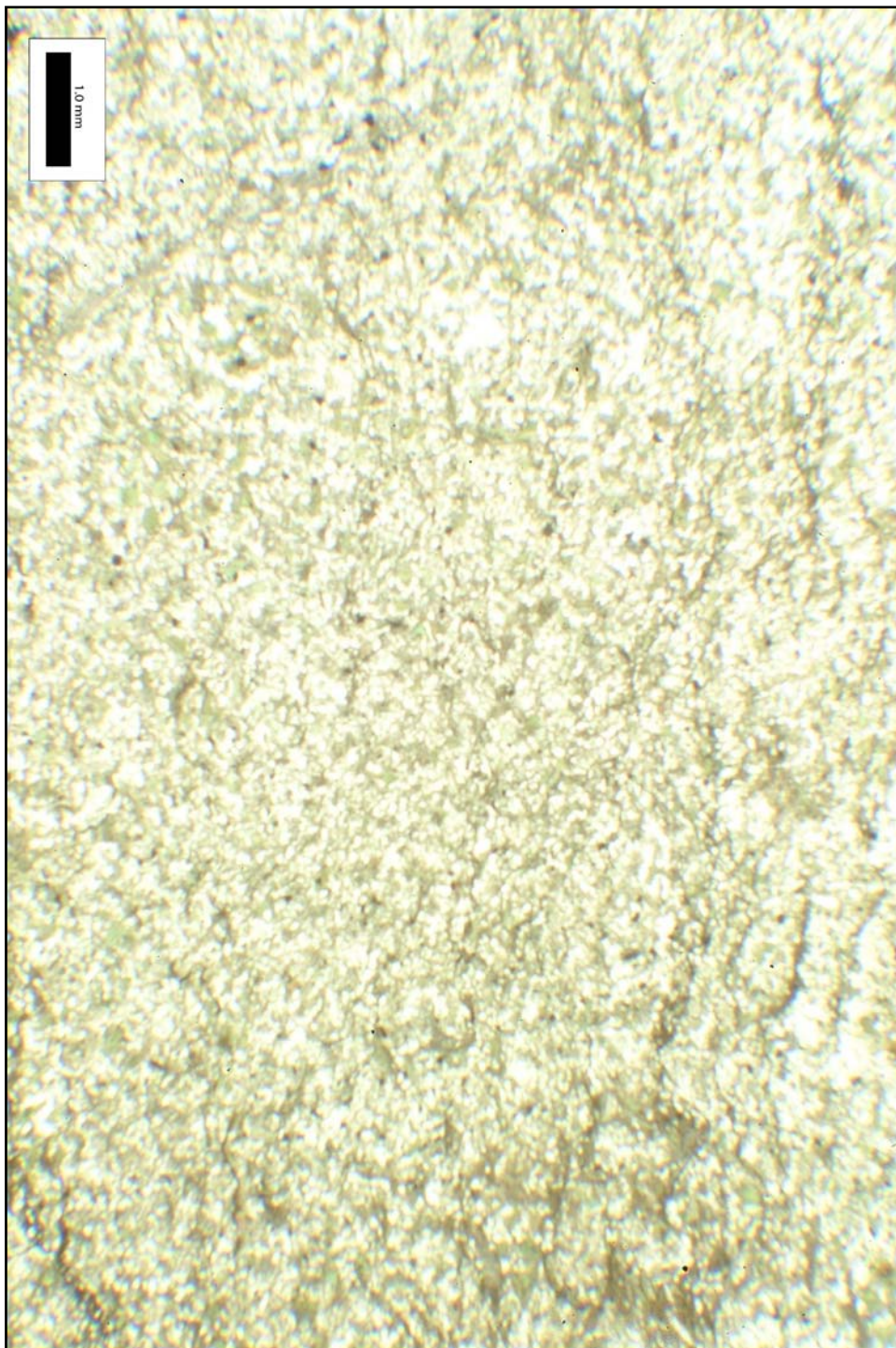
SPECIMEN #	1572.5' Down Hole Footage	
FORMATION	Rogersville Shale	
MEMBER		
TEXTURE:		
Median GS	0.0323 mm	
Sorting	Poor	
Roundness	Angular→ Subround	
Sphericity	Low	
Packing	Dense	
GRAINS:		PRESENT
QUARTZ		
	Round	X
	Broken Round	X
	Angular	X
	Qtz. Overgrowth	
FELDSPAR		
	K-Spar	X
	Plagioclase	
CARBONATES		
	Calcite	
	Sparry	X
	Micrite	
	Void Filling	
	Dolomite	
	Replacement Dolomite	
GLAUCONITE		
	Pelloidal	X
	Clay-Glauconite Intermediate	X
	Platy	X
	Vermiform or Zebra	
	Replacement	
OTHER MINERALS		
	Phosphatic Material (Collophane)	X
	Chert	X
	Clay	X
	Biotite	
	Muscovite	
	Ooids	
	Fecal Pellets	X

ACCESSORIES		
	Organic Matter	
	Heavy Minerals	
	Ironsulfide (Pyrite?)	X
	Ironoxide (Hematite/Illmenite?)	X
FOSSILS		
	Shell Fragments	X
	Other:	
MICROFOSSILS		
	Cryptospores	
	Acritarchs	
CEMENTS		
	Calcite	X
	Sparry	
	Micrite	
	Dolomite	
	Chert	
	Phosphate	
	Clay-Glauconite Intermediate	X
	Quartz	
	Clay	X
SECONDARY FEATURES:	Vugs	
	Stylolites	
	Soft Sediment Deformation	
SEDIMENTARY STRUCTURES:	Finely Laminated	X
	Thickly Laminated	
	Wavy Laminated	X
	Lenticular Laminated	
	Mud Cracks	
	Cross-Bedding	
	Graded-Bedding	
	Fining Upward	X
	Burrows:	
	Surface Trace	
	Shallow Surface Trace	
	Below Substrate Circular Holes	
	Subsurface Mining	
	Escape / Vertical	
	Cryptic	

Hand Lens Observations:		
Glauconite Present?	X	
Laminations:	X	
Bioturbation:		
None:		
Slight:		
Moderate:	X	
Extensive::		
Micro-faulting		
Organic Rich Layers	X	
Facies Present	I, II, III	
OVERALL LITHOLOGIES	Limestone	
	Silty Mudstone	X
	Siltstone	
	Argillaceous Limestone	
	Calcareous Mudstone	
	Argillaceous Siltstone	
	Dolomite	
	Dolomitic Limestone	

Several large cracks throughout this thin section sample are evident in this photograph. This slide was one of several that were damaged.

Percent Composition:	
Brown	75.6
Green	3.7
White	20.7
Total	100.0

Thin Section

Scale Bar = 1 mm
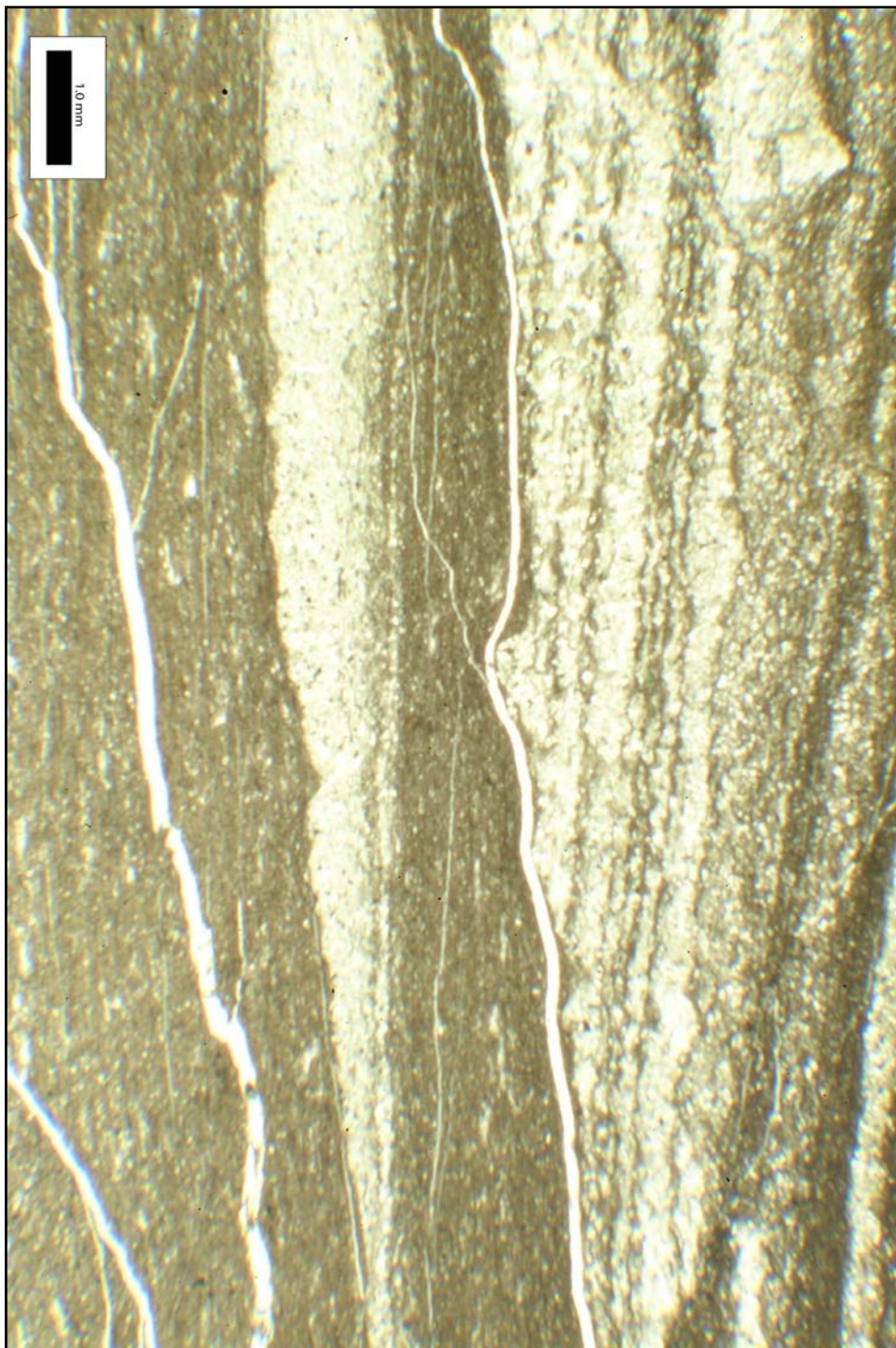
SPECIMEN #	1581' Down Hole Footage	
FORMATION	Rogersville Shale	
MEMBER		
TEXTURE:		
Median GS	0.0429 mm	
Sorting	Poor	
Roundness	Angular→ Subround	
Sphericity	Low	
Packing	Dense	
GRAINS:		PRESENT
QUARTZ		
	Round	X
	Broken Round	X
	Angular	X
	Qtz. Overgrowth	
FELDSPAR		
	K-Spar	X
	Plagioclase	
CARBONATES		
	Calcite	X
	Sparry	
	Micrite	
	Void Filling	
	Dolomite	
	Replacement Dolomite	
GLAUCONITE		
	Pelloidal	X
	Clay-Glauconite Intermediate	X
	Platy	
	Vermiform or Zebra	
	Replacement	
OTHER MINERALS		
	Phosphatic Material (Collophane)	X
	Chert	X
	Clay	X
	Biotite	
	Muscovite	
	Ooids	
	Fecal Pellets	X

ACCESSORIES		
	Organic Matter	
	Heavy Minerals	
	Ironsulfide (Pyrite?)	X
	Ironoxide (Hematite/Illmenite?)	X
FOSSILS		
	Shell Fragments	X
	Other:	
MICROFOSSILS		
	Cryptospores	
	Acritarchs	
CEMENTS		
	Calcite	X
	Sparry	
	Micrite	
	Dolomite	
	Chert	
	Phosphate	
	Clay-Glauconite Intermediate	X
	Quartz	
	Clay	X
SECONDARY FEATURES:	Vugs	
	Stylolites	
	Soft Sediment Deformation	
SEDIMENTARY STRUCTURES:	Finely Laminated	X
	Thickly Laminated	
	Wavy Laminated	
	Lenticular Laminated	
	Mud Cracks	
	Cross-Bedding	
	Graded-Bedding	
	Fining Upward	X
	Burrows:	
	Surface Trace	
	Shallow Surface Trace	X
	Below Substrate Circular Holes	
	Subsurface Mining	
	Escape / Vertical	
	Cryptic	X

Hand Lens Observations:		
Glauconite Present?	X	
Laminations:	X	
Bioturbation:		
None:		
Slight:	X	
Moderate:		
Extensive::		
Micro-faulting	X	
Organic Rich Layers	X	
Facies Present	I, II, III	
OVERALL LITHOLOGIES	Limestone	
	Silty Mudstone	X
	Siltstone	
	Argillaceous Limestone	
	Calcareous Mudstone	
	Argillaceous Siltstone	X
	Dolomite	
	Dolomitic Limestone	

Circled in red is a burrow completely fill with pyrite

Percent Composition:
Brown	67.8
Green	13.9
White	18.1
Total	99.8

Thin Section

Scale Bar = 1 mm

SPECIMEN #	1586' Down Hole Footage	
FORMATION	Rogersville Shale	
MEMBER		
TEXTURE:		
Median GS	0.0443 mm	
Sorting	Poor	
Roundness	Subangular→ Subround	
Sphericity	Low	
Packing	Dense	
GRAINS:		PRESENT
QUARTZ		
	Round	X
	Broken Round	X
	Angular	X
	Qtz. Overgrowth	
FELDSPAR		
	K-Spar	X
	Plagioclase	
CARBONATES		
	Calcite	X
	Sparry	
	Micrite	
	Void Filling	
	Dolomite	X
	Replacement Dolomite	
GLAUCONITE		
	Pelloidal	X
	Clay-Glauconite Intermediate	X
	Platy	
	Vermiform or Zebra	
	Replacement	
OTHER MINERALS		
	Phosphatic Material (Collophane)	X
	Chert	X
	Clay	X
	Biotite	
	Muscovite	
	Ooids	
	Fecal Pellets	X

ACCESSORIES		
	Organic Matter	
	Heavy Minerals	
	Ironsulfide (Pyrite?)	X
	Ironoxide (Hematite/Illmenite?)	X
FOSSILS		
	Shell Fragments	X
	Other:	
MICROFOSSILS		
	Cryptospores	
	Acritarchs	
CEMENTS		
	Calcite	X
	Sparry	
	Micrite	
	Dolomite	
	Chert	
	Phosphate	
	Clay-Glauconite Intermediate	
	Quartz	
	Clay	
SECONDARY FEATURES:	Vugs	
	Stylolites	
	Soft Sediment Deformation	
SEDIMENTARY STRUCTURES:	Finely Laminated	X
	Thickly Laminated	
	Wavy Laminated	
	Lenticular Laminated	
	Mud Cracks	
	Cross-Bedding	
	Graded-Bedding	
	Fining Upward	X
	Burrows:	
	Surface Trace	
	Shallow Surface Trace	X
	Below Substrate Circular Holes	
	Subsurface Mining	
	Escape / Vertical	
	Cryptic	X

Hand Lens Observations:		
Glauconite Present?	X	
Laminations:	X	
Bioturbation:		
None:		
Slight:		
Moderate:	X	
Extensive::		
Micro-faulting	X	
Organic Rich Layers	X	
Facies Present	I, II, III	
OVERALL LITHOLOGIES	Limestone	
	Silty Mudstone	X
	Siltstone	
	Argillaceous Limestone	
	Calcareous Mudstone	
	Argillaceous Siltstone	X
	Dolomite	
	Dolomitic Limestone	
Points of Interest:		

Percent Composition:	
Brown	73.0
Green	19.6
White	7.3
Total	99.9

Thin Section

Scale Bar = 1 mm
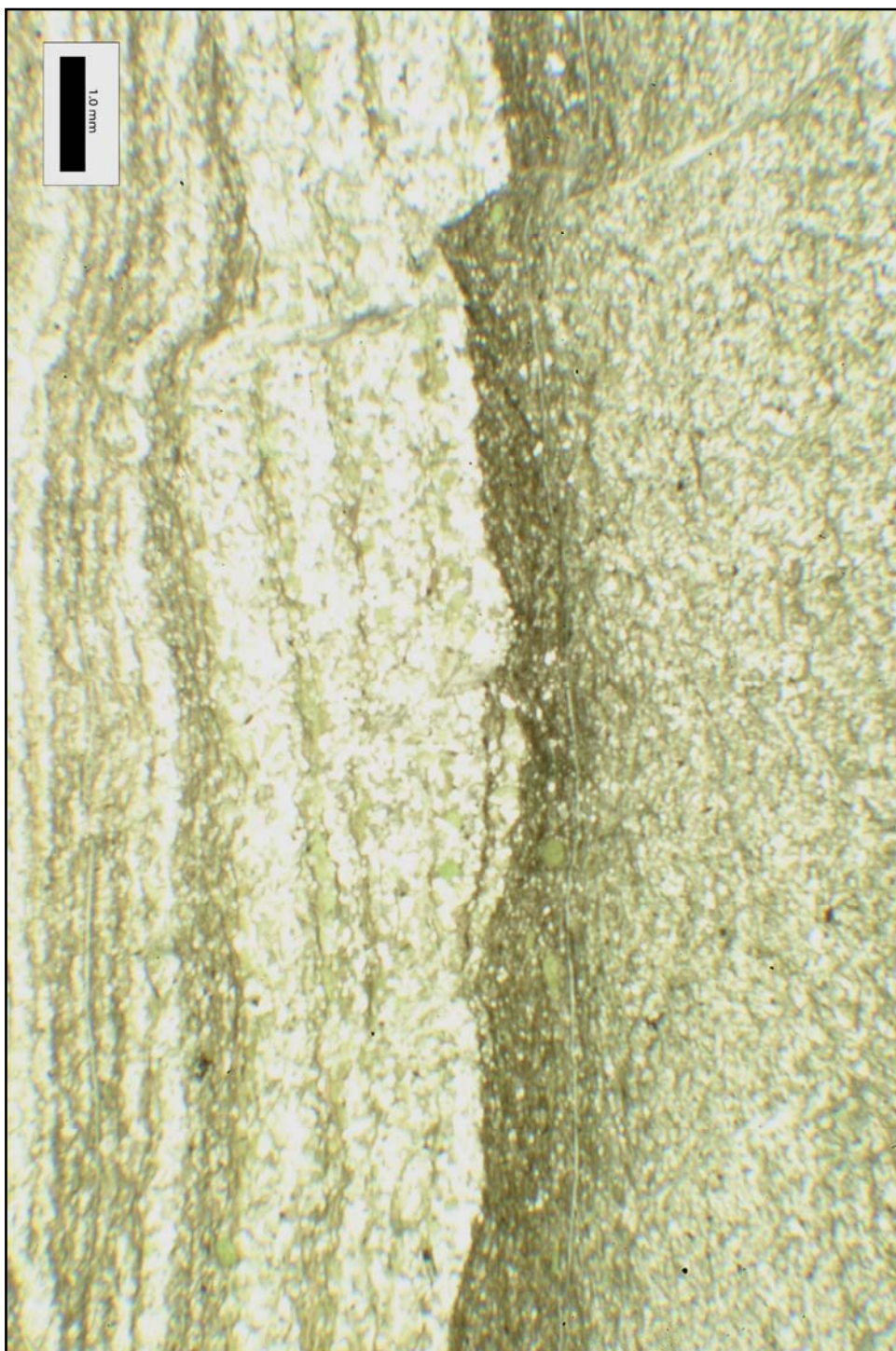
SPECIMEN #	1594' Down Hole Footage	
FORMATION	Rogersville Shale	
MEMBER		
TEXTURE:		
Median GS	0.0436 mm	
Sorting	Poor	
Roundness	Subangular→ Subround	
Sphericity	Low	
Packing	Dense	
GRAINS:		PRESENT
QUARTZ		
	Round	X
	Broken Round	X
	Angular	X
	Qtz. Overgrowth	
FELDSPAR		
	K-Spar	X
	Plagioclase	
CARBONATES		
	Calcite	X
	Sparry	X
	Micrite	
	Void Filling	
	Dolomite	
	Replacement Dolomite	
GLAUCONITE		
	Pelloidal	X
	Clay-Glauconite Intermediate	X
	Platy	X
	Vermiform or Zebra	
	Replacement	
OTHER MINERALS		
	Phosphatic Material (Collophane)	X
	Chert	X
	Clay	X
	Biotite	
	Muscovite	
	Ooids	
	Fecal Pellets	X

ACCESSORIES		
	Organic Matter	
	Heavy Minerals	
	Ironsulfide (Pyrite?)	X
	Ironoxide (Hematite/Illmenite?)	X
FOSSILS		
	Shell Fragments	X
	Other:	
MICROFOSSILS		
	Cryptospores	
	Acritarchs	
CEMENTS		
	Calcite	X
	Sparry	
	Micrite	
	Dolomite	
	Chert	
	Phosphate	
	Clay-Glauconite Intermediate	X
	Quartz	
	Clay	X
SECONDARY FEATURES:	Vugs	
	Stylolites	
	Soft Sediment Deformation	
SEDIMENTARY STRUCTURES:	Finely Laminated	X
	Thickly Laminated	
	Wavy Laminated	
	Lenticular Laminated	
	Mud Cracks	
	Cross-Bedding	
	Graded-Bedding	
	Fining Upward	X
	Burrows:	
	Surface Trace	X
	Shallow Surface Trace	X
	Below Substrate Circular Holes	
	Subsurface Mining	
	Escape / Vertical	
	Cryptic	X

Hand Lens Observations:		
Glauconite Present?	X	
Laminations:	X	
Bioturbation:		
None:		
Slight:	X	
Moderate:		
Extensive::		
Micro-faulting	X	
Organic Rich Layers	X	
Facies Present	I, II, III	
OVERALL LITHOLOGIES	Limestone	
	Silty Mudstone	X
	Siltstone	
	Argillaceous Limestone	
	Calcareous Mudstone	
	Argillaceous Siltstone	X
	Dolomite	
	Dolomitic Limestone	

Circled in red are several burrows the smaller is a surface trace and the larger is a shallow surface trace

Percent Composition:	
Brown	36.7
Green	4.0
White	58.5
Total	99.2

Thin Section

Scale Bar = 1 mm
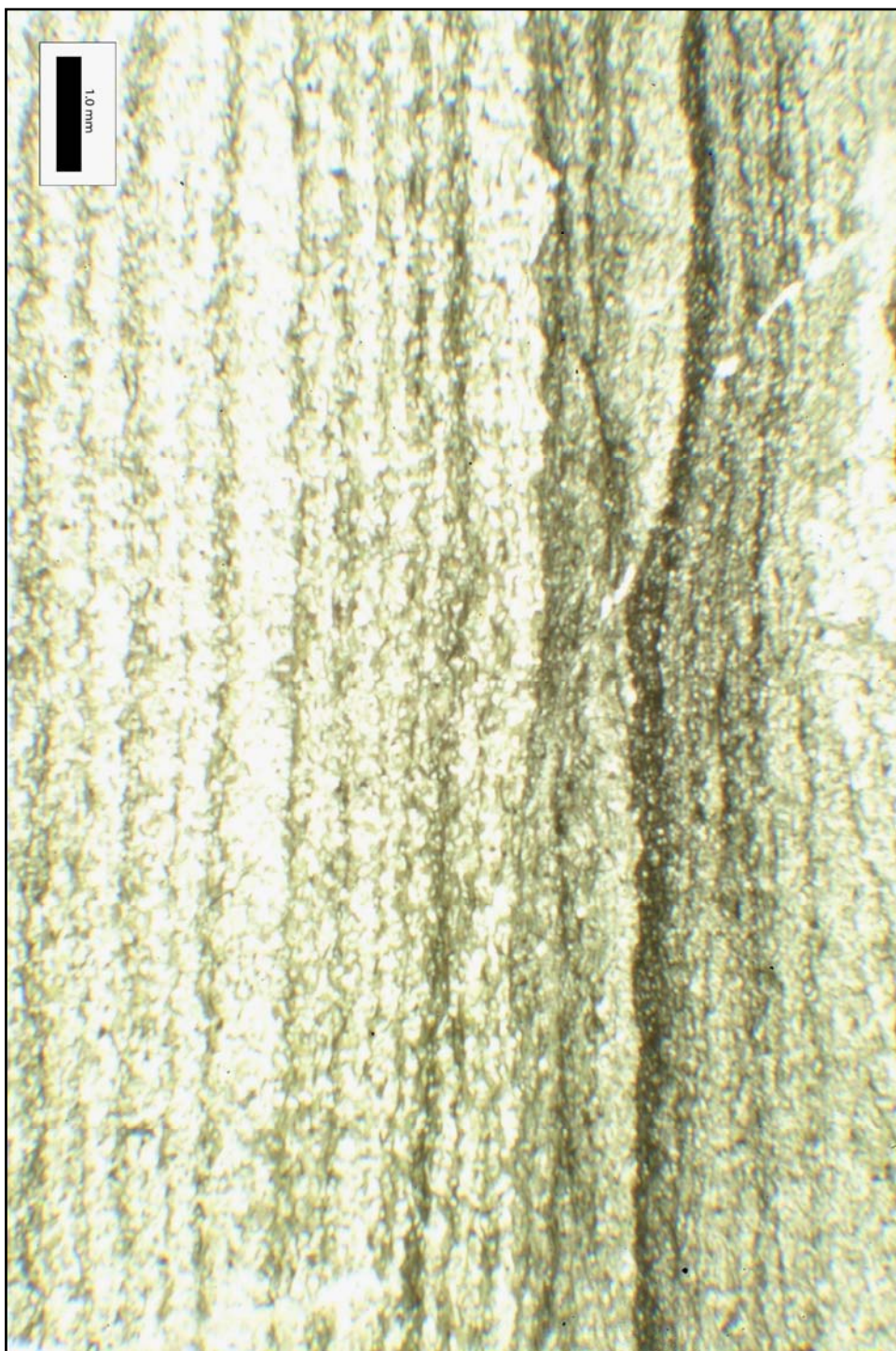
Point of Interest

Scale Bar = 1 mm
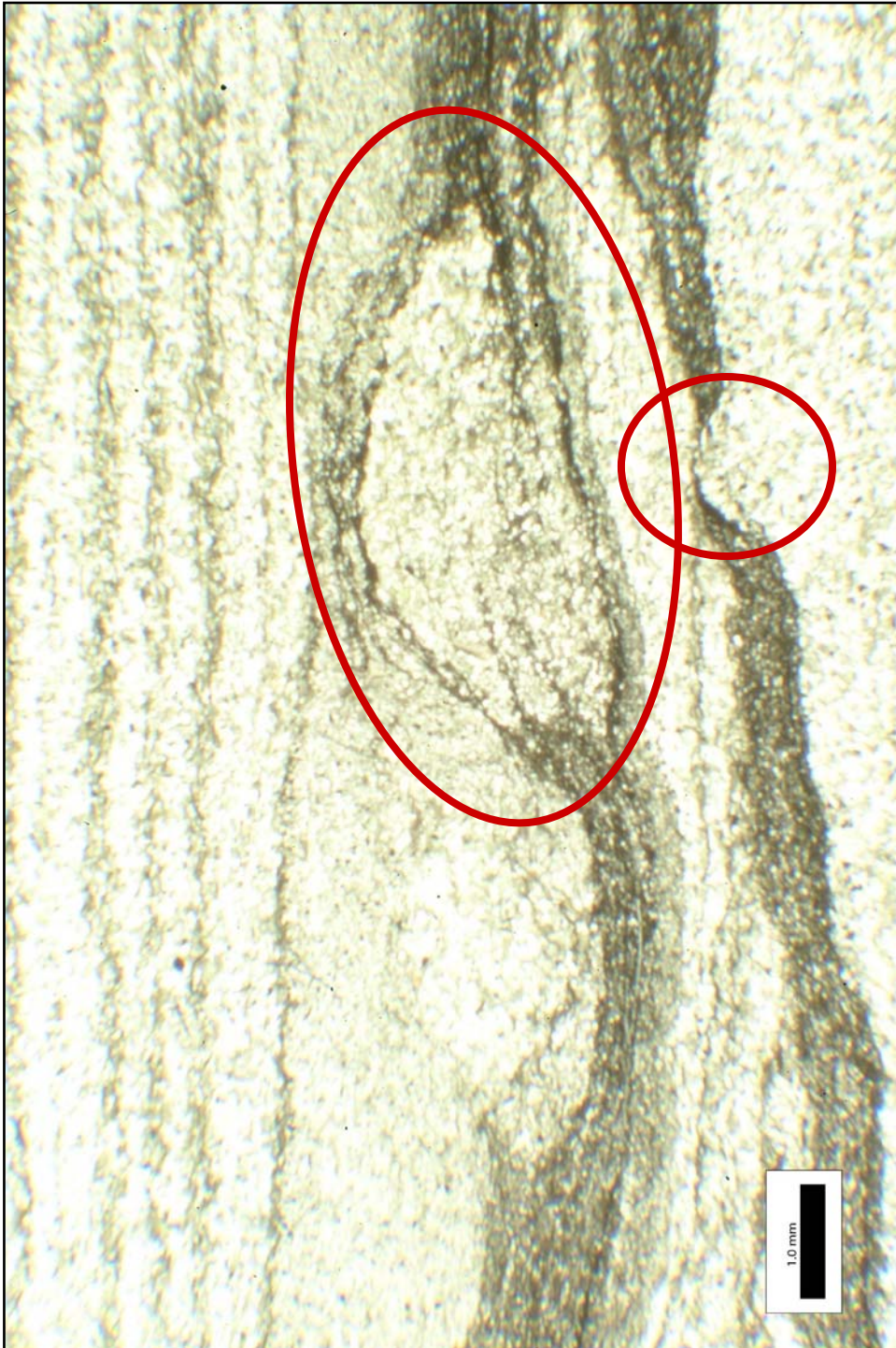
SPECIMEN #	1599.5' Down Hole Footage	
FORMATION	Rogersville Shale	
MEMBER		
TEXTURE:		
Median GS	0.0338 mm	
Sorting	Poor	
Roundness	Angular→ Subround	
Sphericity	Low	
Packing	Dense	
GRAINS:		PRESENT
QUARTZ		
	Round	X
	Broken Round	X
	Angular	X
	Qtz. Overgrowth	
FELDSPAR		
	K-Spar	X
	Plagioclase	
CARBONATES		
	Calcite	X
	Sparry	
	Micrite	
	Void Filling	
	Dolomite	X
	Replacement Dolomite	
GLAUCONITE		
	Pelloidal	X
	Clay-Glauconite Intermediate	X
	Platy	
	Vermiform or Zebra	
	Replacement	
OTHER MINERALS		
	Phosphatic Material (Collophane)	X
	Chert	X
	Clay	X
	Biotite	
	Muscovite	
	Ooids	
	Fecal Pellets	X

ACCESSORIES		
	Organic Matter	
	Heavy Minerals	
	Ironsulfide (Pyrite?)	X
	Ironoxide (Hematite/Illmenite?)	X
FOSSILS		
	Shell Fragments	X
	Other:	
MICROFOSSILS		
	Cryptospores	
	Acritarchs	
CEMENTS		
	Calcite	X
	Sparry	
	Micrite	
	Dolomite	
	Chert	
	Phosphate	
	Clay-Glauconite Intermediate	X
	Quartz	
	Clay	X
SECONDARY FEATURES:	Vugs	
	Stylolites	
	Soft Sediment Deformation	
SEDIMENTARY STRUCTURES:	Finely Laminated	X
	Thickly Laminated	
	Wavy Laminated	
	Lenticular Laminated	
	Mud Cracks	
	Cross-Bedding	
	Graded-Bedding	
	Fining Upward	X
	Burrows:	
	Surface Trace	
	Shallow Surface Trace	
	Below Substrate Circular Holes	
	Subsurface Mining	
	Escape / Vertical	
	Cryptic	

Hand Lens Observations:		
Glauconite Present?	X	
Laminations:	X	
Bioturbation:		
None:		
Slight:	X	
Moderate:		
Extensive::		
Micro-faulting	X	
Organic Rich Layers	X	
Facies Present	I, II, III	
OVERALL LITHOLOGIES	Limestone	
	Silty Mudstone	X
	Siltstone	
	Argillaceous Limestone	
	Calcareous Mudstone	
	Argillaceous Siltstone	
	Dolomite	
	Dolomitic Limestone	

Percent Composition:	
Brown	55.9
Green	13.4
White	32.2
Total	101.5

Thin Section

Scale Bar = 1 mm
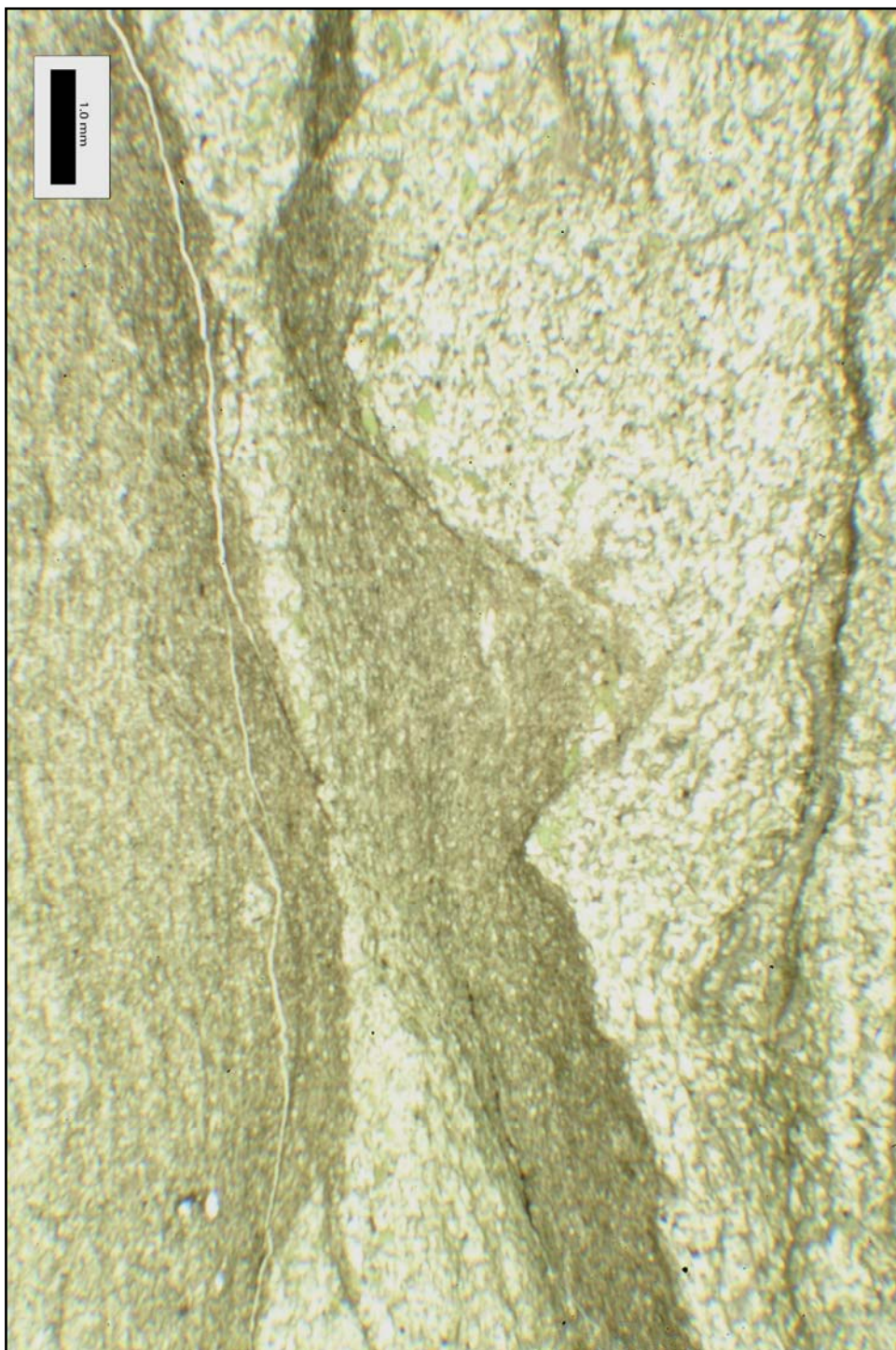
SPECIMEN #	1602' Down Hole Footage	
FORMATION	Rogersville Shale	
MEMBER		
TEXTURE:		
Median GS	0.0307 mm	
Sorting	Poor	
Roundness	Angular→ Subround	
Sphericity	Low	
Packing	Dense	
GRAINS:		PRESENT
QUARTZ		
	Round	X
	Broken Round	X
	Angular	X
	Qtz. Overgrowth	
FELDSPAR		
	K-Spar	X
	Plagioclase	
CARBONATES		
	Calcite	X
	Sparry	
	Micrite	
	Void Filling	
	Dolomite	X
	Replacement Dolomite	
GLAUCONITE		
	Pelloidal	X
	Clay-Glauconite Intermediate	X
	Platy	
	Vermiform or Zebra	
	Replacement	
OTHER MINERALS		
	Phosphatic Material (Collophane)	X
	Chert	X
	Clay	X
	Biotite	
	Muscovite	
	Ooids	
	Fecal Pellets	X

ACCESSORIES		
	Organic Matter	
	Heavy Minerals	
	Ironsulfide (Pyrite?)	X
	Ironoxide (Hematite/Illmenite?)	X
FOSSILS		
	Shell Fragments	X
	Other:	
MICROFOSSILS		
	Cryptospores	
	Acritarchs	
CEMENTS		
	Calcite	X
	Sparry	X
	Micrite	
	Dolomite	
	Chert	
	Phosphate	
	Clay-Glauconite Intermediate	X
	Quartz	
	Clay	X
SECONDARY FEATURES:	Vugs	
	Stylolites	
	Soft Sediment Deformation	
SEDIMENTARY STRUCTURES:	Finely Laminated	
	Thickly Laminated	
	Wavy Laminated	
	Lenticular Laminated	
	Mud Cracks	
	Cross-Bedding	
	Graded-Bedding	
	Fining Upward	
	Burrows:	
	Surface Trace	
	Shallow Surface Trace	X
	Below Substrate Circular Holes	X
	Subsurface Mining	X
	Escape / Vertical	
	Cryptic	X

Hand Lens Observations:		
Glauconite Present?	X	
Laminations:	X	
Bioturbation:		
None:		
Slight:		
Moderate:		
Extensive::	X	
Micro-faulting	X	
Organic Rich Layers	X	
Facies Present	I, II, III	
OVERALL LITHOLOGIES	Limestone	
	Silty Mudstone	X
	Siltstone	
	Argillaceous Limestone	
	Calcareous Mudstone	
	Argillaceous Siltstone	
	Dolomite	
	Dolomitic Limestone	

Percent Composition:	
Brown	49.3
Green	n/a
White	51.4
Total	100.7

Thin Section

Scale Bar = 1 mm

Point of Interest

Scale Bar = 1 mm